An integral predictive model that reveals a causal relation between exposures to non-thermal electromagnetic waves and healthy or unhealthy effects

Hans J Geesink[1] and Dirk K F Meijer[2]

1. Previous Project Leader Nanotechnology, DSM-Research, The Netherlands
2. Em, Professor of Pharmacology, University of Groningen, Groningen, The Netherlands

Keywords: Quantum coherence, coherent and decoherent EMF- frequencies, spectral coherence scale, electromagnetic frequencies, quantum biology, quantum wave equation, healthy and unhealthy frequency patterns, 5G EMF-frequencies, models of Fröhlich and Davydov, GM-scale biophysical principle, health technologies,

07 April 2020

Summary

Conformational states of living cells have typical spatial arrangements of atoms, that are characteristic for building, homeostasis, decay and apoptosis. We earlier found clear evidence, indicating that such states of biomolecules are related to spectral coherence and decoherence frequency bands, providing a quantitative physical resource. The patterned arrangements of EMF frequencies can be described by electromagnetic wave patterns positioned on an acoustic scale, on the basis of an underlying quantum wave equation. The proposed equation shows a discrete distribution of energy: $E_n = \hbar\ \omega_{ref}\ 2^{n+p}\ 3^m$, that supports quantum entanglement, and is in line with the earlier published models of Fröhlich and Davydov. The overall results show the presence of a molecular code-script, which supplies information to realize biological order in life cells and substantiates collective (Bose-Einstein) type of coherent wave behaviour. The particular wave equation was inferred from a meta-analysis of 724 biomedical publications, from 1970 till 2020, reporting either beneficial or detrimental biological effects caused by external non-thermal EMF-frequencies from ELF till THz. Based on this new biophysical principle, solid evidence is provided to support a causal relation between exposure of electromagnetic waves and healthy or unhealthy effects for living cells and biomolecules. External exposures to non-thermal KHz, MHz- and GHz electromagnetic waves can therefore lead to unhealthy conditions depending on wave frequency, pulsing properties, field intensity and exposure time. An additional analysis of 229 experiments confirms that non-thermal electromagnetic waves are able to induce significant changes in human cells. The currently applied single or composed (modulated) frequencies in communication technology, fit for 94.2% with the proposed quantum model as related to either healthy or unhealthy behaviour, offering the potential to optimize calibration of chosen EMF bands. For example, up to 80% of the planned 5G frequencies belong to the detrimental decoherent or modulated coherent frequency bands. Further research to counteract non-thermal unhealthy electromagnetic effects can generate ideas for improving the balance between coherent and decoherent waves, and thereby may open a potential novel road to innovative health technologies.

Introduction of Fröhlich's hypothesis

The appearance of endogenous electromagnetic fields in biological systems has been reviewed by De Ninno and Pregnolato (2016). The existence of fast-moving charged particles in the macromolecules inside both intracellular and extracellular fluids envisage the generation of localized electric currents as well as the presence of closed loops, implying the existence of electromagnetic fields in life systems, see figure 1. Bioelectrical communication generated by the electromagnetic rhythm of coherent groups of cells, and cell-to-cell communication form a complex hierarchy of electromagnetic signals of different frequencies which cover the living being and represent a fundamental information network controlling the cell metabolism. From this consideration the concept of electromagnetic homeostasis emerges: that is, the capability of the human body to maintain a balance of highly complex electromagnetic interactions within cells, in spite of an external electromagnetic noisy environment (De Ninno and Pregnolato, 2016). Various researchers proposed Bose-Einstein condensation as a principle for a self-organizing-synergetic structure, that works in biological processes and is present in several systems of boson-like quasi-particles in condensed inorganic matter: Fröhlich (1968), Davydov (1977), Wu (1978), Reimers (2009), Chukova (2011), Vasconcellos and Luzzi (2012), Lundholm et al. (2015), Ninno and Pregnolato (2016), Nardecchia et al. (2018), Wong (2019) and Zhedong Zhang et al. (2019).

A similar state, with collective excitation frequencies, was predicted basically, in 1924 by Einstein: a Bose–Einstein condensate (BEC) and was defined as a state of matter which is typically formed when a gas of bosons at low densities is cooled to temperatures very close to absolute zero (-273.15 °C). Under such conditions, a large fraction of bosons occupy the lowest quantum state, at which microscopic quantum phenomena, particularly wavefunction interference, becomes macroscopic. Within this context, Devyatkov reported the typical frequency-dependent non-thermal state for biological effects in the GHz-frequency range (Devyatkov, 1974). This frequency-dependent effect of millimetre waves could be further confirmed on the genomic conformational state of E. coli cells in the frequency GHz-range including a power density dependence of the millimetre waves at typical resonance frequencies (Belyaev, 1996). Also, Chukova showed that biological effects of non-thermal electromagnetic waves are subject to Bose – Einstein-like behaviour: millimetre electromagnetic waves exposed to living cells are able to flow in a direction of an increase of the Helmholtz free energy (endergonic processes) or, a contrast, into a direction of decrease (exergonic processes). Thus, both conditions depend upon a frequency spectrum. It has been concluded that thermodynamics do not prohibit processes under the conditions of $h\nu << kT$ (the Rayleigh-Jeans region), (Chukova, 2011).

There is currently scientific evidence that ELF (extreme low frequency) - EMF (electromagnetic field) exposures clearly pose a health risk. The strongest evidence for health effects comes from an association observed with childhood leukaemia. This lies at the basis of a classification performed by the International Agency for Research on Cancer in 2001, ranking ELF magnetic fields as possibly carcinogenic to humans (Group 2B) (IARC, 2002). The classifications, essentially, were based on the fact that epidemiological studies showed a consistent association between magnetic fields above approximately 0.3/0.4 μT (Marino, 2016). Radiofrequency radiation (RF) is increasingly being recognized as a new form of environmental pollution (Russell, 2018). Concerns about health effects caused by exposure to RF are now mainly related to mobile telephones and base stations, becoming a major societal issue. Major improvements have been achieved in measuring the SAR (Specific Absorption Rate) in liquid phantoms and calculating power distribution in the head using numerical phantoms over the last 10 years. Of note, one study computed the temperature elevations in an anatomical human head model exposed to radiation from a dipole antenna and truncated plane waves at 300 MHz-10 GHz. The temperature elevation in the brain at 10 W/kg is at most 0.93 °C and the temperature elevation under this condition for occupational exposure is within the ranges of brain temperature variability for environmental changes in daily life (Kodera, 2018).

A comprehensive understanding of the mechanisms of EMF/life interaction remains to be further elucidated, and there is great interest in evaluating the induced biological responses from the point of view of the

associated interaction mechanisms (Scarfì, 2019). It is further recommended that in future studies, effects of EMF should be investigated more systematically, i.e., studies should consider various frequencies, including their combinations and modulations to identify potential frequency-dependent effects as well as the influence of different field strengths, especially if threshold-dependent effects are expected (Bodewein, 2019).

A dynamic model for cellular oscillations has been proposed by Fröhlich, where part of the cellular energy supplied to the biological system is not used to reach the thermal equilibrium but, rather, to create order (Fröhlich, 1968; Ahmed, 1975). The random supply of energy to non-linearly coupled modes lead to coherent excitations of highly excited modes over an assumed bath that is nearly in thermal equilibrium. If the energy E supplied by metabolic processes exceeds a critical rate E_0, then a phase transition related to a Bose condensation arises in the vibrating system and the particular frequencies are excited in a coherent manner. Importantly, it is possible to excite this mode by external electromagnetic radiation of correct frequencies and this mechanism can explain how under specific circumstances the ordering of a system is enforced by the supply of energy, which is the case of living systems. (Fröhlich, 1968; De Ninno and Pregnolato, 2016).

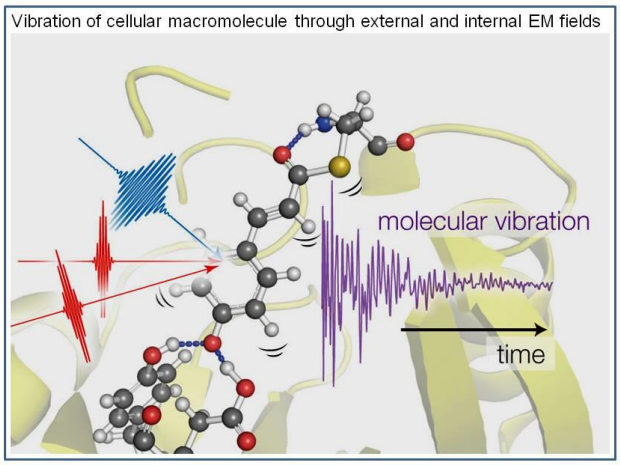

Figure 1. *Internal (blue arrow) and external (red arrows) EM-fields with discrete wave frequencies influence the 3-D structure and vibratory states of macromolecules in life systems.*

Quantum mechanics explains the interactions of wave/particles energy at the scale of atoms and subatomic particles. The theory postulates that physical quantities such as energy and momentum are, under certain conditions, quantized and therefore have only discrete values. This is also true for warm and wet life systems: quantum coherence have been shown not only for micro states but also for macro processes such as photosynthesis, magneto-reception in birds, the human sense of smell as well as the photon effects in vision, all showing a non-trivial role for quantum mechanisms throughout biology (Huelga and Plenio, 2013). One aspect is related to the kT paradox: the existence of long-lasting coherent states and excitations at room temperature, that is not compatible with the energy exchanges due to the thermal random motion. A general theorem of Quantum Electrodynamics (QED) theory shows that under appropriate circumstances, i.e. when T is lower than a critical temperature Tc and the density is greater than a critical density dc, the system spontaneously attains a quantum state. This state has been termed as coherent because all the atoms or molecules belonging to this state can be described by one wave function and related eigenstates (Preparata, 1995; De Ninno and Pregnolato, 2016; Geesink and Meijer, 2017a). Highly efficient energy transfer is a major characteristic of coherent systems and the existence of oscillating dipoles in biological systems can be explained in terms of atoms and molecules sharing the same wave function (Del Giudice, 1983, 1985).

In 1968, H. Fröhlich showed that a driven set of oscillators can condense with nearly all of the supplied energy activating a vibrational mode of lowest frequency. A theory of coherent excitations has been proposed, and describes a state of coherence, called a Fröhlich condensate (Fröhlich, 1968, 1969). Also, he showed that biological organisation is facilitated by the creation of such coherent excited states as driven by a flow of free energy provided by metabolic processes and mediated by molecular motions according to Fröhlich (Fröhlich, 1986; Weightman, 2014). This emerging property is usually compared not only with Bose-Einstein condensation, but also with superconductivity, since both involve macroscopic quantum coherence (Fröhlich, 1968; Reimers, 2009), see figure 2. Fröhlich regarded the high sensitivity of living cells to external waves with non-thermal millimetre waves (MMW) in particular, as created by so-called resonance, representing one central feature of his theory (Fröhlich, 1988). He assumed, for example, that cancer induction pathways include a link with disturbed coherent electric vibrations. A cancer cell may escape from the essential interactions with the surrounding healthy cells and may exhibit an individual (independent) activity if the healthy frequency spectrum is perturbated (Fröhlich, 1978). Meijer and Geesink were able to prove this hypothesis by analysing about 120 biomedical studies related to cancer, showing a frequency band pattern of cancer-promoting and cancer- inhibiting frequencies that could be described by quantum wave interference and was explained by influences on the supposed Bose – Einstein type of cellular behaviour (Meijer and Geesink, 2018e).

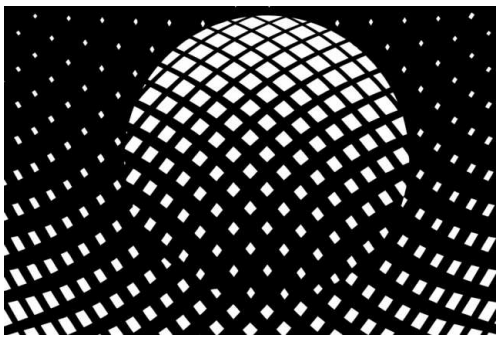

Figure 2. *Bose Einstein Condensate: assembly of ordered states (art impression).*

Also, liquid water plays a clear role in the existence of long-lasting coherent states of healthy cells (De Ninno and Pregnolato, 2016; De Ninno, 2013; Renati, 2019; Hinrikus, 2014; Geesink, 2020a). In order to explain such long-range cohesion of liquid water clusters, special spatial arrangement of structured H-bonded water molecules is considered. In this process, coherent and decoherent vibrating liquid water clusters exhibit a role in the superposition of collective wave patterns of macro-molecules that can show different degrees of mutual correlation and therefore can belong to very different quantum states that constitute cell viability. Recent experimental findings and analyses have confirmed this picture (Taschin, 2013; De Ninno, 2014). Of note, structured domains of pure water molecules and superconductive condensed matter may therefore share similar unique quantum wave states (Geesink, 2020a).

A number of researchers found evidence for the hypothesis of Fröhlich and Davydov:

1) **Lundholm** et al. provided experimental support for the Fröhlich type of condensation in the arrangement of certain proteins, indicating Bose - Einstein condensate-like structures in biological matter at room temperature. The group used a combined terahertz measuring technique with a highly sensitive X-ray crystallographic method to visualize low frequency vibrational modes in the protein structure of lysozyme. The vibrations were sustained for micro- to milli-seconds, which is 3–6 orders of magnitude longer than expected if such structural changes would be due to a redistribution of vibrations according to a Boltzmann's distribution. The influence of a non-thermal signal, at an intensity of 62 mW/cm2, was able to locally change the electron density in a long alfa-helix motif of the protein, being consistent with an observed subtle

longitudinal compression of the helix (Lundholm, 2015). Direct protein atoms probing, using X-ray crystallography in bovine trypsin at 100 K, while irradiating the crystals with 0.5 THz EMF radiation showed alternating on and off states. Thus, an anisotropy of atomic displacements has been clearly observed upon terahertz irradiation. This pattern likely arises from delocalized polar vibrational modes rather than delocalized elastic deformations or rigid-body displacements (Ahlberg Gagnér, 2019).

2) **Nardecchia** et al. described the activation of out-of-equilibrium collective oscillations of a macromolecule and attributed this to classical Bose-like phonon condensation phenomenon (Nardecchia (2018). If a macromolecule is modelled as an open system, that is, if it is subjected to an external energy supply and is in contact with a thermal bath to dissipate the excess energy, the internal nonlinear couplings among the normal modes make the system undergo a nonequilibrium phase transition in particular if the energy input rate exceeds a threshold value. This transition takes place between a state in which the energy is incoherently distributed among the normal modes as opposed to a state where the input energy is channelled into the lowest-frequency mode entailing a coherent oscillation of the entire molecule. The studies on solvated BSA (Bovine Serum Albumine) in the THz and sub-THz frequency range have shown broad resonances due to an efficient coupling of low-frequency modes of the protein with the surrounding EMF field. It was concluded that if biomolecules are positioned in an open system, that is, far from thermal equilibrium with its environment, energy can flow under the simultaneous actions of an external energy supply and a process of dissipation, the latter being due to radiative, dielectric, and/or viscous energy losses (Nardecchia, 2018). The relevance of the coupling of a BSA protein with the surrounding of a watery solution was confirmed in a non-thermal way by optical pumping. This experimental set-up revealed that such a protein, vibrating in its collective mode, has to be dressed by ordered layers of water molecules in order to attain an effective dipole moment. That is, sufficiently large to overcome the strong absorption of bulk water (Lechelon, 2017). It has also been found that long-range interactions involving electromagnetic fields of frequencies 0.1–1THz can be temporarily activated despite radiation losses and solvent dissipation. The theoretical background used to derive the mentioned interactions shed more light on Fröhlich's theory of selective long-range forces between biomolecules.

3) **Pokorný** (2019): Fröhlich-type of nonlinear interaction of coherent electric polar vibrations in cells play a role in structures of tunnelling nanotubes, that form a communication system between cells, and a unified coherent cavity system which enables simultaneity and mutual cooperation in multicellular organisms (Pokorný, 2019).

4) **Kadantsev** et al. (2018) studied the collective excitations in alpha-helical protein structures interacting with environment. Low-frequency vibrational excitations of protein- macromolecules in the terahertz frequency region are suggested to contribute to many biological processes such as enzymatic activity, molecular electron/energy transport, protein folding, and others. Two possible mechanisms of the formation of long-live vibrational modes in protein were earlier proposed by H. Fröhlich and A.S. Davydov in a form of vibrational modes and solitary waves, respectively, to explain high effectiveness of energy storage and transport in proteins. A quantum dynamic model of vibrational mode excitation in alpha-helical protein interacting with environment was therefore developed. In this model we distinguish three coupled subsystems, i.e. (i) hydrogen bond peptide groups (PGs), interacting with (ii) the subsystem of side residuals which in turn interacts with (iii) environment (surrounding water) that is responsible for dissipation and fluctuation processes. It was shown that the equation of motion for phonon variables of the PG chain can be transformed to nonlinear Schrödinger equation for order parameter. The latter admits bifurcation into the solution corresponding to weak damped vibrational modes (Fröhlich-type regime). A bifurcation parameter was shown to determine interaction of protein with environment and in part also energy pumping to the protein due to its interaction. In the bifurcation region, a solution corresponding to the Davydov soliton concept was shown to exist. The suggested mechanism of emergence of the macroscopic dissipative structures is a form of collective vibrational modes in alpha-helical proteins. This is discussed in connection with the recent experimental data on the long-live collective protein excitations in the terahertz frequency region.

5) **Zhedong Zhang** et al. (2019) described the Fröhlich condensation of polar vibrations into the lowest frequency mode when the system is pumped externally. The authors stated that for a full understanding of the Fröhlich condensate one needs to go beyond the mean field level to describe critical behaviour as well as quantum fluctuations. The energy redistribution among vibrational modes, included nonlinearity, and was shown to be essential for forming. The condensate and the related phonon-number distribution, revealed the transition from quasi-thermal to super-Poissonian statistics with regard to the pump. The spectroscopic properties of the Fröhlich condensate especially were revealed by the narrow linewidth. This factor provides the long-lived coherence and the collective motion of the condensate. Proteins such as Bovine Serum Albumin (BSA) and lysozyme are most likely suitable candidates for observing such collective modes in THz regime by means of Raman or infrared (IR) spectroscopy.

6) **Geesink and Meijer** found further support for the Fröhlich condensation not only for the long-range electromagnetic waves but also for shorter waves in a meta-analysis of endogenous and exogenous electromagnetic waves for living cells and biomolecules. Particular unique wave frequency patterns have been found in two meta-analysis of about 750 published articles of biological electromagnetic experiments, in which spectra of biomolecules and exposures to non-thermal electromagnetic waves have been analysed (Geesink and Meijer, 2017a; Meijer and Geesink, 2018f; Geesink, 2020c). It turns out that biological systems show a clear spectral frequency coherence. A similar meta-analysis of Einstein-Podolsky-Rosen (EPR) experiments learned that entanglement, achieved in the experiments is real, and that applied EMF-frequencies are again located at discrete coherent configurations. Strikingly, all analysed EPR-data of the independent studies fit precisely in the inferred GM-scale of coherent frequency bands and turned out to be virtually congruent with the above mentioned semi-harmonic frequency-scale for living organisms (Geesink and Meijer, 2018b). Fröhlich's superconductivity, involving macroscopic quantum coherence, could also be substantiated by a meta-analysis of about 93 independent experiments on the behaviour of superconducting materials (Geesink and Meijer, 2019a). It can be concluded that frequency patterns of biomolecules, frequencies in Einstein-Podolsky-Rosen (EPR) experiments, and frequencies of superconductors obey to a proposed algorithm of frequencies, that describe Bose-Einstein statistics.

Summarized: The earlier proposed theory and underlying experiments, collectively called Fröhlich condensation has now been substantiated by a spectrum of biological and physical experiments. On the basis of these results, a quantum wave equation of coherence was inferred, that expresses the patterned frequency distribution of quantum coherence/decoherence by an acoustic physical resource: $E_n = \hbar\, \omega_{ref}\, 2^{n+p}\, 3^m$ (Geesink and Meijer, 2018a, Sonderkamp, 2019). This quantum wave equation can be applied both to living systems and non-living systems such as superconductors.

Proposed informational law

We submit that an informational law or principle is at work in complex living systems and also in highly coherent inanimate materials, a phenomenon that apparently can be based upon an adapted Pythagorean tuning, in which discrete frequencies of coherent and decoherent oscillations are described by two related equations (Geesink, 2018a, b) and appendix 1. The discrete standing coherent wave pattern of EM wave frequencies has been mathematically expressed in a quantum wave equation as follows,

$$E_n = \hbar\, \omega_{ref}\, 2^n\, 3^m\, (2^p)$$

(En: Energy distribution, ω_{ref}: reference frequency 1 Hz, $\hbar$: Reduced Planck's constant, n: Series of integers: 0, 0.5, 2, 4, 5, 7, 8, -1, -3, -4, -6, -7; m: series of integers: 0, 1, 2, 3, 4, 5, -1, -2, -3, -4, -5; p: series of integers: <-4, -4, -3, -2, -1, 0, 1, 2, 3, 4, 5, 6, > +52)

The detected eigenfrequencies are arithmetically scaled according to a semi-harmonic scale and exhibit a core pattern of twelve eigenfrequency functions with adjacent self-similar patterns, according to octave hierarchy (Geesink, 2018a; 2019a). The typical distribution pattern of EM frequencies also shows entangled conditions in Einstein–Podolsky–Rosen experiments, in which the GM frequencies (eigenstates) selectively promote quantum entanglement of particles/waves. Wave eigenstates, also called pointer states, are less perturbed by decoherence than coherent states, and the particular environment allows them to exist almost as classical states (Zurek, 2017).

Orderings principles of living cells and biomolecules

Biomolecules, beyond being coupled among themselves via the dipolar interaction, are also driven by a common external energy supply. A collective mode emerges by decreasing the average distance among the molecules as testified by the emergence of a clear peak in the power spectrum of the total dipole moment. This is due to a coherent vibration of the most part of the molecules at a frequency definitely larger than their own frequencies corresponding to a partial cluster synchronization of the biomolecule (Olmi, 2018). Proteins are polymers made up of amino acids and have specific cellular functions, such as mediating cell structure, intracellular movements, signal transduction, membrane transport and receptor expression, information storage and communication, as well as being instrumental in the mediation of chemical reactions. There are twenty different amino acids and specific proteins can be made up of hundreds to even thousands of specific amino acids linked together in a particular order. The order of amino acids in a protein is encoded in the genes in our DNA. It has been experimentally found that the DNA segments related to protein coding regions have a tendency to display a strong spectral vibrational component at the frequency of $2\pi/3$ called period-3 property (Inbamalarand, 2015).

The primary amino acid chain is folded into the final 3-dimensional protein, often providing a specific shape that is essential in carrying out its particular function. Folded proteins show a high degree of structural order and undergo (fairly constrained) collective motions related to their functions. If the coding process for the protein is incorrect, the resulting order of amino acids will be perturbed. In such a case the protein may not have the correct shape and thereby may have no optimal function and/or can even cause cellular disorder. On the other hand, intrinsically disordered proteins, although lacking a well-defined three-dimensional structure, still may exhibit some structural and dynamical ordering, but are less constrained in their motions than folded proteins. Particularly, in the context of cancer progression, many oncogenes, tumour-suppressor genes, and regulators of metastatic spread have been identified as due to intrinsically disordered proteins. Protein folding is considered geometrically, as a part of a broader context of different topologies. In this process solitons (electrons dressed by phonons) in the cells are able to constitute stable local electromagnetic fields that both can be involved in intracellular morphogenetic ordering, as well as intercellular communication (Melkikh, 2018; Geesink and Meijer, 2018d; Salford, 2017). This influences of electromagnetic fields (EMFs) on bio-energetic folding processes have, among others, been investigated through analytical and numerical simulation and experimentation. Bio-energy transport along protein molecules as performed by soliton movement causes dipole–dipole electric interactions between neighbouring amino acid residues. As such, electromagnetic fields can directly affect the structure of protein molecules and modulate the bio-energy transported in living systems (Pang, 2016).

Biomolecules, including their precursor molecules, are always embedded in well-defined discrete electromagnetic fields displaying discrete frequency patterns (conformational states with spectral coherence). Accordingly, these are based upon the values of the manifest eigenstates and conditions such as quantum entanglement can be described by the unique quantum wave equation mentioned above. The coherent and decoherent (chaos-like) frequencies can be aligned at a frequency scale and are arranged according to an alternating ordering, while transition frequencies are located just in between the coherent and decoherent frequencies (Geesink and Meijer, 2018a), see figure 3 and 4. This special arrangement of

energies can be conveniently described as integral trajectories displayed in torus-geometry as have been shown by also in acoustic (musical) theories.

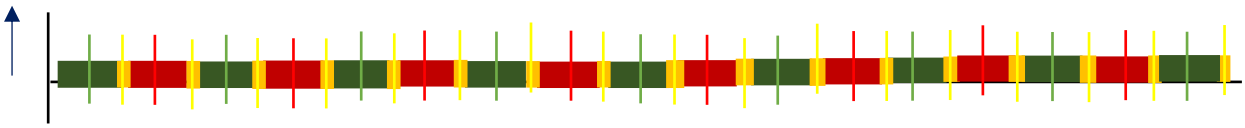

Coherent, decoherent and transient monotone frequencies and bandwidth's (Hz) ⟶

Figure 3. Alternating ordering of *frequency patterns. X-axis: Coherent frequencies and bandwidth (green); decoherent frequencies and bandwidth (red); transition frequencies and bandwidth (yellow). Coherent, decoherent and transient monotones (Hz) (green, red and yellow stripes). Y-axis: intensities.*

A recent analysis of 52 different infrared spectra of normal biomolecules/cells and about 25 precursor molecules of biomolecules, that contain 760 different frequencies at NIR, MIR and FIR, learned that the particular frequency patterns exhibit discrete frequencies, that are, to a large extent, precisely positioned at the abovementioned pointer states of the proposed of quantum coherence equation (Geesink, 2019b). This study demonstrated that frequency patterns of biomolecules in normal cells are precisely positioned at the *coherent* pointer state frequencies of the proposed quantum equation. In contrast, biomolecules present in diseased cells are positioned at typical *decoherent* frequency patterns. On the basis of these results an integral life model can be inferred that makes use of four types of attractors: a static fixed-point frequency; a periodic repetition of sequences of twelve basic intervals; a periodic torus geometry, and a chaos attractor related to decoherence. This set of four attractors have been used to describe the different states of living biomolecules in relation to cell viability (Naarala et al. 2019).

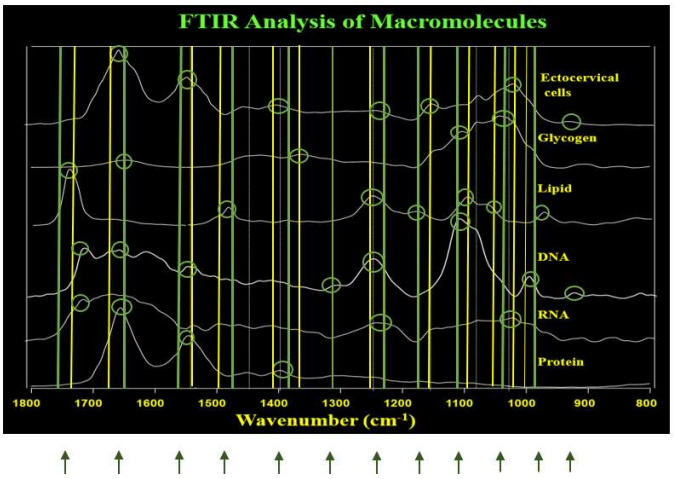

Figure 4*. IR-spectra of biomolecules, depicted: 12 coherent pointer states; green lines of coherence and yellow lines of transition frequencies; H. Geesink and reference picture B.R. Wood.*

In this model transitional vibrations, positioned just in between zones of coherent and decoherent states, are considered as zones of rearrangements of biomolecules, that can collectively be interpreted as rearrangements of ordering. It is estimated that transitions in the cell take place at the borders of order and "controlled disorder". Among others, this complex but integral dynamic system plays a role in the folding and de-folding of proteins, as well as in the twisting arrangements of DNA and during opening and closing of ion channels (Meijer and Geesink, 2017c) and see figure 5.

It has been further observed that life systems, externally exposed to non-thermal electromagnetic fields, can through resonance induce a high extent of coherency in the cell with frequency patterns that are fully in line with the abovementioned pointer states of the proposed quantum equation. The transitions of healthy to unhealthy conformations of the exposed biomolecules in cells can be understood by assuming a combined change of intensities of the wave spectra and detrimental shifts of frequencies. The typical changes involved can be attributed to transition of coherent states to states that are less coherent or even exhibit clearly decoherent modes. In such cases the imposed frequencies induce less order or even complete disorder (Geesink and Meijer, 2018a). Yet, such decomposition of biomolecular order can also be interpreted as programmed cell death.

In fact, the cornerstone of our work is an extensive meta- analysis of about 750 articles from 1950 to 2017, dealing with endogenously measured and exogenously applied electromagnetic field frequencies in tissues, cells and biomolecules. This analysis unequivocally showed band patterns of beneficial (stabilizing) or detrimental (destabilizing) EMF frequencies of the experimentally chosen electromagnetic fields in the sub Hertz till Peta Hertz region as exposed to or within in a large variety of vitro and in vivo life systems. Of note even the pattern of destabilizing and unhealthy biological effects fit with a quantum behaviour that is adequately described by a second quantum equation (see appendix 1). The stabilising electromagnetic field effects (Geesink and Meijer, 2017a; 2018a; 2018b), were observed in a widespread disease window and related therapeutic measures, and see figure 5:

- therapeutic neuro-stimulation,
- therapeutic brain stimulation,
- therapeutic spinal cord stimulation,
- transcranial magnetic stimulation,
- treatment of Parkinson disease,
- anti-proliferative effects on tumour cells,
- inhibition and repression of tumour growth,
- promoting rhythmic neuronal synchronization,
- improvement of memory function
- improvement of conscious attention,
- acceleration of wound healing,
- decrease of inflammatory cells,
- increase in bone growth,
- reduction of diabetic peripheral neuropathy,
- increase of fibroblast proliferation,
- stimulation of angiogenesis,
- improved self-assembly of micro-tubulins,
- granulation in tissue formation and synthesis of collagen,
- promotion of proliferation of human mesenchymal stem cells,
- promoting entorhinal-hippocampal interactions,
- regeneration of cells and others

In contrast, destabilizing experiments of EMF exposure were found in the areas of:

- tumour growth,
- influence on teratogenic potential,
- DNA single-strand breaks,
- gene expression, chromosomal instability,
- inhibition of cell growth,
- influences on sperm viability parameters,
- influence on sleeping,
- influence on the permeability of the blood-brain barrier,
- influence on social behaviour,

- cognitive impairment,
- learning and memory alterations,
- maculopathy,
- influence on specific brain rhythms,
- alter of protein conformation,
- effects on blood pressure,
- cardiovascular responses,
- phototoxic effects on human eye health and on the retina,
- influence on alkaline phosphatase activity
- antigen-antibody interaction,
- ADHD,
- cardiovascular effects as well as in
- several other conditions (Geesink and Meijer, 2017a, 2018a).

Beneficial (green) and detrimental (red) biological frequency data, and transition zones (yellow)

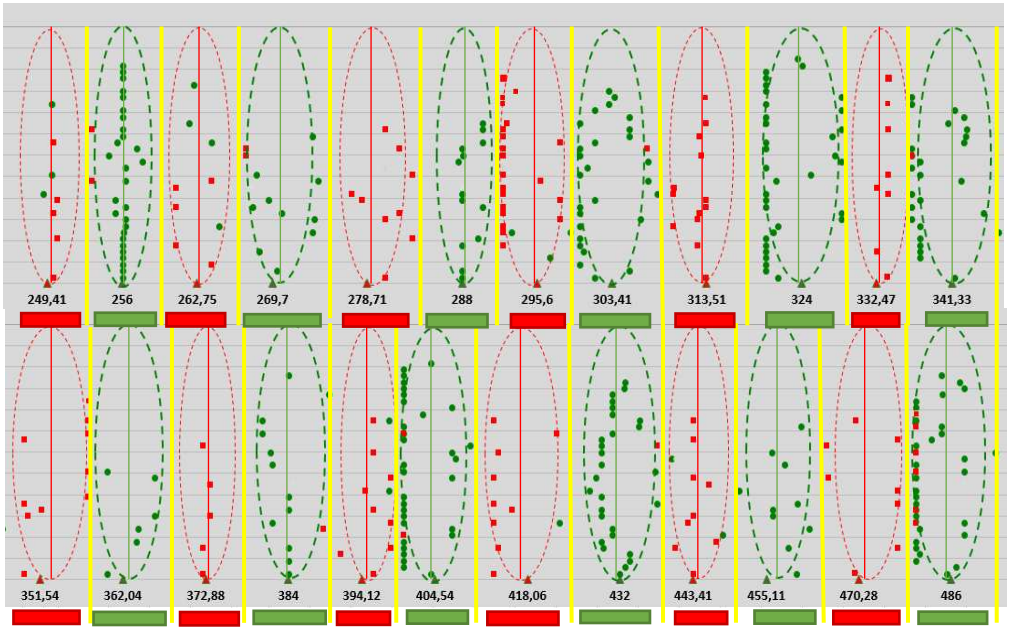

Figure 5. *Measured frequency data of living cells systems that are health-sustaining (coherent data and zones: green), or detrimental for health (decoherent data: red, and transition zones: yellow) versus calculated normalized frequencies. Biological effects measured following exposures or endogenous effects of living cells in vitro and in vivo at frequencies in the bands of Hz, kHz, MHz, GHz, THz, PHz. Green triangles plotted on a logarithmic x-axis represent calculated normalized (Hz) health-sustaining frequencies; red triangles represent calculated health-destabilizing frequencies. Each point indicated in the graph is taken from published biological data and are a typical frequency for a biological experiment(s). For clarity, points are randomly distributed along the Y-axis; Yellow lines are proposed transition frequencies (Geesink, 2018).*

Also, carcinogenesis fits in a frequency pattern during an exposure to electromagnetic waves, in which a gradual loss of cellular organization occurs. Cancer can also be initiated and promoted at distinct decoherent frequencies of electromagnetic waves (Meijer and Geesink, 2016). These observations were revealed by analysing 100 different EMF frequency data reported in a meta-analysis of 123 different, earlier published, biomedical studies. The studied EMF frequencies showed a fractal pattern of 12 basically beneficial (anti-cancer) frequencies, and 12 basically detrimental (cancer promoting) frequencies. This study provided the central pattern of a much wider self-similar EMF spectrum of cancer inhibiting or promoting activities.

Importantly, Inhibition of the cancer process, and even curing of the disease by exposure to the coherent type of electromagnetic fields. can now be chosen in much more detail and predicted efficiency. The apparent stabilization of the disease can be understood by constructive resonance of macromolecules in the cancer cell, through coherent EMF field frequencies, likely in the form of solitons/polarons. For instance, as have been shown earlier, this procedure can also induce repair in DNA/RNA conformation and/or epigenetic changes.

Conformational changes in components of living cells by non-thermal electromagnetic fields

The biological components of living cells, including the solutes dissolved in water, all have their typical resonances and spectra, that respond to electromagnetic fields. The most common are dipole relaxation, ionic, atomic and electron polarization, and such features in the whole cell are ordered according to their resonant frequencies. Endogenous electromagnetic fields are self-generated by internal vibrations of living cells and their constituents play an important role in biological self-organization. On the other hand, external electromagnetic fields at sub-thermal intensities are able to influence the intrinsic endogenous electromagnetic fields, and can have an impact on conformational states and self-organisation of biomolecules (Y. Feng, 1990; Belyaev,1996; Blank, 2008; Lechelon, 2017, Geesink, 2020c).

An external RF field can modulate and rotate charged and polar molecular structures as well as other cellular components of biological materials. The magnitude of these motions depends on the strength and frequency of the field and may be impeded by inertia and viscous forces. The orientation of polar molecules under the influence of external fields usually does not occur instantaneously, but rather follows a time-dependent behaviour known as the relaxation process. After the application of an external field, it also takes some time for electric charges within the cells and tissue structures to accumulate at their interfaces and reach a new equilibrium state (relaxation). Depending on the size/characteristics of polar molecules, different types of relaxation processes can take place in biological tissues. Small charged particles, such as monopolar ions, are able to respond at frequencies up to at least 10^{12} Hz, and the association of ions with water molecules (solvation) means that the dielectric properties of water, with its large dipole moment, are dominant in biological solutions (Sheppard, Swicord and Balzano, 2008). Proteins also contain charged groups, which are located at sites specific to the atomic arrangements of the molecule. Similarly, to isolated ions, these charged groups are associated with water molecules, therefore dielectric properties of biological tissues (at RF) strongly depend on and vary with water content.

Protein molecules show conformational vibrations, that consist of the formation of folds, twisting and compression of protein polypeptide chains. Biological processes exhibit a number of interactions between proteins and their targets (other proteins, DNA regulatory segments or small molecules). Each of these processes imply an energy transfer between the interacting molecules. These interactions are highly selective, and this selectivity is defined by the protein structure. Taking into account frequency resonant effects, taking place in living cells, it becomes possible for such low-intensity EM radiation to become manifest if the energy goes through the resonant path. The cell membrane is supposed to be an important site of interaction for electromagnetic fields. There are many free ions that, in principle, can move bidirectionally across cell membrane, such as K^+, Na^+, Cl^- and Ca^{++}, but attain different concentration gradients. These ions not only control the cell volume, but may also help in essential signalling processes, as well as creating a strong electric field between both sides of the cell membrane. The cell membrane contains ion channel proteins, the opening of which can be regulated by the transmembrane voltage, and mechanical stress in the case of gated channels by ion pressure or chemical signals. The basic mechanism proposed for this dynamic is the forced vibration of all the free ions on the outer surface of a cell membrane, caused by an oscillating electric field. It has been shown that these vibrations of electric charge are able to irregularly affect voltage-gated channels in the plasma membrane by external electromagnetic fields, and thereby can disrupt

the cell's electrochemical balance and function (Lindstrom, 1993). Given the existence of these resonant effects, interactions between external weak electromagnetic fields and living systems were considered in detail (Cosic, 1997).

In addition, extended exposure to broad-spectrum terahertz radiation results in changes in cellular functions that are closely related to DNA-directed gene transcription. The hydrogen bonds in dsDNA vibrate at a THz frequency, and THz radiation has the potential to change important cellular genomic DNA and thus DNA-protein functions. Although the THz photons do not carry enough energy to directly alter chemical reactions, nonlinear resonance effect may cause local changes of the conformational dynamics in systems such as DNA, leading to changes in gene transcription. Such extended exposure to a broad-spectrum of THz radiation (centred at ~10 THz) has indeed been shown to result in specific changes in the functionality of cellular DNA. Of note, certain genes in irradiated mouse stem cell cultures are activated, while other genes are repressed, when exposed to an average power density of 1 mW/cm2, broadband THz radiation, at a high repetition rate (Bock, 2010).

Studies on exposure of proteins to hydrodynamic forces show that very weak forces are able to unfold proteins in flow. The effect of a low strength oscillating electric field at electric field strengths at intensities of 1.6 mW/cm2 till 23.9 mW/cm2 has a distinct influence on the conformation of Bovine Serum Albumin (BSA) and Lysozyme. The applied field strengths are extremely small compared to the protein inter-chain intra-molecular forces. Prolonged electric field exposure results in energy dissipation in the proteins and finally in protein unfolding, which is a critical initial step for protein aggregation and also potentially amyloid fibril formation (Bekard, 2014). A model has been proposed, in which the electrophoretic motion of the proteins leads to a frictional force that results in protein unfolding (Bekard, 2011, 2012, 2014).

Millimetre waves (MMW) are able to rearrange the electron subsystem of DNA (Belyaev, 1992, 1996). It takes place in a magnetic field (Zeeman Effect) or in an electrical field (Stark Effect) and circular polarization may thereby occur. A possibility is that MMW with sub-thermal intensity induce rearrangement at various levels in the electron subsystem of DNA. Some results are explained in the context of electron-conformational interactions. Electron tunnelling can induce electron-conformational transitions which likely involves rearrangement of the ionic framework in a segment of DNA-protein complex. For example, the effect of non-thermal millimetre waves on the genome conformational state of E. coli cells was shown by the method of anomalous viscosity time dependencies in the frequency range of GHz. The results obtained could be explained in the framework of a model of electron-conformational interactions according to multi-quantum processes, that can influence various biological aspects (Betskii and Lebedeva, 2004). The energy estimate suggests that MMW/THz radiation affects life processes in multi-quantum processes, which is a characteristic of coherent oscillations. It was found that different microorganisms exposed to MM-wave (millimetre waves) radiation exhibited a frequency-dependent biological effect and this effect of MM-waves on living beings was called informational (Betskii, 2004).

Microwave absorption seen as a transfer of energy from the microwave field to the very vibrational modes of the macromolecules has earlier been studied (Devi-Prasad and Prohofsky, 1984). Prohofsky (2004) suggested that protein conformation might be affected by RF radiation if amplitudes of specific vibrational modes are thereby altered. A non-thermal effect can occur if a very strong energy coupling between the inter-molecular and intra-molecular modes is present. For instance, the vibrational modes of DNA double helices have been estimated and can be directly measured at various IR frequencies. These calculations indicated the existence of a number of bands within the microwave region of the spectrum. Low-lying vibrational modes are of importance in predicting conformational states, or shape, as well as other changes in the particular macromolecules. Such conformational changes can alter biological function and, in this sense, the low-lying vibrational modes can, in principle, have major effects on cellular function. Indeed, frequency of modes of structural importance are low enough to be affected by electromagnetic radiation. Photonic/phononic pumping on these modes can thus cause instabilities, which can affect the overall cell function (Devi-Prasad, 1984).

Exposures in the extremely low-frequency range have shown that weak fields can also cause charge movement of protein and DNA by electromagnetic fields (Blank, 2008). Redistribution of charges in large molecules, on their turn, can trigger conformational changes that are often driven by large hydration energies. Conformational changes that arise from alterations in charge distribution, for example, may play a key role in membrane transport proteins, including ion channels, and probably can be coding for stimulation of DNA to initiate protein synthesis. Thus, it appears likely that weak EMF can control and amplify biological processes through their effects on charge distribution (Blank, 2008).

A nonlinear model of DNA dynamics on the coupling between conformational dynamics and proton tunnelling has been proposed (Bugay, 2012). Terahertz radiation can influence both vibrational excitations and proton motion in DNA hydrogen bonds. The particular irradiation at the edge of far IR spectral range can promote proton tunnelling. If the radiation frequency matches the vibrational mode, enabling the generation of localized excitations in form of dissipative solitons. It was shown that the theoretical results can qualitatively explain the results of experimental observations of terahertz influence on the number of spontaneous and induced point mutations. In fact, the low-amplitude DNA collective breathing modes can serve as precursors for generation of the transcription bubbles and other large-scale conformational changes. This may be related to experimentally observations of changes in DNA conformation and gene transcription in the presence of terahertz field (Bugay, 2012).

Exposures of artificial human skin tissue to intense, picosecond-duration THz pulses, affects expression levels of numerous genes has been associated with non-melanoma skin cancers, psoriasis and atopic dermatitis (Titova, 2013). Genes that seem to be affected by intense THz pulses include nearly half of the epidermal differentiation complex (EDC) members. Theoretical both modelling as well as derived experiments have shown that many important cellular biomolecules, including DNA and proteins, have intrinsic vibrational resonances in the THz range. Resonant coupling of THz radiation to those vibrational modes may therefore affect conformation states and dynamics of various cellular biomolecules, and thus exhibit potential impact on cellular functions. Based on mesoscopic modelling of DNA breathing dynamics in a THz field, it has been proposed that THz radiation may amplify existing (or create new) open states in the double helix, thereby affecting transcription initiation or binding of transcription factors (Titova, 2013).

Effects of continuous microwaves of different field intensity have also been shown on protein conformation in muscle fractions from frog skeletal muscles (Vukova, 2005). Acetylcholinesterase activity in samples from muscle homogenate fractions, exposed for 30 min to microwaves of low (10 mW/cm2) and high (20 mW/cm2) intensity at almost constant temperature, resulted in non-thermal, intensity-dependent modification of acetylcholinesterase activity in frog skeletal muscles. Infrared spectroscopy data argue for induced conformational changes in the secondary structure of muscle proteins: increased content of beta-structures, random coils, and amorphous structures, were shown at low field intensity (Vukova, 2005). MHz-exposure on human astrocytoma cell line showed typical alterations in cell proliferation, being observed at 8.1 mW/cm2, whereas alteration in cell morphology was noticed at field power density of 40 mW/cm2 (French, 1997). THz-exposures on lyophlized DNA at 20 mW/cm^2 were employed to examine conformational changes in DNA. The data showed that THz radiation causes changes in the optical density of the nucleotides at UV wavelengths. These effects were observed to be dose-dependent and the spectral changes were most pronounced at a number of discrete wavelengths. These results provided clear evidence for a THz radiation caused conformational changes of DNA (Fedorov, 2003).

An analysis of data on biological effects of low intensity RFR lead to a conclusion that this physical agent is also an oxidative stressor for living cell. The oxidative efficiency of RFR can be mediated via changes in activities of key ROS-generating systems, including mitochondria and non-phagocytic NADH oxidases, either via direct effects on water molecules, or via induction of conformation changes in biologically important macromolecules. In turn, a broad biological potential of ROS and other free radicals, including both their mutagenic effects and their signalling regulatory potential, makes RFR a potentially hazardous factor for

human health (Yakymenko, 2015). Reviews revealed that 90% of all studies analysing ROS generation after MW exposure, have reported ROS induction in different cell types. It became clear that the increased level of ROS is often associated with oxidative DNA damage (Durdik, 2019)

It should therefore be emphasized that biomolecules are in a continue process of building, rearrangement, homeostasis, rebuilding and apoptosis. It has now been confirmed that building and homeostasis is related to coherence as a physical quantitative resource, a property that can be described by a unique quantum wave equation. Decay and apoptosis of biomolecules is very likely related to decoherence, seen as as a loss of quantum coherence. Coherence/decoherence transitions of biomolecules occur in a zone just in between these conditions, in which the particular rearrangements take place. Biomolecules exhibit many conformational states: processes of formation, final structuring as well as the related arrangements of parts.

Summarized: All conformational states of biomolecules reflect typical geometric patterns of electromagnetic waves, that can be described by the quantum wave equation proposed by us and can be pictured as being situated at nested torii. (Geesink, 2020c). Many biophysical research experiments have shown that non-thermal external electromagnetic waves are able to influence conformational states of crucial component of living cells, thereby perturbing normal function in this way being decisive for healthy or unhealthy conditions.

Overview of research on the influences of electromagnetic waves on living cells

Research about electromagnetic pulses on living cells has been systematically undertaken the past eighty years. As much as around 35.000 biological/physical reports are available, of which a part is dealing with non-thermal biological effects on cells. Influences of electromagnetic waves causing thermal effects on biological systems are relatively well understood, and more detailed knowledge about non-thermal effects of electromagnetic waves were urgently required. Additional physical principles have now been discovered to describe the effects of non-thermal electromagnetic waves on living and we can nowadays refer to a spectrum of potential mechanisms: ion-cyclotron resonances, parametric resonance, interactions between electromagnetic fields and electrons, resonant frequencies and polarisation, resonant recognition, radical concentrations, and stability of quantum coherence. The earlier mentioned analysis of more than 700 bio-medical articles from 1950 to 2020, dealing with effects of external electromagnetic waves on in vitro and in vivo life systems has put many of these effects in perspective, (Geesink and Meijer, 2017a).

This comprehensive review addressed non-thermal electromagnetic fields (EMF) that are able to cause either beneficial or detrimental responses of living cells (Geesink and Meijer, 2017a, Meijer and Geesink, 2018 e, f). This pattern has been observed in the wide frequency ranges of extremely low frequencies (1 - 300 Hz) and microwave frequencies (300 MHz to 300 GHz). There is strong evidence therefore from many studies that biological effects of EMF depend on a large variety of physiological and physical parameters. The particular EMF frequency energies can affect overall cell viability, for instance influencing neural and osteogenic differentiation, gene expressions, epigenetic mechanisms, as well as chromatin modifications. Of note, stem cells are probably much more sensitive to EMF exposure than differentiated human primary cells, lymphocytes, and fibroblasts, whereas fibroblasts seem to be the least sensitive.

The International Commission on Non-Ionizing Radiation Protection (ICNIRP) included the radiofrequency electromagnetic field (RF-EMF) of mobile phones on the category 2B as ‘possibly’ carcinogenic to humans. Epidemiological studies noticed a causal association between the exposure to RF-EMF and the incidence of brain neoplasm in different populations, since this is the organ with the highest EMF specific absorption rate. The fact that so many of the ipsilateral tumours found are statistically significant with RF-EMF exposure provided the weight suggesting this causality. In this way, the higher the exposure (ipsilateral vs contralateral), the longer the cumulative exposure (hours of exposure) and the longer the latency (beyond 10 years); the greater the risk has been proposed (Pareja-Peña and Ruiz-Gómez, 2020).

Non-thermal EMF's biological effects depend on various physical wave or field parameters:

- exposure intensity,
- overall duration of exposure
- intermittent or permanent exposure,
- wave frequency,
- modes of polarization,
- wave modulations such as pulsed modes,
- wave amplitudes and phases,
- intermittent or continues exposure,
- near field/far field features
- static or dynamic magnetic fields

Of note, even small changes in carrier wave frequency can result in disappearance of non-thermal microwave (MW) effects, because of the selectivity of resonance like responses. Relatively small changes in carrier frequency, has reproducibly resulted in cell-type-dependent generation of effects upon non-thermal EMF exposure, for instance with respect to DNA repair foci in human cells. Non coherent modulations of MW waves have often been shown to play a crucial role (Geesink and Meijer, 2018a). It has been usually observed that MMW effects are frequency-dependent and that the time of exposure is especially an important modulating parameter, whereas the applied power has a weaker effect (Devyatkov, 1974, 1991, 1994). Also, recent experiments have shown that RF-EMF exposure can cause DNA-damage and significantly affect RE-DNA transcription and that such effects strongly depend on the cellular context and the tissue type of cells (Smith-Roe, 2019; Del Re, 2019). Millimetre waves can have a major health impact, according to the review of Simko, who analysed 94 publications performing in vivo or in vitro investigations. It could be concluded that 80% percent of the in vivo studies showed biological responses to exposure, while 58% of the in vitro studies demonstrated biological effects (Simko, 2019).

A study of radiofrequency radiation (RF) on living organisms in vitro studies, using data from 300 peer-reviewed scientific publications (1990–2015) in total describing 1127 experimental observations, learned that (RF) induces significant changes in human cells (45.3% of the studies), and in faster-growing rat/mouse cell dataset (47.3%). In parallel with this finding, analysis of faster-growing cells from other species (chicken, rabbit, pig, frog, snail) indicates that most undergo significant changes (74.4%) when exposed to RF. The study confirmed observations from the REFLEX project, Belyaev and others that cellular response may largely vary with the signal properties chosen. It has also been concurred that differentiation of cell type constitutes a critical piece of information (Halgamuge, 2020). Thus, biological effects have been reproducibly reported in rodents exposed to radiofrequency fields (RF), that is without significant changes in the body temperature. These observations clearly invalidate the controversial proposition of a general lack of consistent non-thermal effects of RF. In further substantiating such effects, one should consider to systematically registrate RF energy absorption/interaction in tissues, not as volume-averaged manner, but defined locally down to the microscale. This is of potential importance especially at frequencies beyond 3 GHz (Vanderstraeten, 2020). Of note, using a longitudinal birth cohort study design, an association has been found between maternal exposure to MF nonionizing radiation during pregnancy and risk of ADHD in offspring throughout childhood up to age of 20 years (De-Kun Li, 2020).

In conclusion: the impact of electromagnetic waves on health has been clearly established by many studies in recent decades as reviewed by among others Simkó, 2019, Halgamuge, 2020, and Deruelle, 2020.

Overview of Physical Principles in EMF Effects

Principles of atomic and molecular interactions

The shortest-range interactions that occur between molecules are excluded volumes forces, also known as steric repulsions. Such repulsions are electromagnetic interactions due to the inability of the molecular electron clouds to overlap, leading to repulsive forces. The excluded volume can be described as the volume that is inaccessible to the other molecules in the system and their physical origin is laid down in the Pauli's exclusion principle (Pauling, 1974). On a slightly larger scale, Van der Waals forces are at stake, that induce interactions between all atoms and molecules, charged or neutral, with an action range in the order of Angstrom's. Van der Waals forces' is a general term used to define the attraction of intermolecular forces between molecules. There are two kinds of Van der Waals forces: weak London Dispersion Forces and stronger dipole-dipole forces. The van der Waals force has the same origin as the well-known Casimir effect, arising from quantum interactions with the zero-point field. Electrostatic interactions basically describe the attractive or repulsive interaction between objects having electric charges. Brownian motion is the random motion of particles resulting from their collision with the fast-moving molecules in for example a fluid. Within such a fluid, there exists no preferential direction of flow as in transport phenomena.

The same forces and motions can in principle be found in living systems, but in addition properties such as of self-regulation or self-organisation may play a role. Self-regulation and organisation have been described in the dynamical model of Herbert Fröhlich, in which a part of the energy supply is not completely thermalized, but is used to create order in response to environmental perturbation. Fröhlich published in 1968 his first article related to biology, named "Long-Range Coherence and Energy Storage in Biological Systems" and stated that biological systems are expected to have a branch of longitudinal electric vibration modes in a frequency region between 10^{11} and 10^{12} sec-1. These would be due to electric dipole components present at the cell membrane, certain chemical bonds, and particularly hydrogen bonds and regions containing non-localized electrons (Fröhlich, 1968).

Physical models describing biological influences on cells by non-thermal electromagnetic waves

Differently acting physical principles have been discovered and reviewed the past fifty years to describe the effects of non-thermal electromagnetic waves on living cells: a) ion cyclotron resonances, b) parametric resonances, c) interactions of electromagnetic fields and electrons, d) resonant frequencies and polarizations, e) resonant recognition, f) radical concentrations, g) quantum coherence and entanglement as well as h) local resonance synchronization. The following models have become well known:

1) **Fröhlich** (1968) proposed the so-called Quantum coherence model and Davydov (1973) the Soliton model; Both models describe the effects of coherent states of waves and the involvement of various modes of electromagnetic waves: electrons, phonons, polarons, polaritons and magnons with regard to wave stability. Polarons pseudo-particles of electrions, dressed with phonons and are similar to solitons, and the name soliton will be further used.

2) **Davydov** (1997) discovered the principle of longitudinal wave forms called solitons (Davydov, 1977). In the same time Fröhlich proposed a Hamiltanion model for polarons, through which their dynamics can be treated quantum mechanically as acoustic phonons located in a Bose–Einstein condensate (BEC). A soliton is defined as a self-reinforcing solitary wave that travels at constant speed without changing shape. Davidov proposed that the solitons play a role in the energy transfer and conformational states of biomolecules. This model, describes, among others, the interaction of the amide vibrations of peptide groups with the hydrogen bonds that stabilize the α-helix of proteins. The supposed excitation and deformation processes balance each other and thereby form a soliton. His theory showed how a soliton could travel along the hydrogen bonded spines of the alfa helix protein molecular chains (Davydov, 1977). The author stated that solitons are able to suppress anharmonicity (the deviation of a system from being a harmonic oscillator) by the excitation of high quantum levels, a process that facilitates the crossing of potential barriers and the transfer of a molecule to a new conformational state. His concept of the excitations of atoms and solitons, as the quanta of collective vibrational motions of atoms and molecules in living cells, is also known from solid-state theory. Also, so-

called excitons, known from quantum biology, interact with the lattice vibrations, under the action of electromagnetic fields and show a bound state. A bound state in quantum physics describes a system where a particle, or wave is subject to a potential such that the particle has a tendency to remain localized in one or more space regions. The energy spectrum of the set of bound states is discrete, unlike the continuous spectrum of free particles. They show typical eigen-frequencies, at which a system tends to oscillate on its own, nearly in the absence of any driving or damping force. Davydov also introduced a mathematical model to show how solitons could travel along the three spines of hydrogen-bonded chains of proteins. Davydov's Hamiltonian is formally similar to the Fröhlich-Holstein Hamiltonian for the interaction of electrons with a polarizable lattice.

3) **Liboff** (1985) and **Blackman** (1984) described the role of ion cyclotron resonances (ICR's) that involve a combined action of an Extreme Low Frequency (ELF) electromagnetic field and a static geomagnetic field on the resonance of typical ions (Blackman, 1984; Liboff, 1985). The model of Lednev (1991) proposes the ion parametric resonance hypothesis, which predicts that when frequencies of a combined dc-ac magnetic field parametrically equals the cyclotron frequency of an ion, for example calcium, the affinity of the calcium for calcium-binding proteins such as calmodulin will be affected. It is considered that ions bonded to proteins (Ca^{++}, K^{+}, and/or Mg^{++}) behave as isotropic coupled oscillators (Lednev, 1991, 1993). The Warburg observation concerning ATP generation in cancer cells has been analysed with regard to the likely involvement of H+ resonance effects on the angular velocity of the ATP synthase rotor. It is reasonable to expect that the variety of diseases associated with mitochondrial dysfunction may in part be related to the ATP synthase rate of rotation. Experimental measurements of ATP synthase rotational rate are consistent with what might be expected from the ion cyclotron resonance (ICR) frequencies of protons moving under a Lorentz force determined by the approximate surface intensity of the geomagnetic field (~26-65 μT) (Liboff, 2020).

4) **Blank** (1970) pictured the interactions between electromagnetic fields and electrons, as particles with the highest charge/mass ratio, that play a role in relation to the DNA-molecule, gene activation, Na/K-ATPase, and cytochrome oxidase (Blank and Findl, 1970).

5) **Cosic** (1997) introduced the concept of dynamic electromagnetic field interactions implying that molecules recognize their particular targets and vice versa by the principle of electromagnetic resonance: she designed the "Resonant Recognition Model "(RRM). In this concept, all molecules have their own spectrum of vibrational frequencies and DNA itself can function as an aggregate of EM antennae that could discern, differentiate, and transform EM energies to perturbations in protein sequences (Blackman, 1984). Periodicities within the distribution of energies of delocalized electrons along a protein molecule are crucial to the protein's biological function, i.e. interaction with its target. The RRM makes use of the equation of the Electron Ion Interaction Potential (EIIP), which is coupled to a theoretical modulated weak potential experienced by electrons in the vicinity of ions and the cloud of surrounding electrons. The RRM calculates indirectly the spectral characteristics of proteins at frequencies of infrared, visible light and ultraviolet (Cosic, 1997; Cosic, 2015, 2016; Pirogova and Cosic, 2001; Veljkovic, 1972, 1985).

6) **Pakhomov** (1998) looked at the biological effects of MMW (millimetre-waves). He examined dozens of studies and cited research demonstrating profound effects of MMW on all biological systems including cells, bacteria, yeast, animals and humans. Some effects were clearly thermal, however, many of the studies showed non-thermal biological effects at low intensities. Both negative and positive responses were seen depending on frequency, power, resonance and exposure time. Researchers found at times even small difference in frequencies could have very different biological effects.

7) **Butikov** (2004) showed that non-linear parametric resonance is possible at fixed resonance frequencies, but also inside the zones of instability at frequencies lying on either side of their resonance values. Parametric excitation occurs within ranges of rotary oscillations of a torsion spring pendulum excited by periodic variations (Butikov, 2004). Hinrikus showed that the modulated microwave radiation causes periodic alteration of neurophysiologic parameters and parametric excitation of brain bioelectric oscillations

(Hinrikus, 2016). The experiments with a single frequency-modulated microwave radiation demonstrated that this effect on EEG depended on modulation frequency (Hinrikus, 2008). The theory of parametric excitation was demonstrated being appropriate for interpretation of the modulated microwave effect on EEG (Hinrikus, 2011).

8) **Sheppard, Swicord and Balzano** (2008) considered the possibility that demodulation of high-frequency incident RF signals might arise from nonlinear interactions with biochemically induced transient oscillators in living tissues e.g. the uncoupled electrons of free radicals. If this were to occur, then the spectrum of RF emission energy emitted from the exposed tissue would be altered. Weak RF fields that do not cause heating, would be likely to require frequency-dependent resonant absorption or multiple-photon absorption to induce an amplified signal strong enough to overcome intrinsic molecular thermal noise. This is because the photon energy of RF radiation is much smaller than molecular thermal energy at body temperature. Biological systems may appear to absorb RF signals like a broadband receiver rather than eliciting line spectra characteristic of resonant vibrational motion (Prohofsky, 2004; Sheppard, Swicord & Balzano, 2008).

9) **Hinrikus et al.** (2014) Microwave radiation may affect hydrogen bonding between dipolar water molecules and through that diffusion in water at constant temperature. The experimental study was performed on the setup of two identical reservoirs filled with pure water and 0.9% NaCl solution and connected by a thin tube. The applied 450 MHz continuous-wave microwave field had the maximal specific absorption rate of 0.4 W/kg on the connecting tube. The standard deviation of water temperature in the setup was 0.02 ^{0}C during the experiment. The experimental data demonstrated that microwave exposure makes faster the process of diffusion in water. The time required for reduction of initial resistance of the solution by 10% was 1.7 times shorter with microwave (Hinrikus (2014).

10) **Belyaev** (2010) proposed that the millimetre waves (MMW) with sub-thermal intensity induce rearrangement of levels in the electron subsystem of DNA and will take place in a magnetic field (Zeeman Effect) or in an electrical field (Stark Effect) and circular polarization occurs. A possibility is that MMW left-handed polarization was shown to be more effective than right-handed polarization at certain resonance frequencies and electron tunnelling could induce electron-conformational transitions which should involve rearrangement of the ionic framework in a segment of DNA-protein complex. The strongest microwave effects were observed in stem cells. Experimental data indicated that non-thermal biological MMW effects occur depending on several physical parameters: carrier frequency, modulation, amplitude, polarization, intermittence and static field (Belyaev, 2010; Belyaev, 2015).

11) **Pall** (2013) proposed that the direct target of the EMFs is what is called the voltage sensor, a part of the VGCC (voltage-gated calcium channels) structure that produces its activation to a partial depolarization of the plasma membrane. The voltage-gated calcium channel (VGCC) protein molecule contains a four-domain structure with each domain carrying an alpha helix, each designated an S4 helix, containing 5 positive charges. Those four charged alpha helixes act together as what is called the voltage sensor, the structure that responds to electrical changes across the plasma membrane to open the channel. It has been shown that not only 4 distinct types of VGCCs, but also a voltage gated sodium channel, potassium channel and chloride channel are all activated by low intensity EMFs of various frequencies, suggesting that the EMFs act on the voltage sensor. In plants, EMFs apparently act via activation of some other channels, known as TPC channels, which also contain a similar voltage sensor. The structure and location of the voltage sensor and the Coulomb's law and Ohm's law, predict that the EMF forces on the voltage sensor are strong, approximately 7.2 million times stronger than the forces on singly electrically charged groups in the aqueous parts of our cells and bodies. The voltage-gated sodium, potassium and chloride channels apparently play only minor roles in producing EMF effects, so that to a first approximation, effects can be explained as being predominantly from VGCC activation and consequent increases in intracellular calcium [Ca2+]i. This explains why the voltage sensor is the main direct target of the EMFs. Large numbers of non-thermal pathophysiological EMF effects can be explained through the action of VGCC activation as produced by two

different pathways of action: the calcium signalling pathway and the peroxynitrite/free radical/oxidative stress/inflammation pathway (Pall, 2013).

12) **Barnes and Greenebaum** (2014), and Buchachenko (2015) pictured that radical concentrations of biomolecules can be influenced by combinations of steady and alternating magnetic fields that modify the population distribution of the nuclear and electronic spin states at a relatively low magnetic field strength in the range of 1microTesla till 100 micro Tesla (Barnes and Greenebaum, 2014; Buchachenko, 2015). Free radical concentrations have the potential to lead to biological significant changes. Usselman et al. found that oscillating magnetic fields at Zeeman resonance alter relative yields of cellular superoxide ($O2^{\bullet-}$) and hydrogen peroxide ($H2O2$) ROS products, indicating coherent singlet-triplet mixing at the point of reactive oxygen species (ROS) formation. The results reveal quantum effects in live cell cultures that bridge atomic and cellular levels by connecting ROS partitioning to cellular bioenergetics. The radical pair mechanism hypothesis for ROS-related quantum biology has been tested by exposing human umbilical vein endothelial cells (HUVECs) to either 50 µT static magnetic fields and combined with MHz-waves (Usselman, 2016).

13) **Lundholm et al.** (2015) presented a model, that supports the model of Fröhlich condensation in the arrangement of proteins, by detecting Bose-Einstein condensate-like structures in biological matter at room temperature. The group used a combined terahertz measuring technique with a highly sensitive X-ray crystallographic method to visualize low frequency vibrational modes in the protein structure of lysozyme. The vibrations were sustained for micro- to milli-seconds, which is 3–6 orders of magnitude longer than expected if the structural changes would be due to a redistribution of vibrations upon terahertz absorption according to a Boltzmann's distribution. The influence of this non-thermal signal is able to changes locally the electron density in a long alfa-helix motif, which is consistent with an observed subtle longitudinal compression of the helix (Lundholm, 2015).

14) **Romanenko et al.** (2017) presented a model about the resonance interactions between electromagnetic fields and cells, tissues and organisms. Electromagnetic fields have been shown to affect the activity in cell membranes (sodium versus potassium ion conductivities), non-selective channels, transmembrane potentials and even the cell cycle. MMWs are known to alter active transport across cell membranes, and it has been reported that terahertz radiation may interfere with DNA and cause genomic instabilities. Application of an external electromagnetic field to biological objects induces a redistribution of internal charges with respect to the field lines. This time-consuming process is characterized by 'relaxation' time and different types of relaxation. The most common are dipole relaxation and ionic, atomic and electron polarization, that are ordered according to their resonant frequencies. The dominance of any one of these types of relaxation in a whole system depends on the frequency of the external stimulus. Those findings are consistent with the original Fröhlich theoretical conclusions about the role and importance of MMW and terahertz electromagnetic oscillations in biology (Romanenko, 2017).

15) **Nardecchia et. al.** (2018) presented a model about out-of-equilibrium collective oscillation as phonon condensation in a model protein, that generally supported the model of Fröhlich. The activation of out-of-equilibrium collective oscillations of a macromolecule was described as a classical phonon condensation phenomenon. If a macromolecule is modelled as an open system—that is, it is subjected to an external energy supply and is in contact with a thermal bath to dissipate the excess energy—the internal nonlinear couplings among the normal modes make the system undergo a nonequilibrium phase transition when the energy input rate exceeds a threshold value. This transition takes place between a state where the energy is incoherently distributed among the normal modes and a state where the input energy is channelled into the lowest-frequency mode entailing a coherent oscillation of the entire molecule. The experimental outcomes are in good qualitative agreement with the theory developed and in quantitative agreement with the theoretical result, allowing to identify the observed spectral feature with a collective oscillation of the entire molecule (Nardecchia, 2018).

16) **Naarala et al.** (2019) are studying cellular oscillations as a measure of the state of biological systems. A central concept of dynamical (i.e., time-dependent) systems is that of state space. The state itself can be defined as a complete description of a physical system i.e., everything that can be possibly known about it. The state space of a dynamical system is then the set of all possible states of the system. Each coordinate of the state space is a state variable, and the values of all state variables completely describe the state of the system. Consequently, each point in the state space corresponds to a different state of the system. The trajectories (time developments) in the state space advance toward limit sets are called attractors. In principle four types of attractors can exist: 1) fixed point: static attractor; 2) limit cycle: periodic attractor; 3) torus: quasiperiodic attractor; 4) chaos: strange attractor. Genomic instability has been discussed in the framework of the dynamical systems theory, and describe the hypothesis that environmentally induced genomic instability corresponds to abnormal attractor states; large enough environmental perturbations can force the biological system to leave normal evolutionarily optimized attractors (corresponding to normal cell phenotypes) and migrate to less stable variant attractors (Naarala et al. 2019).

17) **Simkó and Mattsson** (2019a, 2019b) present a hypothesis regarding the biological aspect of interaction between low frequency magnetic fields (LF MF) from 1 to 100 kHz and cells. The endoplasmic reticulum (ER) membrane protein STIM1, which functions as a sensor for several cellular conditions (low Ca2+ levels, temperature increase, increased levels of oxygen radicals, hypoxia), is a candidate LF MF sensor. Such a sensor function can be either direct (via local temperature increase caused by intracellularly induced electric fields), or indirect due to responses to increased reactive oxygen species (ROS) levels. Activated STIM1 leads to downstream effects by activation of signal transduction processes and changes in gene expression leading to secondary events. The nature of these changes would be dependent on both cell type and the particular physiological state the cell displays at the time of STIM1 activation. Therefore, it is assumed that oxidative processes triggered by MF play a key role for the effectiveness of electromagnetic fields. Studies confirmed this finding, as shown in LF MF exposure in vitro, that causes changes in oxidative status as an early response, and the strongest association between MF exposure and effects occurred at 0.1 or 1 mT. Also, static magnetic fields (SMF) have been shown to influence a number of cellular activities, including formation of ROS and transmembrane Ca2+-transport. Such interactions are suggested to be dependent on that biomolecules contain magnetic dipole moments (Zhang, 2016). Whether or not this is a prerequisite also for LF MF interactions with cells in the context here is unknown. Furthermore, at present it is not known if, STIM1 does contain epitopes that suggest the presence of magnetic dipole moments (Simkó Mattsson and Simkó, 2014).

18) **Meijer and Melkikh** (2018) proposed an approach, based on the embedding of proteins in the whole cellular context: in this concept the protein molecule is influenced by various long and short distance force fields of nature such as coherent electromagnetic waves and zero-point energy. In particular, the role of solitons is reviewed in relation to a novel GM-scale biophysical principle, revealed by the authors. This finding of a set of discrete EM frequency bands, that either promote or endanger life conditions, could explain directed the morphogenetic aspects of protein folding in a biological evolutionary context. In addition, an alternative hypothesis is presented in which each individual cell may store integral 3-D information holographically at the virtual border of a 4-D hypersphere that surrounds each living cell, providing a field receptive memory structure that is instrumental in guiding the folding process towards coherently oscillating protein networks that are crucial for cell survival. (Meijer and Melkikh, 2017, Meijer and Geesink, 2018).

19) **Geesink and Meijer** (2020) propose a model, that is in line with the models and concepts of Fröhlich, Davydov, Chukova and Naarala. The proposed model has a direct relation with Bose-Einstein behaviour and describes quantum coherence (Geesink and Meijer, 2016a, 2016b, 2017b, 2018a). The model, has been validated by three extensive meta-analyses of published measurements of: 1) discrete frequency spectra of biomolecules and its precursors, 2) discrete frequency windows for beneficial and detrimental biological effects related to endogenous and exogenous frequency patterns of non-thermal electromagnetic waves, 3) frequency patterns of superconductors. Evidence of a quantum wave equation of coherence has been found, that can be addressed to quantum coherence as a physical resource: $E_n = \hbar\ \omega_{ref}\ 2^{n+p}\ 3^m$. The particular frequency pattern could be revealed by a meta-analysis of 720 biomedical publications that reported life-

sustaining as well as life-decaying EMF frequencies. The model fits with a good precision the frequency windows of the different biological experiments, and has been validated by a statistical analysis. Decoherent frequencies are described by a second quantum wave equation (Geesink and Meijer, 2018a, 2018b).

Conformational states of superconducting systems

A relation between conformational coherent states of high-temperature superconductors and the ordering of living matter has earlier been proposed by Vasconcellos (Vasconcellos, 2012), and Poccia (Poccia, 2011a, 2011b), as well as in the theory of Fröhlich (Fröhlich, 1968). The central item here is that a particular wave-information or conformational state, is able to affect living cells at frequencies in the surrounding of a thermal bath, in which a large number of quanta condense into a single state. The latter has been defined as a Bose-Einstein condensate, and is supposed to induce physical and non-thermal interactions between bio-molecules. The waves can take dimensions that are many orders of magnitude larger than that of the microscopic objects, due to the fact that the resulting overall wave field is highly correlated, and therefore has an analogy with the behaviour of high temperature superconductors (Jerman, 2016). It has been found that typical coherent frequencies in superconductors resemble that of the living cells/biomolecules and can be described by the proposed same quantum coherence equation, that is related to entanglement (Geesink and Meijer 2019a, 2020b). Spectral energy gaps of superconducting materials could well be positioned at the pointer states of a pattern of coherent frequencies, and can be described by the proposed GM-scale quantum wave equation. This idea is supported by the finding that HTSC's show patterns of frequencies, in which frequency ratios of 2:3 (third harmonic) are incorporated in ratios of 1:2 (fundamental frequency). The observations highlight a potential quantum bridge between superconducting properties in physics and biology.

While conventional superconductors are explained by the Bardeen-Cooper-Schrieffer (BCS) theory (Bardeen, 1957), high temperature superconductivity is still in search of a theoretical explanation. In the BCS theory, each electron pairs with an electron of opposite spin to form a new entity, a Cooper pair, that can move without electronic resistance through the material. The pairing is made possible by interactions between the electrons and the metal atoms vibrating in place in the crystal lattice. But there is also a relation between the Bardeen-Cooper-Schrieffer (BCS) wave function applied for superconductors and the quantum state for Bose Einstein condensates (BECs). The similarity between the systems BEC and BCS can be understood by considering the presence of exciton-polaritons, and polarons. The exciton-polariton, formed in microcavities as a bosonic system, represent hybrid particles/waves made up of photons strongly coupled to electric dipoles, and their presence demonstrates quantum coherent phenomena (Kavokin, 2010).

A manifestation of electron-hole pairing as a nonlinear electromagnetic response of layered superconductors show that the pairing causes the appearance of a number of peaks in the frequency dependence of the intensity of the third-harmonic generation (Tranquada, 2018; Rajasekaran, 2018; Germash, 2017; Cea, 2018; Gioacchino, 2010). If the HTSC's show the proposed frequency patterns, then the geometry of these patterns can be described by a torus geometry (Geesink and Meijer, 2016c) and see figure 6.

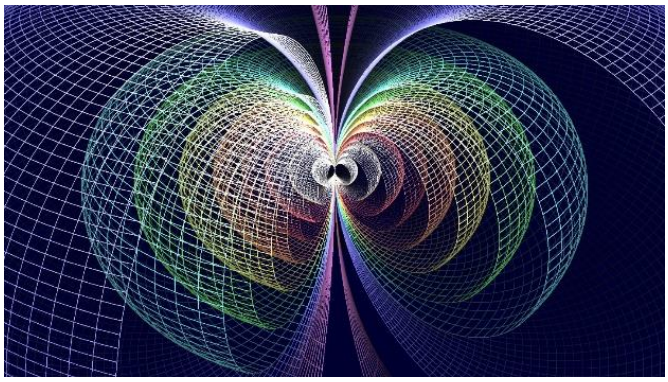

Figure 6. *Nested torii, Reference Wolfgang W. Daeumler*

The coherent states of this semi-harmonic oscillator can be conceived to be positioned at the surfaces of nested torii, which are maximally localized in a phase space (Fremling, 2013). The classification of closed lines on the torus corresponds to discrete sets of energy levels, mirroring the analogous quantization of energy levels of an atom (Jantzen, 2010). In mathematics, a dynamical system is a system in which a function describes the time dependence of a point in a geometrical space and state space is the set of all possible states of a dynamical system; each state of the system corresponds to a unique point in the state space. Cellular oscillations are a measure of the state of the biological system and a concept of dynamical systems is that of state space, in which a torus plays a role as periodic attractor (Naarala, 2019).

For the soliton and phonon guided principle, a torus model has been elaborated, making use of the basic principles of the Neo-Riemannian Tonnetz, which is extended with sequences of twelve basic intervals described by the proposed quantum wave equation (Meijer and Geesink, 2016c). In the Tonnetz (German: tone-network) systematic the parameter pitch refers not only to the perceived frequency of sound, but in addition describes the distance between repeated elements in a musical structure possessing translational symmetry. Pitch/space relationships typically use distance parameters to model the degree of relatedness of closely related pitches, placed near one another, and less closely related pitches placed farther apart of which all intervals of this network can be described by a 3D toroidal space (Amiot, 2013), see also figure 7. The dynamics of a quantum system with fluctuations may also induces a decoherence phenomenon on the reduced density matrix of the fermionic string which is characteristic of the chaotic behaviour since it presents a horizon of coherence. These dynamics are associated with an invariant torus which involves extra-dimensions emerging from the fluctuations for the viewpoint of the fermionic string, extending a three-dimensional space by six compact dimensions. The situation studied can be considered as a model of qubit (supported by the fermionic string) in interaction with a quantum black hole (Viennot, 2018).

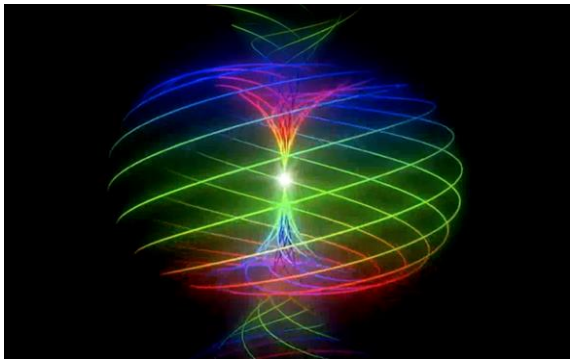

Figure 7. *Torus and standing rotary waves, Reference: John Hagstrand*

It is estimated that the composed static coherent waves of the torus geometry can be disturbed by decoherent or chaotic called information. Differences between quantum coherent counterparts and chaotic systems have been examined and models show the emergence of quantum effects to destruct chaos or the onset of quantum-chaotic behaviour (Rozenbaum, 2017). It has been proposed that the quantification of chaos in a quantum setting can calculated and all decoherent positions can be described by a proposed quantum chaotic equation (Geesink and Meijer, 2018a, 2018e), see also the onset of chaos in figure 8.

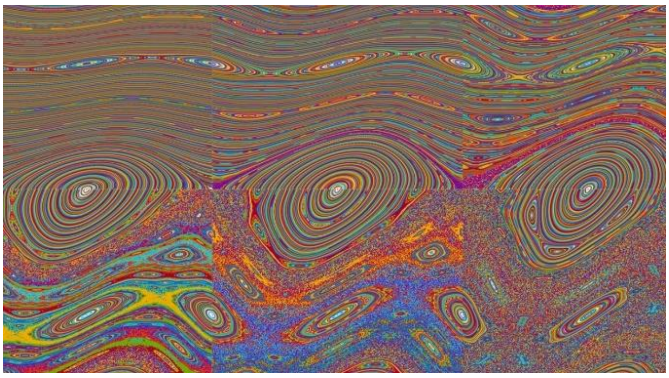

Figure 8*. Onset of quantum-chaotic behaviour (Reference E. Rozenbaum and E. Edwards, 2017).*

Coherence and Decoherence

Coherence is an ideal property of waves that enables stationary (i.e. temporally and spatially constant) interference. Coherence was originally conceived in connection with Thomas Young's double-slit experiment in optics but is now used in any field that involves waves, such as acoustics, electrical engineering, and quantum mechanics. Coherence has been defined as the physical congruence of wave properties within wave packets, and it is a property of stationary waves (i.e. temporally and spatially constant) that enables a type of wave interference, known as constructive. The particular processes are called coherent when the variability of the phase differences between the signals is relatively small, whereas the wave processes are defined as incoherent, the phase difference has a high degree of variability.

Quantum coherence can be expressed in discrete frequency patterns, and is one of the underlying factors that contributes to life, health and diseases (Geesink and Meijer, 2017a). Quantum decoherence is the loss of quantum coherence, and decoherence can be viewed as the loss of information from a system into the environment (often modelled as a heat bath), since every system is loosely coupled with the energetic state of its surroundings (Bacon, 2001). It was Schrödinger who recognized that coherent interaction of waves is coupled to entanglement as “the characteristic aspect of quantum mechanics” and suggested that “eigenstates” are able to survive interaction with the environment. In quantum mechanics, all objects have wave-like properties (see de Broglie waves).

Our meta-analyses of a more than 700 publications showed a distinct frequency band pattern not only with *coherent* (beneficial) frequency values, but also with alternately localized *decoherent* (detrimental) frequency bands precisely positioned between the coherent bands (Figure 12).

How to explain such a typical combined alternating character? We considered two possibilities: 1) this could imply a type of symmetry that is established in many phenomena in nature. It is as if both coherent and decoherent modalities reflect a sort of balanced guiding principle. In cells this could be expressed for instance in various regulatory processes such as programmed cell survival versus cell death. A second possibility is

that the alternating bands represent an EMF wave interference process, well known from classical quantum physics. For instance, in Young's double-slit experiment *single electrons* can be used instead of bundles of photons acting as light waves. Each single electron's wave has been shown to go through both slits due to its broad wave front, and hence provides two separate split-beams that contribute to the patterned wave interference pattern on the projection screen (see figure below), giving rise to an alternate pattern of bright bands, due to constructive wave interference, interlaced with dark bands due to destructive interference, as shown on the downstream screen, see figure 9 and 10. This ability to interfere and diffract is related to coherence of the waves produced at both slits,(French, 2003). When the incident beam is represented by a quantum pure state, they will be represented as superpositions of the pure states (Feynman, 1963). The typical coherent-like frequencies are combinations of coherent tones and coherent overtones. They show a resemblance with the entanglement monotones, that are used to quantify quantum coherence (Baumgratz, 2014). Strikingly, a comparable pattern of waves was found by us when the eigenstates of biomolecules and living cells were positioned on an acoustic frequency scale (Geesink, 2020c).

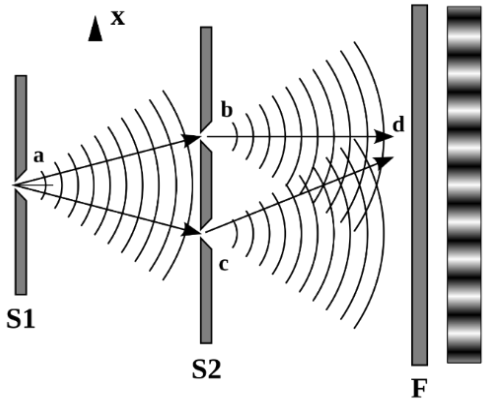

Figure 9. *Young's two slit experiment. Coherent light source: Diffraction spreading of light around barriers; bright and dark bands called "interference fringes", caused by constructive and destructive interference. When the incident beam is represented by a quantum pure state, the split beams downstream of the two slits are represented as a superposition of the pure states representing each split beam (Feynman, 1963).*

Quantum resource theories have been formulated related to entanglement and superposition and make use of quantum coherence (Baumgratz, 2014; Dana, 2017, Streltsov, 2017). A perfect coherent state exhibits a density matrix that can be described by a wave function (resembling the quantum coherence equation proposed by us.

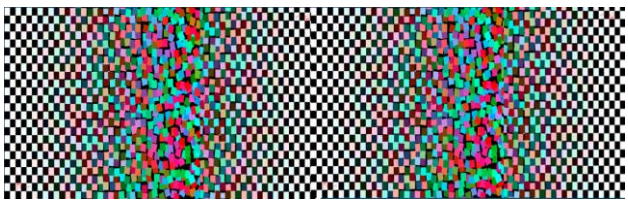

Figure 10. *Typical spatial arrangements of order and disorder according to the proposed quantum model (art impression H. Geesink, 2020).*

For example, a theory of quantum coherence as a physical quantitative resource has earlier been proposed in our work on, based on four different meta-analyses of:
1) EMF-frequency spectra of Einstein-Podolsky-Rosen experiments used in physics studies on entanglement,
2) EMF-frequency spectra of biomolecules and their precursors,

3) the abovementioned EMF-frequency windows for beneficial and detrimental biological effects after exposure of life systems to either endogenous or exogenous EMF (non-thermal) electromagnetic waves, and 4) frequency patterns of energy gaps in superconductors.

All of the related frequency patterns can be described by ratios of 1:2, or 2:3. Therefore consistent evidence for of a quantum wave equation of coherence could be inferred, exhibiting quantum coherence as a physical resource: $E_n = \hbar\, \omega_{ref}\, 2^{n+p}\, 3^m$ (Geesink and Meijer, 2018, 2019) and see appendix 1.

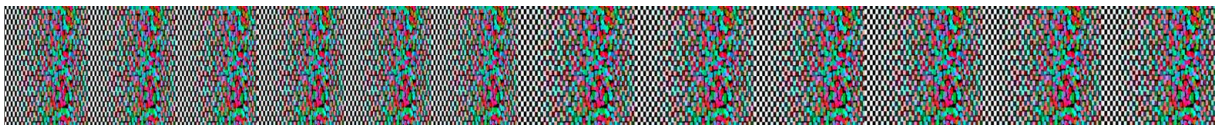

Figure 11. Alternating ordering of *patterns of 12 basic frequency zones. Coherent frequencies and bandwidth (ordered blocks); decoherent frequencies and bandwidth (disordered blocks), and transition zones in between ordered and disordered zones (art impression H. Geesink, 2020).*

Evidently, the information of the proposed quantum coherence equation of EMF-frequencies follows typical eigenstate functions, that are differentiated by discrete coherent, decoherent and also apparent transient frequencies. Thus, typical spatial arrangements of order and disorder were revealed, that can be attributed to twelve basic frequency bands, see figure 11 and 12. The discrete coherent and decoherent frequencies are arranged according to an alternating ordering, while transition frequencies are located just in between the coherent and decoherent frequency-zones with a typical band-width, suggesting an analogy of the Young's experiment treated above (Geesink, 2020c)or alternatively representing a balanced symmetry phenomenon in nature as mentioned above.

Generalized scale of non-coherent frequencies

The non-coherent-scale can be calculated based upon the finding that *decoherent parameters are located logarithmically just in between the coherent parameters and can be calculated as follows* (m=0 till 54):

$Dm(decoh.1) = 10^{(0.5\log F1 + 0.5\log F2)}$ $Dm(decoh.2) = 10^{(0.5\log F2 + 0.5\log F3)}$

$Dm(decoh.3) = 10^{(0.5\log F3 + 0.5\log F4)}$ $Dm(decoh.4) = 10^{(0.5\log F4 + 0.5\log F5)}$

$Dm(decoh.5) = 10^{(0.5\log F5 + 0.5\log F6)}$ $Dm(decoh.6) = 10^{(0.5\log F6 + 0.5\log F7)}$

$Dm(decoh.7) = 10^{(0.5\log F7 + 0.5\log F8)}$ $Dm(decoh.8) = 10^{(0.5\log F8 + 0.5\log F9)}$

$Dm(decoh.9) = 10^{(0.5\log F9 + 0.5\log F10)}$ $Dm(decoh.10) = 10^{(0.5\log F10 + 0.5\log F11)}$

$Dm(decoh.11) = 10^{(0.5\log F11 + 0.5\log F12)}$ $Dm(decoh.12) = 10^{(0.5\log F12 + 0.5\log F13)}$

m = 0 till 54.

The currently applied single or composed (modulated) frequencies in communication technology, fit for 94.2% with the proposed quantum model, related to either healthy or unhealthy behaviour, offering the potential to optimize calibration of chosen EMF bands. For example, up to 80% of the planned 5G frequencies belong to the detrimental decoherent or modulated coherent frequency bands. Further research to counteract non-thermal unhealthy electromagnetic effects can generate ideas for improving the balance between coherent and decoherent waves, and thereby may open a potential novel road to innovative health technologies.

The role of neurons, ATP and water molecules

Neurons are able to sense Ghz and THz resonances and responses of cortical slices of the adrenal gland are at terahertz frequencies and power densities of 0.3-1.0 microWatt/cm2 (Pikov, and Siegel, 2010). Studies, conducted on neurons, revealed that MMW radiation can cause suppression of neuronal activity. Ganglia subjected to MMW's (1 - 4 mW/cm2) revealed a dose-dependent decrease in neurons' spiking rate along with hyperpolarization of the membrane baseline potential and narrowing of the action potential width (Romanenko, 2014; 2016). Also, variations and neurochemical inhibition in amino acid neurotransmitters in brain areas of adult and young male albino rats, due to electromagnetic radiation exposure, have been found at power densities of 0.02 mW/cm2 (Noor, 2011). It has been shown in experiments that the mechanical, ionic, electrical and electromagnetic resonance in neural firing are connected together (Agrawal et al., 2016). accordance with our concept, the group of Bandyopadhyay (Agrawal e al., 2018, Sahu er al., 2013, 2015**,**) found evidence for firing *below the synaptic threshold* in EMF guided information processing in the brain. The particular oscillatory activities are supposed to be generated not only in microtubule, but also in many other protein complexes in the cell, that is, in a fractal setting that is expressed in circular and periodic modes in 12 fractal memory layers. This on the basis of 3-D resonance chains that also contain un-occupied elements that can be filled up by electromagnetic oscillator activity to produce proper information processing in the required integrated time cycles (resembling our concepts for superconductors). In the brain they identified 350 different classes of cavities in the nested (fractal) 12 layers and described each *cavity resonator as an octave musical flute* that together with silence periods collectively generates the known brain rhythms. Thus their fundamental basis is fractally organized, representing a geometric information that finally become expressed in the EEG. Bandyopadhyay et al., identified 12 discrete resonance frequencies, among others with a solitonic (quasi-wave-particle) frequencies, very much resembling the mathematics of our GM-scale EMF pattern.

Thermal imaging of a living cell by triggering 1 kHz to 1 GHz ac signal suggests that the components of a living cell are interconnected over the entire electromagnetic frequency range (Legrand et al., 2015).The effects of EHF-EMF (53.37 GHz–39 mW) on the propagation of the electric impulse have been investigated and the exposure potentiates the action of valinomycin – a K+ carrier – increasing the extent of K+ transport across the lipid membrane and facilitates the electrical signal propagation by increasing transmembrane potassium efflux (D'Agostino, 2018). Adenosine Triphosphate (ATP) is referred to as a molecular unit of currency of intracellular energy transfer. It is used for transport work, mechanical work and chemical work in the cells. It is notably used as substrate for kinases: enzymes that catalyses the transfer of phosphate groups from the high-energy, phosphate-donating molecules to transfer phosphate groups onto proteins through a process called phosphorylation. When a phosphate group is removed from ATP, the reaction is exothermic and an important amount of energy is released (up to 30.5 kJ.mol-1). ATPases are capable of absorbing energy from oscillating electric fields of defined frequency and amplitude and using it to perform chemical work. An example is the 0.42 eV energy, released under hydrolysis of ATP molecule, as studied by Davydov (1973) and Pang (2001) (Davydov, 1973, 1977; Pang and Chen, 2001, 2016). A hypothesis is that the energy is transferred along the alfa-helical protein molecules, while the oscillation energy of the C = O moieties of the peptide groups (amide-I vibration) is at 0.21 eV or 1665 cm−1, which is in resonance with the 0.42 eV of the ATP process. Interestingly, the energy released under hydrolysis of ATP molecule, the oscillation energy of the C = O of the peptide groups and the different bending modes of interfacial water molecules fit precisely with the calculated coherent frequencies of the proposed quantum wave-function, respectively: 0.415 eV, 0.2073 eV and 1660–1693 cm−1.

All surface-promoted reactions require molecular species to interact with the particular surface and these interactions are likely mediated by water molecules, protons, or hydroxyl groups, through relatively weak physical interactions. The importance of water to living organisms originates from its peculiar features including quantum entanglement of structured water domains. In addition, water owes these unique properties to the polarity (dipole character) of its constituent molecules and in particular to the ability to

form hydrogen bonds internally and with other molecules. The particular spectral frequency patterns of water are located in many frequency bands at FIR, MIR, NIR, VIS and UV including overtones and combination absorption bands. Water molecules are building blocks for the proposed coherent spectrum, in which several transitions play a role: 1) harmonic transitions from the ground state, 2) an-harmonic transitions, 3) combination transitions between ground states and excited states, and can be described by informational functions (Geesink, 2020a).

Experimental data demonstrated that microwave exposure accelerates the process of diffusion in water (Hinrikus (2014). The effect of the weak EMF on the solutions of Glutamic acids is mediated by the organisation of water molecules: the exposure to the field seems to modify the structure of water in terms of the relative abundance of the coherent and non-coherent fraction (De Ninno, 2011). The amount of water molecules forced out the coherent phase increases the quantity of molecules at the boundary of the coherence domains, that has been called intermediate population. Such a region is the most reactive place in liquid water because of the abundance of quasi-free electrons and of the existence of the evanescent tail of the electrodynamic field which acts as a source acting on the ions in proportion to the inverse of their masses, thereby inducing the formation of a zwitterion form of water (Voiekov and, Del Giudice, 2009).

Divalent cations such as Mg^{++} and Ca^{++}, in particular, enhance and maintain the long-range dipole wave fields in water solutions. The reorientation of water molecules around ions and interaction with solvated ions slows down during external THz-waves, shifting the absorption peak to typical frequencies (Tielrooij, 2009). The presence of different types of ions causes the stabilization of localized water clusters over their state in the bulk of the solution as they are able to influence the hydrogen bonding exchanges of the affected water molecules (Musumeci, 2012). It may be considered that if molecules in pure water have a comparable configuration with water molecules in living cells, than a reversible coherent interaction between living matter and water molecules may occur. Inorganic ions may stabilize the coherent domains while macromolecules together with the activated water can therefore produce macro-coherent collective oscillation fields. The band's intensity depends on the extent of the harmonic and anharmonic coupling between those motions and on their own oscillator strengths (De Ninno, 2018).

For example, the existence of a DNA minor groove's "spine of hydration" being surrounded by ions at room temperature, showed that the chiral structure of biomolecules can be imprinted on the surrounding solvation structure. The observation reported a robustness of the DNA's chiral spine of hydration, and the fact that a change in the hydration state can lead to dramatic changes to the DNA structure, also indicates that such a water superstructure actually constitutes a detailed mould or "electromagnetic image" (Dermott, 2017). Coherent EM field frequencies are hypothesized to promote the formation of strong quantum coherences, increasing the strength and fidelity of intra-and inter-cellular signalling. Decoherent EM field frequencies are hypothesized to promote a chaotic way of non-coherent waves that show a high level of phase differences. The potential long-range resonant influence was further worked out in a study of 3-dimensional protein folding in the intact cell that can be largely influenced by the formation of coherent oscillation domains in the cell water interacting with the protein backbone (Meijer and Geesink, 2020a).

Our meta-analysis of the particular literature showed that semi-harmonic frequency patterns in purified water have discrete coherent bands and are very much in line with those found in biological systems (Geesink, 2020a). The meta-analysis of about 700 measured frequencies of pure water molecules shows that 192 subsequent first and second derivatives of spectral frequency curves of water molecules can be precisely positioned at the pointer states of the proposed calculated pattern of coherent eigen-frequencies. It was concluded that water molecules assemblies show electromagnetic and electronic collective states that contain "quantum imprints or moulds" for living cells. A potential explanation for this feature is that water molecules are ordered in a partially distorted tetrahedral geometry and related network structure. Since water molecules have a comparable distribution of coherent EMF bands to that of fluid assemblies in living cells, a mutual wave resonance interaction between cytoplasm and macromolecules of life matter with surrounding water molecules can be expected. Of note, the coherence of liquid water is affected by applied

external electromagnetic waves much weaker than those allowed according to the kT threshold (Del Giudice, 2010) and the reorientation of water molecules might take place at energy levels of less than 100 mW/cm2, which is at a non-thermal energy level.

External electromagnetic waves are able to disturb conformational states of biological systems

The organisation of the many components of a life system seem to be logically- and well-organized in a biological sense or, alternatively, may show chaotic aspects, which conditions can be related to the terms coherent or non-coherent respectively. The organised patterns of the cell components can be stable, or instable as well as in equilibrium or far from equilibrium. In physics, waves are called coherent when the phase differences between the waves is small, whereas, if waves are defined as incoherent, these phases have a high degree of variability. It is proposed that life bio-molecules and viable cells are functioning within narrow coherent EM field frequency bands over a broad spectrum of frequency energies. The individual discrete frequency values were found by us to form quite narrow frequency bands, being randomly localized around the algorithmically defined coherent frequencies. This discrete pattern of coherent waves is likely co-responsible for the architectures of living cells. The particular, highly coherent, frequencies of living cells/molecules are positioned in “coherent zones” and exist within small bandwidth’s of about 1.40% of the local coherent algorithmic frequency calculated from the proposed quantum wave equation. In contrast, non-coherent zones are positioned just in between the coherent zones and are responsible for a destabilization of cellular organization, also within a small bandwidth of about 1.40% of the local decoherent algorithmic frequency (see figures 12, and 13 based on data of 724 published biomedical reports) .

In the present study, a complementary third series of 226 different electromagnetic biological studies, mainly carried out also in the period 1970-2020, about influences of external electromagnetic waves on biological properties with different frequencies in the band of MHz, GHz and THz have been analysed, with exposures of 0.1 - 30 mW/cm^2, and 0.014 - 10 W/kg, see appendix 2 and 3.

Analysing these data, it can be concluded that this series of published experiments fit for not less than 94.2% with the earlier applied composed frequency scale, in accordance with the proposed quantum model of coherent and decoherent frequencies, see figure 13. All applied 103 different frequencies of unhealthy conditions according to the biomedical publications can be addressed to pointer states, that are characteristic for typical decoherent frequencies, within a, distinctly small, mean bandwidth of 0.86%, see appendix 2.1 and 3.1. All 47 differently applied frequencies of healthy conditions according to the biomedical publications, could be addressed to pointer states, that are characteristic for typical coherent frequencies, within again a typical mean small frequency bandwidth of 0.70%, see appendix 2.2 and 3.2. Also, coherent frequencies combined with coherent modulations show a healthy behaviour, see appendix 2.6.

On the contrary, coherent frequencies *modulated* with incoherent frequencies, of which by the modulation the band position is forced into a bandwidth of incoherent frequencies, show an unhealthy behaviour: see the 27 different experiments in appendix 2.5. Also, the decoherent frequencies, after being modulated with incoherent frequencies, show a position associated with unhealthy behaviour: see the 18 different experiments in appendix 2.3. An amount of 5.8% of the studies could not be ascribed to the proposed quantum equation of coherence and decoherence. They originated, among others, either from relatively short exposure times, or were exposed to relatively high energy levels, for example: 100 Mw/cm^2 or minor health effects have been found, see appendix 2.8, 2.9, 2.10 and 2.11.

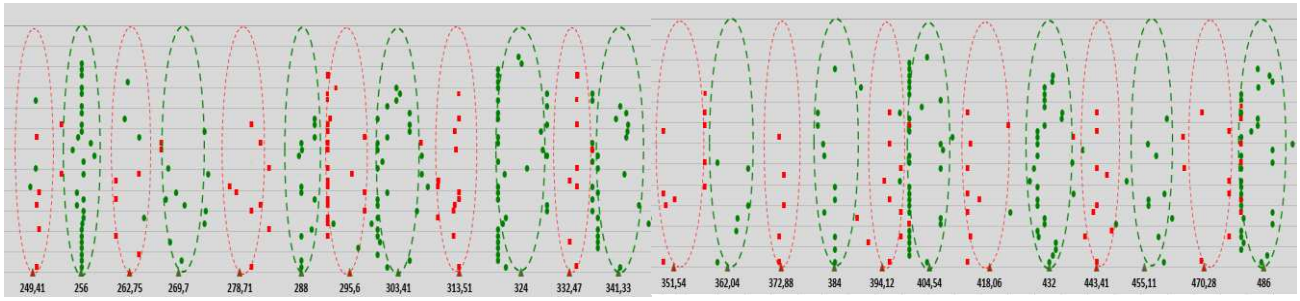

Normalized scale 249.41- 486.0 Hz ------>

Figure 12. *Meta-analysis Geesink and Meijer: healthy and unhealthy related electromagnetic frequencies (2018):*

Measured frequency data of living cells systems that are health-sustaining (coherent data and zones: green), or detrimental for health (decoherent data: red) versus calculated normalized frequencies, from 1970 till 2020. Biological effects measured following exposures or endogenous effects of living cells in vitro and in vivo at frequencies in the bands of Hz, kHz, MHz, GHz, THz, PHz. Green triangles plotted on a logarithmic x-axis represent calculated normalized (Hz) health-sustaining frequencies; red triangles represent calculated health-destabilizing frequencies. Each point indicated in the graph is taken from published biological data and are a typical frequency for a biological experiment(s). For clarity, points are randomly distributed along the Y-axis; Yellow lines are proposed transition frequencies (Geesink, 2018).

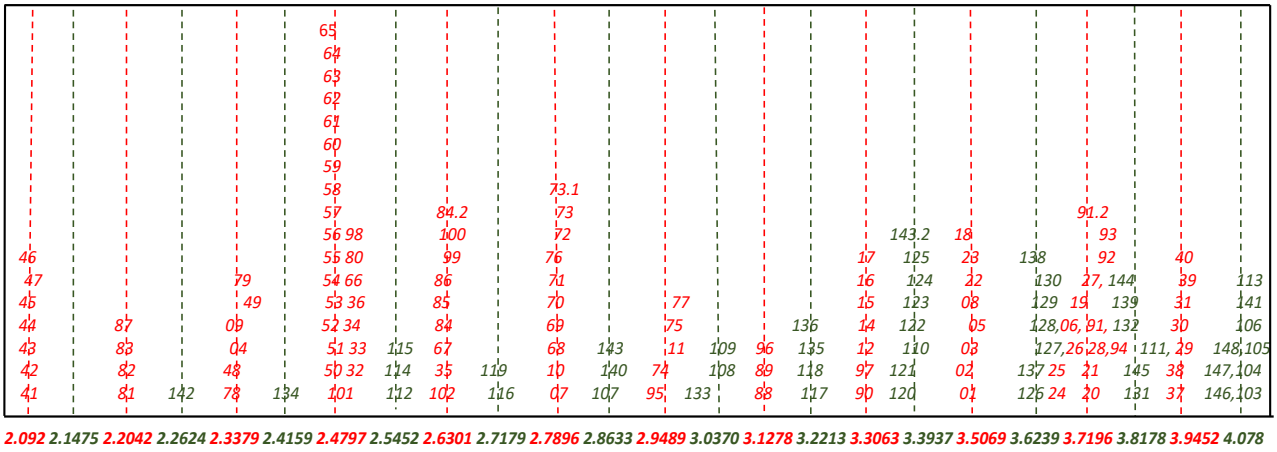

Normalized scale 2.0 - 4.0 GHz ------>

Figure 13. *Meta-analysis Geesink and Meijer: healthy and unhealthy related electromagnetic frequencies (2020):*

Measured frequency data of living cells systems that are health-sustaining (coherent data: green), or detrimental for health (decoherent data: red) versus calculated normalized frequencies, from 1970 till 2020. Biological effects measured following exposures or endogenous effects of living cells in vitro and in vivo at frequencies in the bands of MHz, GHz and THz. Green numbers plotted on a logarithmic x-axis represent calculated normalized GHz-health-sustaining frequencies; red numbers represent calculated GHz-health-destabilizing frequencies. Each point: green numbers (see references) or red numbers (see references) indicated in the graph is taken from published biological data and are a typical frequency for a biological

experiment(s). For clarity, points are randomly distributed along the Y-axis; Yellow lines are proposed transition frequencies (Geesink, 2020).

References Figure 13:

1. Brown-Woodman et al. (1988); 2. Tofani et al. (1986); 3. Lary et al. (1982, 1983); 4.Bawin et al. (1973); 5.Guo et al. (2019); 6.Klos-Witkowska et al. (2019); 7. Jauchem and Frei (1997); 8. Holt JA (1977); 9. Sanders et al. (1980); 10.Frei et al. (1989); 11. Daniells et al. (1998); 12. Mashevich et al. (2003); 13. Mashevich et al.: (2003); 14. Maskey et al. (2014); 15. Donnellan et al. (1997); 16. Maskey et al. (2010); 17. Kim et al. (2018); 18. Pavicic I and Trosic I (2006); 19. Zmyslony et al. (2004); 20.Pavicic I and Trosic I (2008); 21. Maes et al. (1997); 22. Herrala et al. (2018); 23. Luukkonen et al. (2009); 24. Hao et al. (2012); 25. Yang, L. et al. (2012); 26. Johnson and Guy (1972); 27. Zmyslony et al. (2004); 28. Maes et al. (1997); 29. Jauchem and Frei (2000); 30. De Pomerai et al. (2003); 31. Todorova et al. (2020); 32. Todorova et al. (2020); 33. Todorova et al. (2020); 34. Lu et al. (1992); 35. Oscar and Hawkins (1977); 36. Schirmacher et al. (1999); 37. Mancinelli et al. (2004); 38. Miyakoshi et al. (2005); 39. Iyama et al. (2004); 40. Senavirathna et al. (2014); 41. Esmekaya et al. (2013); 42. Esmekaya et al. (2017); 43. Bedir et al. (2015); 44. Sahin et al. (2016); 45. Gokcek-Sarac et al. (2017); 46. Jong Jin Oh et al. (2018); 47. Kesari et al. (2014); 48. Chandel et al. (2019); 49. Shandalal et al. (1979); 50. Lai et al. (1987, 1988); 51. Deshmukh et al. (2015); 52. D'Andrea et al. (1986); 53. Switzer and Mitchell (1977); 54. Meena et al., (2014); 55. Szmigielski et al. (1982); 56. Kesari et al. (2010); 57. Shokri S. et al. (2015); 58. Marcickiewicz et al. (1986); 59. Roszkowski et al. (1980b); 60. Szudzinski et al. (1982); 61. Usikalu et al. (2013); 62. Megha et al. (2015); 63. Karimi et al. (2018); 64. Varghese et al. (2018); 65. Topsakal et al. (2017); 66. Figueiredo et al. (2004); 67. Liburdy R. (1979); 68. Thomas et al. (1982); 69. Albert et al. (1977); 70. Frei and Jauchem (1989); 71. Gandhi et al. (1989); 72. Hai-juan Li et al. (2015); 73. Zuo H. et al. (2014); 73.1 Hui Wang et al. (2017); 74. Siekierzynski et al. (1972); 75. Pu et al. (1997); 76. D'Ándrea et al., (1994); 77. Jensh et al. (1984); 78. Goldstein and Sisko et al. (1974); 79. Zhang Y et al. (2014); 80. Sharma et al. (2014); 81. Millenbaugh et al. (2008); 82. Sypniewska et al. (2008); 83. Foster et al. (2008); 84. Makar et al. (2005); 84.2. Gapeyev et al. (2011); 85. Lushnikov et al. (2003); 86. Gapeev et al. (2003); 87. Frei et al. (1995); 88. Kesari et al. (2009); 89. Albini et al. (2014); 90. D'Agostino et al. (2018); 91. Habauzit et al. (2018); 91.2. Bellossi et al. (2018); 92. Le Quément et al. (2014); 93. Mahamoud et al. (2019); 94. Le Pogam et al. (2019); 95. Foster et al. (2003); 96. Homenko et al. (2009); 97. Tafforeau et al. (2004); 98. Sheng Zhi Tan et al. (2019); 99. Sheng Zhi Tan et al. (2019); 100. Ahlberg Gagnér et al. (2019); 101. Wilmink et al. (2010); 102. Ol'shevskaia et al. (2009). 103. Kyung Shin Kang et al. (2013); 104. Kyung Shin Kang et al. (2013); 105. Takebe et al. (2013). 106. Bandyopadhyay et al. (2014). 107. Usselman et al. (2016); 108. Kyung Shin Kang et al. (2013); 109. Takebe et al. (2013); 110. Agulan et al. (2015); 111. Bandyopadhyay et al. (2014); 112. Zou et al. (2007); 113. Pokorny et al. (2009); 114. Chen X. et al. (2012, 2014); 115. Bandyopadhyay et al. (2014); 116. Stolfa et al. (2007); 117. Garon et al. (2007); 118. Lary et al., (1983); 119. Alessio et al. (2019); 120. Roti et al. (2001); 121. LaRegina et al. (2003); 122. Roti et al. (2001); 123. LaRegina, (2003); 124. Lee et al., (2010); 125. Kim et al., (2010); 126. Keleş et al. (2018, 2019); 127. Surducan et al. (2020); 128. D'Andrea et al. (2000); 129. Masuda al. (2009); 130. Trošic et al., (2013); 131. Furtado-Filho et al., (2015); 132. Seyednour et al. (2011); 133. Gibot et al. (2019); 134. Gibot et al. (2019); 135. Vijayalaxmi et al. (2003); 136. Anderson et al., (2004); 137. Gurbuz et al., (2014);138. Guler et al., (2016); 139. McNamee et al. (2003); 140. Miyakoshi et al. (2019); 141. Hansteen et al. (2009); 142. Hansteen et al. (2009); 143. Beneduci et al. (2005); 143.2. Samoilov et al. (2015); 144. Nicolaz et al. (2009); 145. Radzievsky et al. (2004); 146. Kalantaryan et al. (2010); 147. Beneduci et al. (2005); 148. Bantysh et al. (2018).

A comparison between both analyses of 2018, see figure 12, and the analysis of 2020, see figure 13, learns that the addition of 229 data positioned in MZ, GHz, and THz, further more precisely substantiates the calculated pointer frequencies of coherent and decoherent states, including the bandwidth of the measured data. Eleven different situations can be addressed:

1. A number of 105 different experiments of applied electromagnetic frequencies show a proposed unhealthy behaviour, that can be related to decoherent frequency signals at MHz and GHz (not modulated), and fit in the proposed algorithm.
2. A number of 48 different experiments of electromagnetic frequencies that are proposed as healthy, that can be related to coherent frequency patterns at MHz and GHz, and fit in the proposed algorithm.
3. A number of 18 different experiments electromagnetic frequencies, that are proposed as unhealthy, can be related to a decoherent base signal at MHz and GHz, combined with estimated decoherent modulations, and fit in the proposed algorithm.

4. A number of 1 different experiment electromagnetic frequency that is proposed as healthy, can be related to coherent frequency patterns at MHz and GHz, and fit in the proposed algorithm, but at a relatively high exposure rate.
5. A number of 29 different experiments electromagnetic frequencies, that are proposed as unhealthy can be related to a coherent base signal at MHz and GHz, combined with estimated decoherent modulations.
6. A number of 7 different experiments electromagnetic frequencies, that are proposed as healthy, can be related to coherent base signal at MHz and GHz, combined with coherent modulations, and fit in the proposed algorithm.
7. A number of 8 different experiments of electromagnetic frequencies, that are proposed as healthy, can be related to coherent base signal at MHz and GHz, combined with estimated decoherent modulations.
8. A number of 5 different experiments of electromagnetic frequencies, that are proposed as healthy, can be related to decoherent frequency signals at MHz and GHz (not modulated), and do not fit in the proposed algorithm.
9. A number of 3 different experiments of electromagnetic frequencies, that are proposed as unhealthy, that can be related to coherent frequency signals at MHz and GHz (not modulated), do not fit in the proposed algorithm.
10. A number of 4 different electromagnetic frequency experiments, that are proposed as healthy, can be related to decoherent frequency base signals at MHz and GHz and estimated decoherent modulations, and do not fit in the proposed algorithm.
11. A number of 1 electromagnetic frequency experiment, that are proposed as healthy that can be related to a coherent base signal at MHz and GHz, combined with estimated decoherent modulations, and does not fit in the proposed algorithm.

The analysis of the second series of 229 different electromagnetic biological investigations is in line with the analysis made in 2016 for about 500 investigations and reviews, and show that external coherent and decoherent frequency patterns of non-thermal electromagnetic waves according to the proposed algorithm can be related to cause respectively healthy or unhealthy behaviour for exposed living cells and biomolecules (Geesink and Meijer, 2017a). The discrete coherent and decoherent frequency bands are arranged according to an alternating ordering, while decoherent bands and transition frequencies are located just in between these frequency bands (Geesink, 2018a), see figures 8 and 9.

Mutual coherent ordering of biomolecules can occur in a surrounding in which small frequency shifts can take place, that balance between coherent and transition zones, on the contrary apoptosis and necrosis can take place by morphological patterns, that are characterized by decoherent patterns. It is proposed that frequency shifts from coherent to transition zones and vice versa can occur by: 1) intensity changes of overlapped bands, 2) (de)bonding of hydrogen bonds, 3) changing of dipole–dipole interactions. It has been found in the meta-analyses that underlying causes of unhealthy situations by non-thermal external electromagnetic waves can be related to the different states of biological aspects, that can be disturbed: conformational states of proteins, pre-conformational states of protein folding, genome conformational states, conformational states of ion-gates, conformational states of neurotransmitters, conformational dynamics of DNA, and ATP-arrangements. The disturbances of the mentioned biological aspects can be further related to corresponding physical disturbances like: conformational states of ion water clathrates, short- and long-range electromagnetic interactions, conformational states of electrons, soliton waves and tunnelling frequencies.

To ensure acceptable levels of safety of exposure to external non-thermal electromagnetic waves acting on living cells and biomolecules disturbances of the conformational states of bio-systems have to be prevented. Therefor it is proposed to additional install a certain level of coherent waves into external man-made electromagnetic waves, according to the proposed quantum wave equation, to guarantee sufficient coherent wave conditions for living cells and biomolecules.

Coherent signal generation

It has been discussed in the prior sections, that external non-thermal electromagnetic waves are able to steer the proposed transitional modes in living cells, located just between the coherent and decoherent modes, into one of the other zones: the coherent or decoherent ones. This is depending upon the types of the external EMF frequencies employed and thus if they are located in the coherent or decoherent modes. Not only decoherent electromagnetic base signals are able to cause unhealthy situations, but also coherent base signals modulated with estimated decoherent frequency patterns are also able to cause unhealthy situations, see appendix 2.5, and for example the 900 MHz GSM-pulsed studies of Franzellitti (2010); Mausset-Bonnefont (2004); Schneider (2014); Pandey (2018); Narayanan (2018) and Wyde (2016). Noticeable, studies that apply a single coherent signal at for example 900 MHz show no biological effect (Keleş, 2018; 2019). Coherent base signals, when combined with coherent modulations also show no or healthy effects (Oberto, 2007; Ren Z., 2015; Wang J. 2012; Yao, 2008; Chen X., 2012, 2014; Grospietsch, 1995).

It should be mentioned here that, noise can play a facilitatory role in neuronal processing and reliability of communication, according to principles of stochastic resonance (SR). It has been shown that, if the exogenous noise is properly filtered and its level is adjusted, a clear optimization of the network encoding of an electromagnetic signal, is obtained through the stochastic resonance (Paffi et al. 2013). Noise intensities maximizing spiking activity coherence with the exogenous EM signal are clearly shown, indicating a stochastic resonant behaviour, strictly connected to the model frequency sensitivity. In this study SR exhibits a window of occurrence in the values of field frequency and intensity, which is a kind of effect long reported in bioelectromagnetic experimental studies (Gianni, 2006).

It is proposed that safety of external non-thermal electromagnetic waves can be further improved to a proper ratio of coherent and decoherent signals, as defined the quantum wave equation used by us and has been shown in the meta-analysis of many other investigations. It is proposed that an additional supply of coherent waves, that are positioned in the THz-gap at estimated low intensities of 0.01 till 0.2 mW/cm2, may be efficient to sustain health. Further improvements of coherency of man-made signals can be realised by a coherent coupling of additional FIR, MIR and NIR-waves (Geesink, 2020).

Mathematical concepts of coherence and decoherence can be calculated by a linear algebraic theory of partial coherence that allows mathematical definitions. The mathematical definitions are related to the physical understanding of the corresponding concepts by considering them in the context of Young's experiment. Scalar measures have been proposed for the degree of partial coherence and the measures are unity for fully coherent fields, zero for incoherent fields, and between zero and one for partially coherent fields (Ozaktas, 2016). When the carrier frequency is positioned within a coherent frequency band of the coherence spectrum, the coherence ratio will be > 0.5, on the other hand when the carrier frequency is positioned within a decoherent band, than the coherence ratio will be much lower than 0.5 (Golińska, 2011).

Semi- and super-conductors are candidates to add the proposed additional coherent waves to man-made electromagnetic technology. In polar semiconductor materials, LO phonons produce a macroscopic electric field, which interacts with the electrons. This coupling of long range is known as Fröhlich interaction and due to the interaction of an electron with LO phonons, a quasi-particle is formed known as polaron. The strength of this coupling is expressed by a dimensionless Fröhlich coupling constant. Due to the polar coupling to LO phonons, the carriers lose their initial kinetic energy to the lattice by a very efficient relaxation mechanism in III-V bulk semiconductors. And a theoretical model has been developed to determine threshold pump field for the onset of parametric process (Dubey, 2016). HTSC's (High Temperature Super Conductors) show patterns of frequencies, in which frequency ratios of 2:3 (third harmonic) are incorporated in ratios of 1:2 (fundamental frequency). A manifestation of electron-hole pairing as a nonlinear electromagnetic response of layered superconductors show that the pairing causes the appearance of a number of peaks in the frequency dependence of the intensity of the third-harmonic generation (Germash, 2017, Cea, 2018,

Gioacchino, 2010). The highest peak corresponds to $\hbar\,\omega = (2/3)\,\Delta$, where ω is the incident wave frequency, and Δ is the order parameter of the electron-hole pairing (Germash, 2017). For samples with three-dimensional superconductivity, the superconducting signature can be seen at both the fundamental frequency and at the third harmonic. By driving the system out of equilibrium with an infrared light at a typical frequency, a net coupling between the layers is induced, and a superconducting signature shows up in the third harmonic (Tranquada, 2018, Rajasekaran, 2018).

Quantum coherence in condensed matter systems is a broad avenue to be explored toward the enhancement of its quantum properties by means of material engineering. In this regard, work has reported about a study of the influence of temperature, and magnetic fields on the quantum coherence of a metal-silicate framework: $KNaCuSi_4O_{10}$ (Cruz, 2019). Chip-based technological advancements enable the assessment of pulsed electric field effects on bio-nanostructures. The results contribute to the chip-based high-frequency bioelectronics technology for modulating the function of biological matter at the nanoscale level (Havelka, 2019). Since a nanosecond pulsed electric field can penetrate the tissues and cellular membranes due to its broadband spectrum, the results are also potentially significant for the development of new protocols (Marracino, 2019).

Conclusions

1. A meta-analysis of about 721 papers has shown that external non-thermal electromagnetic waves can be beneficial or detrimental for living cells and biomolecules, depending on the nature of the typical external electromagnetic frequency patterns that can stabilise internal coherent frequency patterns or induce internal decoherent frequency patterns.
2. A number of current researchers further support the known models of Fröhlich and Davydov.
3. Many investigations show a stabilisation of conformational states of biomolecules that can lead to healthy conditions, whereas destabilisation of conformational states can produce unhealthy conditions.
4. Frequency patterns that stabilize or destabilise living systems can be calculated by the quantum wave equation (coined by us the GM-scale biophysical principle) that can be seen as is a further precision of Fröhlich's wave equation.
5. About 226 published investigations in the period 1972 till 2020 were analysed and show that external non-thermal electromagnetic exposures to living cells at typical MHz- and GHz-frequencies are associated with healthy or unhealthy conditions depending on their position on the patterned GM-scale of coherent and decoherent frequency bands.
6. It is considered that acceptable levels of safety of non-thermal external electromagnetic waves acting on living cells, biomolecules and living beings can be realised when a sufficient level of coherent signals are present in man-made signals.
7. Inorganic semi- and superconductors are able to mimic these coherent signal patterns. It is envisioned that chip-technology can become available to improve the safety of external non-thermal electromagnetic waves.
8. The total actualized meta-analysis of about 721 papers of external non-thermal electromagnetic biological influences very clearly obeys the proposed quantum wave equation that is based on Bose-Einstein type of wave behaviour.
9. There seems to be consensus between researchers that: 1) non thermal electromagnetic waves have an impact on health, 2) frequency modulations of coherent frequencies for a major part show a disadvantageous influence on health properties, 3) since selected frequencies can either be related to health promoting effects or to frequencies related to unhealthy situations, presently used communication technology can be fine-tuned to greater extent of safety
10. The proposed frequency algorithm of healthy and unhealthy modes of EMF radiation offer attractive possibilities for the design of dedicated protective technologies.

References

Agrawal, L., Sahu, S., Ghosh, S. Shiga, T., Fujita, D., Bandyopadhyay, A. Inventing atomic resolution scanning dielectric microscopy to see a single protein complex operation live at resonance in a neuron without touching or adulterating the cell, Journal of Integrative Neuroscience, Vol. 15, No. 4 (2016) 435-462 World Scientific Publishing Europe Ltd. DOI: 10.1142/S0219635216500333.

Ahlberg Gagnér V., Ida Lundholm, Maria-Jose Garcia-Bonete, Helena Rodilla, Ran Friedman, Vitali Zhaunerchyk, Gleb Bourenkov, Thomas Schneider, Jan Stake, Gergely Katona. Clustering of atomic displacement parameters in bovine trypsin reveals a distributed lattice of atoms with shared chemical properties. Scientific Reports | (2019) 9:19281 | https://doi.org/10.1038/s41598-019-55777-5.

Ahmed, N. A. G., Calderwood, J. H., Fröhlich, H., Smith, C. W. (1975). Evidence for collective magnetic effects in an enzyme likelihood of room temperature superconductive regions. Phys. Lett. A. 53:129–130.

Amiot E. The Torii of Phases. In: Yust J, Wild J, Burgoyne J A (eds) Mathematics and Computation in Music. MCM 2013. Lecture Notes in Computer Science. 2013;7937.

Bacon, D. "Decoherence, control, and symmetry in quantum computers". arXiv:quant-ph/0305025. Impaired coherence contributes to the progressive, 2001.

Bardeen J, Cooper LN, Schrieffer JR. “Theory of superconductivity” Phys. Rev. 1957; vol. 108, pp. 1175–1204, http://link.aps.org/doi/10.1103/PhysRev.108.1175.

Barnes, F. S., Greenebaum, B. (2014). The Effects of weak magnetic fields on radical pairs. Bioelectromagnetics. 36 (1):45–54. doi: 10.1002/bem.21883 Wiley Periodicals, Inc. B.

Baumgratz, T.; Cramer, M.; Plenio, M.B. (2014). "Quantifying Coherence". Phys. Rev. Lett. 113 (14): 140401. arXiv:1311.0275.

Bekard, I.B., K. J. Barnham, L. R. White and D. E. Dunstan, α-Helix unfolding in simple shear flow, Soft Matter, 2011, 7, 203.

Bekard, I.B., P. Asimakis, C. L. Teoh, T. Ryan, G. J. Howlett, J. Bertolini and D. E. Dunstan, Bovine serum albumin unfolds in Couette flow, Soft Matter, 2012, 8, 385.

Bekard I.B., Dave E. Dunstan. Electric field induced changes in protein conformation. Soft Matter, 2014, 10, 431.

Belyaev I.Y., Shcheglov V.S., Alipov Y.D., Polunin V.A. 1996 Bioelectromagnetics 17 312.

Belyaev, I.Y., Alipov, Y.D. and Shcheglov, V.S. (1992) Chromosome DNA as a Target of Resonant Interaction between Escherichia-Coli-Cells and Low Intensity Millimeter Waves. Electro- and Magnetobiology, 11, 97-108. https://doi.org/10.3109/15368379209009820

Belyaev, I. Y., V.S. Shcheglov, Y.D. Alipov, Resonance effect of millimeter waves in the power range from 10-19 to 3 × 10-3 W/cm2 on Escherichia coli cells at different concentrations. January 1996. Bioelectromagnetics 17(4):312-321

Belyaev, I. Y. (2010) Dependence of Non-Thermal Biological Effects of Microwaves on Physical and Biological Variables: Implications for Reproducibility and Safety Standards. In: Giuliani, L. and Soffritti, M., Eds., European Journal of Oncology—Library Non-Thermal Effects and Mechanisms of Interaction between Electromagnetic Fields and Living Matter.

Belyaev, I.Y., 2015. Biophysical mechanisms for nonthermal microwave effects. In: Markov, M. (Ed.), Electromagnetic Fields in Biology and Medicine, vol. 2015. CRC Press, Boca Raton, London, New York, pp. 49e68.

Blank, M., Findl, E. (1970). Mechanistic Approaches to Interactions of Electric and Electromagnetic Fields with Living Systems. 1987. Springer Science+Business Media, LLC. ISBN: 978-1-4899-1970-0.

Blank, M. Protein and DNA Reactions Stimulated by Electromagnetic Fields. February 2008. Electromagnetic Biology and Medicine 27(1):3-23. DOI: 10.1080/15368370701878820.

Bodewein, L. Schmiedchen K., Dechent D., Stunder D., Graefrath D., Winter L., Kraus T., Driessen S. Systematic review on the biological effects of electric, magnetic and electromagnetic fields in the intermediate frequency range (300 Hz to 1 MHz). Environmental Research Volume 171, April 2019, Pages 247-259.

Buchachenko, A. (2015). Why magnetic and electromagnetic effects in biology are irreproducible and contradictory? Bioelectromagnetics. 37:1–13. Wiley Periodicals, Inc. and Buchachenko (2015).

Bugay, A.N. INTERACTION OF TERAHERTZ RADIATION WITH DNA. NANOSYSTEMS: PHYSICS, CHEMISTRY, MATHEMATICS, 2012, 3 (1), P. 51–55.

Butikov, E. I. (2004). Parametric excitation of a linear oscillator. Eur. J. Phys. 25:535–554.

Betskii, O.V., Lebedeva, N.N., 2004. Clinical Application of Bioelectromagnetic Medicine. Marcel Dekker, USA, N-Y, Ch. Low-intensity Millimeter Waves in Biology and Medicine, pp. 741e760.

Blackman, C.F. (1984) Sub-Chapter 5.7.5 Biological Effects of Low Frequency Modulation of RF Radiation. In: Elder, J.A. and Cahill, D.F., Eds., Biological Effects of Radiofrequency Radiation.

Bock J., Yayoi Fukuyo, Sona Kang, M. Lisa Phipps, Ludmil B. Alexandrov, Kim Ø. Rasmussen, Alan R. Bishop, Evan D. Rosen, Jennifer S. Martinez, Hou-Tong Chen, George Rodriguez, Boian S. Alexandrov, Anny Usheva. 2010 Mammalian stem cells reprogramming in response to terahertz radiation.PLoS ONE 5, e15806. (doi:10.1371/journal.pone.0015806).

Del Re B., Fernando Bersani, Gianfranco del Georgi. Effect of electromagnetic field exposure on the transcription of repetitive DNA elements in human cells, Electromagnetic Biology and Medicine Volume 38, 2019 - Issue 4.

Cea, T, Barone P, Castellani C, Benfatto L. Polarization dependence of the third-harmonic generation in multiband superconductors. Phys. Rev. 2018; B 97, 094516.

Chukova YP. Doubts about Nonthermal Effects of MM Radiation Have no Scientific Foundations, 9th International Fröhlich's Symposium IOP Publishing, Journal of Physics: Conference Series 329 (2011) 012032 doi:10.1088/1742-6596/329/1/012032.

Devi-Prasad, K.V., and Prohofsky, E.W. (1984), "Low frequency mode prediction in A-DNA compared to experimental observations and significance for A to B conformational change," Biopolymers, 20, 853–864.

Devyatkov N. D. at al., 1974 Soviet Physics USPEKHI, p.568.

Deruelle F. The different sources of electromagnetic fields: Dangers are not limited to physical. Journal Electromagnetic Biology and Medicine, Published online: 10 Mar 2020

Cosic, I. (1997). The Resonant Recognition Model of Macromolecular Bioactivity Theory and Applications.
Basel, Boston, Berlin: Birkhauser Verlag. ISBN: 978-3-0348-7477-9.

Cosic, I., Cosic, D., Lazar, K. (2015). Is it possible to predict electromagnetic resonances in proteins. DNA and RNA? EPJ Nonlinear Biomedical Physics. 3:5.

Cosic, I., Cosic, D., Lazar, K. (2016). Environmental light and its relationship with electromagnetic resonances of biomolecular interactions, as predicted by the resonant recognition model. Int. J. Environ. Res. Public Health. 13:647.

Cruz C., Anka M.F. Quantifying quantum coherence in a metal-silicate framework. arXiv:1910.04199v3 [quant-ph] 5 Dec 2019.

D'Agostino, S., Chiara Della Monica, Eleonora Palizzi, Fabio Di Pietrantonio, Massimiliano Benetti, Domenico Cannatà, Marta Cavagnaro, Dariush Sardari, Pasquale Stano & Alfonsina Ramundo-Orlando. Extremely High Frequency Electromagnetic Fields Facilitate Electrical Signal Propagation by Increasing Transmembrane Potassium Efflux in an Artificial Axon Model. SCIENTIfIC REPORS | (2018) 8:9299 | DOI:10.1038/s41598-018-27630-8.

Dana K. D., Mar´ıa Garc´ıa D´ıaz, Mohamed Mejatty, Andreas Winter. Resource Theory of Coherence — Beyond States. arXiv:1704.03710v4 [quant-ph] 20 Nov 2017.

Davydov, A. S. (1973). The theory of contraction of proteins under their excitation. J. Theor. Biol. 38:559–569. Doi 10.1016/0022-5193(73)90256-7. PMID 4266326.

Davydov, A. S. (1977). Solitons and energy transfer along protein molecules. J. Theor. Biol. 66:379–387. Doi 10.1016/0022-5193(77)90178-3. PMID 886872.

De-Kun Li, MD, PhD; Hong Chen, MPH; Jeannette R. Ferber, MPH; Andrew K. Hirst, MS; Roxana Odouli, MSPH. Association Between Maternal Exposure to Magnetic Field Nonionizing Radiation During Pregnancy and Risk of Attention-Deficit/Hyperactivity Disorder in Offspring in a Longitudinal Birth Cohort. Original Investigation Environmental Health, March 24, 2020.

Del Giudice, E., Doglia, S., Milani, M., Vitiello, G. (1983). Spontaneous symmetry breakdown and boson condensation in biology. Phys. Lett. A. 95:508–510.

Del Giudice, E., Doglia, S., Milani, M., Vitiello, G. (1985). A quantum field theoretical approach to the collective behaviour of biological systems. Nucl. Phys. B. 251(C):375–400.

Del Giudice E, Tedeschi A, 2009. Water and Autocatalysis in Living Matter, Electromagnetic Biology and Medicine, 28: 46–52.

Del Giudice E, Spinetti P R, Tedeschi A, 2010. Water dynamics at the root of metamorphosis in living organisms. Water 2: 566–586.

De Ninno A., Castellano AC. On the Effect of Weak Magnetic Field on Solutions of Glutamic Acid: The Function of Water, 2011 J. Phys.: Conf. Ser. 329 012025.

De Ninno, Congiu Castellano and Del Giudice. The supramolecular structure of liquid water and quantum coherent processes in biology. Journal of Physics: Conference Series 442 (2013) 012031 doi:10.1088/1742-6596/442/1/012031

De Ninno, A., Del Giudice, E., Gamberale, L., Congiu Castellano, A. (2014). The structure of liquid water emerging from the vibrational spectroscopy: Interpretation with QED theory. Water 6:13–25.

De Ninno, A., Pregnolato, M. Electromagnetic homeostasis and the role of low-amplitude electromagnetic fields on life organization, ELECTROMAGNETIC BIOLOGY AND MEDICINE, http://dx.doi.org/10.1080/15368378.2016.1194293, 2016.

De Ninno, A., De Francesco, M. ATR-FTIR study of the isosbestic point in water solution of electrolytes, Chem Phys. 513, (2018) 266 -272.

Devyatkov, N.D. (1974) Influence of Millimetre Band Electromagnetic Radiation on Biological Objects. Sov Phys Usp, 16, 568-569. https://doi.org/10.1070/PU1974v016n04ABEH005308

Devyatkov, N.D., Golant, M.V. and Betskii, O.V. (1991) Millimeter Waves and Their Role in Processes of Vital Activity (in Russian). Radio and Svyaz, Moscow.

Devyatkov, N.D., Pletnyov, S.D., Chernov, Z.S., Faikin, V.V., et al. (1994) Effect of Low-Energy Nanosecond-Pulse EHF and Microwave Radiation with a Giant Peak Power on Biological Structures (Malignant Tumors). DAN SSSR, 336. (In Russian)

Dubey S., Ayushi Paliwal, S.Ghosh. Fröhlich Interaction in Compound Semiconductors: A Comparative Study, Advanced Materials Research Online: 2016-08-26, ISSN: 1662-8985, Vol. 1141, pp 44-50, doi:10.4028/www.scientific.net/ AMR.1141.44

Durdik, M., Pavol Kosik, Eva Markova, Alexandra Somsedikova, Beata Gajdosechova,Ekaterina Nikitina, Eva Horvathova, Katarina Kozics, Devra Davis4 & Igor Belyaev. Microwaves from mobile phone induce reactive oxygen species but not DNA damage, preleukemic fusion genes and apoptosis in hematopoietic stem/progenitor cells. Scientific Reports | (2019) 9:16182 | https://doi.org/10.1038/s41598-019-52389-x 1

Fedorov, P. S.S, and P. A.N., Dynamic Effects of Submillimeter Wave Radiation on Biological Objects of Various Levels of Organization. International Journal of Infrared and Millimeter Waves, 2003. 24(8): p. 1235–1254.

Feng Y, Prohofsky EW. Vibrational fluctuations of hydrogen bonds in a DNA double helix with nonuniform base pairs. Biophys J. 1990 Mar;57(3):547–553.

Feynman, R.P., Robert B. Leighton and Matthew Sands (1963). "Quantum Behaviour". The Feynman Lectures on Physics. III. Addison-Wesley.

Fremling M. Coherent State Wave Functions on the Torus, Licentiate Thesis, 2013.

FRENCH, P.W., DONNELLAN, M. & MCKENZIE, D.R. 1997. Electromagnetic radiation at 835 MHz changes morphology and inhibits proliferation of a human astrocytoma cell line. Bioelectrochem. Bioenerg. 43: 13–18.

French, P. (2003). Vibrations and Waves. Norton. ISBN 978-0-393-09936-2.

Fröhlich, H. (1968). Long-range coherence and energy storage in biological systems. Int. J. Quantum. Chem. 2:641–649.

Fröhlich, H. (1969). Quantum mechanical concepts in biology. In: Marois, M.Ed. From Theoretical Physics to Biology. Amsterdam, the Netherlands: North-Holland. pp. 13–22.

Fröhlich, H. (1978). Coherent electric vibrations in biological systems and the cancer problem. Microwave theory and techniques. IEEE Trans. 26:33.

Fröhlich, H.: Further evidence for coherent excitations in biological systems, Phys. Lett, 110A, 480-481, 1985. [2] Frohlich, H.: Coherent excitation in active biological systems, In: Modern Bioelectrochemistry, F. Gutmann, & H. Keyzer, eds., New York: Plenum, 1986, pp. 241-261, 1986.

Fröhlich, H. (1988). Biological Coherence and Response to External Stimuli. Berlin, Heidelberg, New York: Springer.

Hinrikus, H., Bachmann, M., Lass, J. (2011). Parametric mechanism of excitation of the electroencephalographic rhythms by modulated microwave radiation. Int. J. Rad. Biol. 87:1077–1085.

Hiie Hinrikus, Jaanus Lass, Denis Karai, Kristjan Pilt, and Maie Bachmann. Microwave effect on diffusion: a possible mechanism for non-thermal effect. Electromagn Biol Med, Early Online: 1–7! 2014 Informa Healthcare USA, Inc. DOI: 10.3109/15368378.2014.921195.

Hinrikus, H., Bachmann, M., Karai, D., Lass, J. (2016). Mechanism of low-level microwave radiation effect on nervous system. Electromagn Biol Med. 36:202–212. doi: 10.1080/15368378.2016.1251451.

Jerman I. The Origin of Life from Quantum Vacuum, Water and Polar Molecules. American Journal of Modern Physics, 2016;5(4-1):34-43.

Geesink, J.H. and Meijer, D.K.F. (2016a) Quantum Wave Information of Life Revealed: An algorithm for EM Frequencies That Create Stability of Biological Order, with Implications for Brain Function and Consciousness. NeuroQuantology, 14, 106-125. https://doi.org/10.14704/nq.2016.14.1.911.

Geesink, J.H. and Meijer, D.K.F. (2016b) Quantum Wave Information of Life Revealed: An Algorithm for EM Frequencies that Create Stability of Biological Order, with Implications for Brain Function and Consciousness. NeuroQuantology, 14, 106-125. https://doi.org/10.14704/nq.2016.14.1.911.

Geesink JH and Meijer, DKF. Bio-Soliton Model that Predicts Non-Thermal Electromagnetic Frequency Bands, that Either Stabilize Living Cells. Electromagnetic Biology and Medicine, 2017a; 36, 357-378. https://doi.org/10.1080/15368378.2017.1389752.

Geesink J H, Meijer D K F (2017b). Electromagnetic Frequency Patterns that are Crucial for Health and Disease Reveal a Generalized Biophysical Principle: the GM scale. Quantum Biosystems, 8, 1-16.

Geesink J H, Meijer D K F, (2018a) Mathematical Structure of the GM Life Algorithm that May Reflect Bohm's Implicate Order. J. Modern Physics, 9, 851- 897.

Geesink J H, Meijer D K F (2018b) A semi-harmonic electromagnetic frequency pattern organizes non-local states and quantum entanglement in both EPR studies and life systems. J. Modern Physics, 9, 898-924.

Geesink, J H, Meijer, D K F (2018d) Evidence for a Guiding Coherence Principle in Quantum Physics, Quantum Biosystems | 2018 | Vol 9 | Issue 1 | Page 1- 7.

Geesink, J H, Meijer, D K F (2018e) Is the Fabric of Reality Guided by a Semi-Harmonic, Toroidal Background Field? International Journal of Structural and Computational Biology, 2018e.

Geesink, J H, Meijer, D K F (2019a) A novel biophysical quantum algorithm predicts super-conductive properties in animate and inanimate systems, Quantum Biosystems | 2019a | Vol 10 | Issue 1 | Page 1- 32.

Geesink, J H, Jerman, I, Meijer, D K F. Water: the cradle of life in action, cellular architecture is guided by coherent quantum frequencies as revealed in pure water, Water Journal, 2020a.

Geesink J H, Jerman I, Meijer D K F. Clay minerals: information network linking quantum coherence and first life, submitted, 2020b.

Geesink, JH. Informational code of biomolecules and its building blocks: quantum coherence versus decoherence, in preparation, 2020c.

Germash KV, Fil DV. Strong enhancement of third-harmonic generation in a double layer graphene system caused by electron-hole pairing, EPL (Europhysics Letters), 2017; Volume 118, Number 6.

Giannì, M, Liberti M. Apollonio F., D'Inzeo G. Modeling electromagnetic fields detectability in a HH-like neuronal system: stochastic resonance and window behaviour. Biological Cybernetics Volume 94, Issue 2, January 2006.

Gioacchino DD, Marcelli A, Puri A, Bianconi A. The a.c. susceptibility third harmonic component of NdO1-0.14F0.14FeAs: A flux dynamic magnetic analysis. Journal of Physics and Chemistry of Solids 71,2010; 1046–1052.

Golińska K., A. Coherence function in biomedical signal processing: a short review of applications in Neurology, Cardiology and Gynecology, Studies in Logic, Grammar and Rhetoric
2011 | 25(38) | 73-82.

Halgamuge M. N., Efstratios Skafidas, Devra Davis. A meta-analysis of in vitro exposures to weak radiofrequency radiation exposure from mobile phones (1990–2015), Environmental Research, Available online 13 February 2020, 109227.

Huelga, S. F., Plenio, M. B. (2013). Vibration, quanta and biology. Contemp. Phys. 54:181. and E-print: arxiv: 1307.3530.

Inbamalarand T.M., R.Sivakumar. Improved Algorithm for Analysis of DNA Sequences Using Multiresolution Transformation, Hindawi Publishing Corporation The Scientific World Journal Volume 2015, Article ID 786497, 9 pages http://dx.doi.org/10.1155/2015/786497.

Jantzen, R.T. Geodesics on the Torus and other Surfaces of Revolution Clarified Using Undergraduate Physics Tricks with Bonus: Nonrelativistic and Relativistic Kepler Problems. Physics, MathematicsPublished 2012.

Kadantsev, V.N., Goltsov, A. Collective excitations in alpha-helical protein structures interacting with environment. doi: https://doi.org/10.1101/457580.

Kavokin, A. Exciton-polaritons in microcavities: Recent discoveries and perspectives. Phys. Status Solidi B 2010; 247, 1898;1906.

Kodera S, Gomez-Tames J, Hirata A. Temperature elevation in the human brain and skin with thermoregulation during exposure to RF energy. Biomedical Engineering Online, 08 Jan 2018, 17(1):1, DOI: 10.1186/s12938-017-0432-x.

LECHELON, M.Thesis: Long-range electrodynamic interactions among biomolecules, Defended on December 11th, 2017.

Legrand, R. et al., Thermal microscopy of single biological cells. Appl. Phys. Lett. 2015, 107, 263703.

Liboff, A. R. (1985). Geomagnetic cyclotron resonance in living cells. J. Biol. Phys. 13:99–102.

Lindstrom, E., E. Lundgren, “Intracellular Calcium Oscillations Induced in a T-cell Line by a Weak 50 Hz Magnetic Field”. J. of Cellular Physiology 1993, 156:395-398.

Lednev, V. V. (1991). Possible mechanism for the influence of weak magnetic fields on biological systems. Bioelectromagnetics. 12:71–75. doi 10.1002/bem.2250.120202.

Lednev, V. V. (1993). Possible mechanism for the effect of weak magnetic fields on biological systems: Correction of the basic expression and its consequences. In: Blank, M. Ed. Electricity and Magnetism in Biology and Medicine. San Francisco: San Francisco Press. pp. 550–552.

Lundholm, I.V., Helena Rodilla, Weixiao Y. Wahlgren, Annette Duelli, Gleb Bourenkov, Josip Vukusic, Ran Friedman, Jan Stake, Thomas Schneider, Gergely Katona. Terahertz radiation induces non-thermal structural changes associated with Fröhlich condensation in a protein crystal. Structural Dynamics, 2015; 2 (5): 054702 DOI: 10.1063/1.4931825.

Marino C., Galloni P., and Merla C., Biological Effects of Electromagnetic Fields. In: Saleem Hashmi (editor-inchief), Reference Module in Materials Science and Materials Engineering. Oxford: Elsevier; 2016. pp. 1-9.
ISBN: 978-0-12-803581-8.

Marracino P., Daniel Havelka, Jiří Průša, Micaela Liberti, Jack Tuszynski, Ahmed T. Ayoub, Francesca Apollonio & Michal Cifra. Tubulin response to intense nanosecond-scale electric field in molecular dynamics simulation, Scientific Reports | (2019) 9:10477 | https://doi.org/10.1038/s41598-019-46636-4.

Mc Dermott M Let al., 2017. DNA’s Chiral Spine of Hydration. ACS Central Science 3: 708-714. https://doi.org/10.1021/acscentsci.7b00100.

Meijer, D.K.F. and Geesink, J.H. (2016c) Phonon Guided Biology: Architecture of Life and Conscious Perception Are Mediated by Toroidal Coupling of Phonon, Photon and Electron Information Fluxes at Discrete Eigenfrequencies. Neuro-Quantology, 14, 718-755. https://doi.org/10.14704/nq.2016.14.4.985

Meijer, D.K.F. and Geesink, J.H. (2017c) The Folding of Life Proteins: Being a Guest in a Multi-Scale Landscape; On the Role of Long- and Short-Range Electromagnetic Pilot Mechanisms, in an Evolutionary Context. Biological Physics, Research Gate.

Melkikh, A.V. and Meijer, D.K.F. (2018) On a Generalized Levinthal's Paradox: The Role of Long- and Short Range Interactions on Complex Bio-Molecular Reactions, including Protein and DNA Folding. Progress in Biophysics and Molecular Biology, 132, 57-79. https://doi.org/10.1016/j.pbiomolbio.2017.09.018.

Meijer, D.K.F. and Geesink (2018f) Favourable and Unfavourable EMF Frequency Patterns in Cancer: Perspectives for Improved Therapy and Prevention. Journal of Cancer Therapy, 2018, 9.

Musumeci F., Rosaria Grasso, Luca Lanzanò, Agata Scordino, Antonio Triglia, Salvatore Tudisco, Marisa Gulino. Delayed luminescence: a novel technique to obtain new insights into water structure. J Biol Phys (2012) 38:181–195. DOI 10.1007/s10867-011-9245-5.

Naarala J., Mikko Kolehmainen and Jukka Juutilainen. Electromagnetic Fields, Genomic Instability and Cancer: A Systems Biological View, Genes 2019, 10, 479; doi:10.3390/genes10060479.

Nardecchia I., Jeremie Torres, Mathias Lechelon, Valeria Giliberti, Michele Ortolani, Philippe Nouvel, Matteo Gori, Yoann Meriguet, Irene Donato, Jordane Preto, Luca Varani, James Sturgis, and Marco Pettini. Out-of-Equilibrium Collective Oscillation as Phonon Condensation in a Model Protein
PHYSICAL REVIEW X 8, 031061 (2018).

Noor NA, Mohammed HS, Ahmed NA, Radwan NM. Variations in amino acid neurotransmitters in some brain areas of adult and young male albino rats due to exposure to electromagnetic radiation. med./bio. Eur Rev Med Pharmacol Sci 2011; 15 (7): 729-742.

Olmi S., Gori M., Donato I., Pettini M. Collective behaviour of oscillating electric dipoles, CieNtifiC REPOrTS | (2018) 8:15748 | DOI:10.1038/s41598-018-33990-y.

Ozaktas H.M., Talha Cihad Gulcu, and M. Alper Kutay. Linear algebraic theory of partial coherence: continuous fields and measures of partial coherence. Journal of the Optical Society of America A Vol. 33, Issue 11, pp. 2115-2124 (2016) •https://doi.org/10.1364/JOSAA.33.002115.

Paffi A, Apollonio F, d'Inzeo G, Liberti M. Stochastic resonance induced by exogenous noise in a model of a neuronal network. Network. 2013;24(3):99-113. doi: 10.3109/0954898X.2013.793849. Epub 2013 May 8.

Pang, X. F., Chen, X. R. (2001). Distribution of vibrational energy levels of protein molecular chains. Commun. Theor. Phys. (Beijing, China). 35:323–326.

Pareja-Peña F., Antonio M. Burgos-Molina, Francisco Sendra-Portero & Miguel J. Ruiz-Gómez. Evidences of the (400 MHz – 3 GHz) radiofrequency electromagnetic field influence on brain tumor induction. Journal International Journal of Environmental Health Research, 2020.
https://doi.org/10.1080/09603123.2020.1738352

Pakhomov, A.G., Akyel, Y., Pakhomova, O.N., Stuck, B.E., Michael, R., Murphy, M.R., 1998. Current state and implications of research on biological effects of millimetre waves: a review of the literature. Bioelectromagnetics 19, 393–413. ⟨https://www.ncbi.nlm.nih.gov/pubmed/9771583⟩.
Pang, X. F., Chen, S., Wang, X., Zhong, L. (2016). Influences of electromagnetic energy on bio-energy transport through protein molecules in living systems and its experimental evidence. Int. J. Mol. Sci. 17:1130.

Pauling, L. Molecular basis of biological specicity. Nature, 248(5451):769{771, apr 1974.

Pikov, V., X. Arakaki, M. Harrington, S. E. Fraser, and P. H. Siegel, "Modulation of neuronal activity and plasma membrane properties with low-power millimeter waves in organotypic cortical slices," J. Neural Eng., vol. 7, no. 4, p. 045003, Aug. 2010.

Pirogova, E., Cosic, I. (2001). Examination of amino acid indexes within the resonant recognition model,
Proceedings of the 2nd Conference of the Victorian Chapter of the IEEE EMBS, Melbourne, Australia

Poccia, N, Ricci, A, Bianconi, A. Fractal structure favouring superconductivity at high temperatures in a stack of membranes near a strain quantum critical point. J. Supercond. Nov. Magn. 2011a; 24, 1195–1200.

Poccia N. and Bianconi A. Meeting Report The Physics of Life and Quantum Complex Matter: A Case of Cross-Fertilization Life 1, 3-6; 2011b; doi:10.3390/life1010003 life ISSN 2075-1729 www.mdpi.com/journal/life.

Pokorný, J., Jiří Pokorný; Jan Vrba. Electromagnetic communication between cells through tunnelling nanotubes, 2019 European Microwave Conference in Central Europe (EuMCE).

Preparata, G. (1995). QED Coherence in Condensed Matter. New Jersey, Singapore, London: World Scientific, pp. 25–40.

Prohofsky EW (2004). RF absorption involving biological macromolecules. Bioelectromagnetics, 25(6):441-451.

Reimers J.R., Laura K. McKemmish, Ross H. McKenzie, Alan E. Mark, and Noel S. Hush.Weak, strong, and coherent regimes of Fröhlich condensation and their applications to terahertz medicine and quantum consciousness. PNAS March 17, 2009 106 (11) 4219-4224; https://doi.org/10.1073/pnas.0806273106.

Romanenko S, Siegel PH, Wagenaar DA, Pikov V. 2014 Effects of millimeter wave irradiation and equivalent thermal heating on the activity of individual neurons in the leech ganglion. J. Neurophysiol. 112, 2423–2431. (doi:10.1152/jn.00357.2014)

Romanenko S, Siegel PH, Pikov V, Wallace V. 2016, Alterations in neuronal action potential shape and spiking rate caused by pulsed 60 GHz millimetre wave radiation. In 41st Int. Conf. on Infrared, Millimeter, and Terahertz Waves (IRMMW-THz), Copenhagen, Denmark, 25–30 September, pp. 1–2. Piscataway, NJ: IEEE.

Romanenko S., Ryan Begley, Alan R. Harvey, Livia Hool and Vincent P. Wallace. The interaction between electromagnetic fields at megahertz, gigahertz and terahertz frequencies with cells, tissues and organisms: risks and potential. Published:06 December 2017https://doi.org/10.1098/rsif.2017.0585.

Efim B. Rozenbaum, Sriram Ganeshan, and Victor Galitski. Lyapunov Exponent and Out-of-Time-Ordered Correlator's Growth Rate in a Chaotic System. Phys. Rev. Lett. 118, 086801 – Published 21 February 2017.

Rajasekaran SJ, Okamoto L, Mathey M, Fechner V, Thampy, Gu GD, Cavalleri A. Probing optically silent superfluid stripes in cuprates. Rajasekaran et al., Science 2018; 359, 575–579.
Reimers JR., Laura K. McKemmish, Ross H. McKenzie, Alan E. Mark, and Noel S. Hush, Weak, strong, and coherent regimes of Fröhlich condensation and their applications to terahertz medicine and quantum consciousness. PNAS March 17, 2009 106 (11) 4219-4224; https://doi.org/10.1073/pnas.0806273106.

Renati P., Zoltan Kovacs, Antonella De Ninno, Roumiana Tsenkova, Temperature dependence analysis of the NIR spectra of liquid water confirms the existence of two phases, one of which is in a coherent state Journal of Molecular Liquids 292 (2019) 111449.

Russell, CL. 5 G wireless telecommunications expansion: Public health and environmental implications. Environmental Research 165 (2018) 484–495.

Sahu S, Ghosh S, Ghosh B, Aswani K, Hirata K, Fujita D, Bandyopadhyay A**,** 2013. Atomic water channel controlling remarkable properties of a single brain microtubule: Correlating single protein to its supramolecular assembly. Biosensors and Bioelectronics. 47**,** 141-148 10.1016/j.bios.2013.02.050

Sahu S, Ghosh S, Fujita D, Bandyopadhyay **A**, 2015. Live visualizations of single isolated tubulin protein self-assembly via tunneling current: effect of electromagnetic pumping during spontaneous growth of microtubule. Scientific Reports. **4** [1] (2015) 10.1038/srep07303

Salford, L.G., Nitty, H., et al. (2017) The Mammalian Brain in the Electromagnetic Fields Designed by Man with Special Reference to Blood-Brain Barrier Function, Neuronal Damage and Possible Physical Mechanisms. Progress of Theoretical Physics Supplement, 173, 283-309. http://ptp.ipap.jp/link?PTPS/173/283.

Scarfì, MR, Mats-Olof Mattsson, Myrtill Simkó, Olga Zeni. Special Issue: "Electric, Magnetic, and Electromagnetic Fields in Biology and Medicine: From Mechanisms to Biomedical Applications" Int. J. Environ. Res. Public Health 2019, 16, 4548; doi:10.3390/ijerph16224548 www.mdpi.com/journal/ijerph.

Simkó M., Mats-Olof Mattsson. 5G Wireless Communication and Health Effects—A Pragmatic Review Based on Available Studies Regarding 6 to 100 GHz. Int. J. Environ. Res. Public Health 2019, 16, 3406; doi:10.3390/ijerph16183406.

Smith-Roe SL, Wyde ME, Stout MD, Winters JW, Hobbs CA, Shepard KG, Green AS, Kissling GE, Shockley KR, Tice RR, Bucher JR, Witt KL, NTP study, conclusions 2019. Environ Mol Mutagen 2019.

Sonderkamp, T, Geesink J H, Meijer D K F, (2019). Statistical analysis and prospective application of the GM-scale, a semi-harmonic EMF scale proposed to discriminate between "coherent" and "decoherent" EM frequencies on life conditions, Quantum Biosystems. 10(2) 33-51.

Streltsov A. Colloquium: Quantum coherence as a resource, REVIEWS OF MODERN PHYSICS, VOLUME 89, OCTOBER–DECEMBER 2017.

Taschin, A., Bartolini, P., Eramo, R., et al. (2013). Evidence of two distinct local structures of water from ambient to supercooled conditions. Nat. Commun. 4:2401–2411.

Pall, M. L. (2013). Electromagnetic fields act via activation of voltage-gated calcium channels to produce beneficial or adverse effects. J. Cell. Mol. Med. XX:1–9.

Sheppard AR, Swicord ML, Balzano Q (2008). Quantitative evaluations of mechanisms of radiofrequency interactions with biological molecules and processes. Health Phys, 95(4):365-396.

Tranquada J. Hidden superconductivity revealed. Kathryn Allen, Materials World magazine, 2018.

Tielrooij K J, Timmer R L A, Bakker H J, Bonn M, 2009. Structure Dynamics of the Proton in Liquid Water Probed with Terahertz Time-Domain Spectroscopy. Phys. Rev. Lett., 102:198303.

Usselman, R. J., Chavarriaga, C., Castello, P. R., et al. (2016). The quantum biology of reactive oxygen species partitioning impacts cellular bioenergetics. Sci Rep. 6:38543. Doi 10.1038/srep38543.

Vanderstraeten J, Verschaeve L. Biological effects of radiofrequency fields: Testing a paradigm shift in dosimetry. Environmental Research Volume 184, May 2020, 109387

Vasconcellos AR, Vannuchi FS, Mascarenhas S, Luzzi R. Fröhlich. Condensate: Emergence of synergetic Dissipative Structures in Information Processing Biological and Condensed Matter Systems, Information, 2012.

Veljkovic, V., Cosic, I., Dimitrijevic, B., Lalovic, D. (1985). Is it possible to analyze DNA and protein sequence by the method of digital signal processing? IEEE Trans. Biomed.
Eng. 32:337–341.

Veljkovic, V., Slavic, I. (1972). Simple General-Model Pseudopotential. Phys. Rev. Lett. 29:105–107.

Viennot, D., Aubourg, L. Chaos, decoherence and emergent extra dimensions in D-brane dynamics with fluctuations. arXiv:1802.08541v2 [hep-th], 16 May 2018.

Voiekov V, Del Giudice E 2009 Water respiration – The Basis of the Living State Water 1 52-75.

Vukova T.,Andrey Atanassov, Radoy Ivanov, Nicolina Radicheva. Intensity-dependent effects of microwave electromagnetic fields on acetylcholinesterase activity and protein conformation in frog skeletal muscles. March 2005 Medical science monitor: international medical journal of experimental and clinical research 11(2):BR50-6.

Weightman P. "Investigation of the Frohlich hypothesis with high intensity terahertz radiation", Proc. SPIE 8941, Optical Interactions with Tissue and Cells XXV; and Terahertz for Biomedical Applications, 89411F (13 March 2014); https://doi.org/10.1117/12.2057397.

Wong KW, Fung PCW, Chow WK. 5D Model Theory for the Creating of Life Forms. Journal of Modern Physics, 2019, 10, 1548-1565, https://www.scirp.org/journal/jmp, ISSN Online: 2153-120X.

Wu, TM., Austin S. Bose-Einstein condensation in biological systems. Journal of Theoretical Biology, Volume 71, Issue 2, 20 March 1978, Pages 209-214.

Yakymenko I., Olexandr Tsybulin, Evgeniy Sidorik, Diane Henshel, Olga Kyrylenko4 and Sergiy Kyrylenko. Oxidative mechanisms of biological activity of low-intensity radiofrequency radiation. Electromagn Biol Med, Early Online: 1–16, 2015 Informa Healthcare USA, Inc. DOI: 10.3109/15368378.2015.1043557.

Zhedong Zhang, Girish S. Agarwal, Marlan O. Scully. Institute for Quantum Science and Engineering, Quantum fluctuations in Fröhlich condensate of molecular vibrations driven far from equilibrium. Phys. Rev. Lett. 122, 158101 (2019), DOI:10.1103/PhysRevLett.122.158101.

Zurek, W H. DECOHERENCE, EINSELECTION, AND THE EXISTENTIAL INTERPRETATION. Theoretical Astrophysics T-6, MS B288, LANL Los Alamos, New Mexico 87545 February 1, 2008; arXiv:quant-ph/9805065 865 (2017) 012007 doi :10.1088/1742-6596/865/1/012007.

Appendix 1. Quantum informational code: calculated examples of coherent frequencies from sub Hertz till PHz

Factor	F1,m	F2,m	F3,m	F4,m	F5,m	F6,m	F7,m	F8,m	F9,m	F10,m	F11,m	F12,m
m=0	1.0000	1.0535	1.1250	1.1852	1.2656	1.3333	1.4142	1.5000	1.5803	1.6875	1.7778	1.8984 Hz
m=1	2.0000	2.1070	2.2500	2.3704	2.5312	2.6666	2.8284	3.0000	3.1606	3.3750	3.5556	3.7968 Hz
m=2	4.0000	4.2140	4.5000	4.7408	5.0624	5.3332	5.6568	6.0000	6.3212	6.7500	7.1112	7.5936 Hz
m=5	32.000	33.712	36.000	37.9264	40.4992	42.6656	45.2544	48.000	50.5696	54.000	56.8896	60.7488 Hz
m=8	256.00	269.70	288.00	303.41	324.00	341.33	362.04	384.00	404.54	432.00	455.12	486.00 Hz
m=12	4.0960	4.3151	4.6080	4.8546	5.1839	5.4613	5.7926	6.1440	6.4729	6.9120	7.2819	7.7759 KHz
2^24	16.777	17.675	18.874	19.884	21.233	22.370	23.726	25.166	26.513	28.312	29.827	31.850 MHz
2^32	4.2950	4.5248	4.8318	5.0904	5.4357	5.7266	6.0739	6.4425	6.7873	7.2478	7.6356	8.1536 GHz
2^40	1.0995	1.1583	1.2370	1.3031	1.3915	1.4660	1.5549	1.6493	1.7376	1.8554	1.9547	2.0873 Thz
2^48	281.47	296.53	316.66	333.60	356.23	375.29	398.06	422.21	444.81	474.99	500.41	534.35 Thz

Equation of discrete energy distribution

$E_n = \hbar\, \omega_{ref}\, 2^{n+p}\, 3^m$

En: Energy distribution, ω_{ref}: reference frequency 1 Hz, $\hbar$: Reduced Planck's constant, n: Series of integers: 0, 0.5, 2, 4, 5, 7, 8, -1, -3, -4, -6, -7; m: series of integers: 0, 1, 2, 3, 4, 5, -1, -2, -3, -4, -5; p: series of integers: <-4, -4, -3, -2, -1, 0, 1, 2, 3, 4, 5, 6, > +52

Generalized scale of coherent frequencies

$F_m(coh.1) = 2^0 3^0 2^m$ $F_m(coh.7) = 2^{0.5} 2^m$

$F_m(coh.2) = 2^8 3^{-5} 2^m$ $F_m(coh.8) = 2^{-1} 3^1 2^m$

$F_m(coh.3) = 2^{-3} 3^2 2^m$ $F_m(coh.9) = 2^7 3^{-4} 2^m$

$F_m(coh.4) = 2^5 3^{-3} 2^m$ $F_m(coh.10) = 2^{-4} 3^3 2^m$

$F_m(coh.5) = 2^{-6} 3^4 2^m$ $F_m(coh.11) = 2^4 3^{-2} 2^m$

$F_m(coh.6) = 2^2 3^{-1} 2^m$ $F_m(coh.12) = 2^{-7} 3^5 2^m$

m = 0 till 54.

Appendix 2. Frequencies that are health or unhealthy, related to the proposed algorithmic frequency patterns

Algorithmic coherent reference scale:

2.1475 2.2624 2.4159 2.5452 2.71785 2.8633 3.03695 3.22125 3.39365 3.6239 3.8178 4.0768 GHz

Algorithmic decoherent reference scale:

2.0922 2.2042 2.3379 2.4797 2.6301 2.7896 2.9489 3.1278 3.3063 3.5069 3.7196 3.9452 GHz

2.1 Frequencies that are proposed unhealthy, related to decoherent frequency signals at MHz and GHz (not modulated), that fit in the algorithm

Name, (year): (applied frequency, calculated decoherent pointer frequency; difference between applied frequency and pointer frequency); calculated normalized applied frequency.

1) **Brown-Woodman et al. (1988)**: (27.12 Mhz; 27.40; 1.0%); norm.: 3.4714 GHz

Brown-Woodman PDC & J. A. Hadley; Studies of the Teratogenic Potential of Exposure of Rats to 27.12 MHZ Pulsed Shortwave Radiation, Journal of Bioelectricity, Volume 7, 1988 - Issue 1.

2) **Tofani et al. (1986)**: (27.12 MHz; 27.40; 1.0%); norm.: 3.4714 GHz

Tofani S, Agnesod G, Ossola P, Ferrini S, Bussi R. Effects of continuous low-level exposure to radiofrequency radiation on intrauterine development in rats. Health Physics. 1986;51(4):489-99.

3) **Lary et al. (1982, 1983)**: (27.12 MHz; 27.40; 1.0%); norm.: 3.4714 GHz

Sprague-Dawley rats (F), 27.12 MHz 11 W/Kg 30 min, Una tantum at gestation days 1, 3, 5, 7, 9, 11, 13, or 15, 30 min NR Viable litter size/live birth index, neonatal growth, neonatal survival indices, prenatal mortality Increased incidence of pre-implantation and post-implantation fetal malformations ($p < 0.05$), reduced fetal weight and crownrump length, increased incidence of dead or resorbed fetuses ($p < 0.05$).

Lary, J.M.; Conover, D.L.; Foley, E.D.; Hanser, P.L. Teratogenic effects of 27.12 MHz radiofrequency radiation in rats. Teratology 1982, 26, 299–309. Lary, J.M.; Conover, D.L.; Johnson, P.H.; Burg, J.R. Teratogenicity of 27.12-MHz radiation in rats is related to duration of hyperthermic exposure. Bioelectromagnetics 1983, 4, 249–255.

4) **Bawin et al. (1973)**: (147 Mhz; 146.1; 0.62%); norm.: 2.352 GHz

Bawin, S.M., Gavalas-Medici, R.J. and Adey, W.R., Effects of modulated very high frequency fields on specific brain rhythms in cats. Brain Res 58:365-384, 1973.

L. Guo et al., "Effects of 220 MHz Radiofrequency Field on Sperm Quality of SD Rat," 2019 IEEE MTT-S International Microwave Biomedical Conference (IMBioC), Nanjing, China, 2019, pp. 1-4.

5) **Guo et al. (2019)**: (220 Mhz; 219.18; 0.37); norm.: 3.520 GHz

These data collectively suggested that under the present experimental conditions, 220 MHz RF exposure could affect sperm quality in rats, and the disruption of secreting function of Leydig cells and increased apoptosis of testis cells induced by RF field might both account for this damaging effect.

6) **Klos-Witkowska et al. 2019:** (230 MHz; 232.48; 1.07%); norm.: 3.680 GHz

Klos-Witkowska A., Vasyl Martsenyuk; Mikolaj Karpinski; Ibrahim Obeidat. Influence of radiation at different RF frequencies on Bovine Serum Albumin stability in the aspect of biosensor, 2019 Advances in Science and Engineering Technology International Conferences (ASET)

Scans of electromagnetic field distribution for (125, 180 and 230 MHz) have been collected with the use of 3D EMC scanner and specially constructed experimental setup. The analysis of UV/Vis spectrum was used for testing influence of electromagnetic field on Bovine Serum Albumin and changes through 19 days. The protein beyond the wide application in pharmacokinetics and pharmacodynamics drug study, is also widely used in the biosensor construction. Increase of absorption of BSA with time, related to conformational changes of protein was observed. The differences between irradiated and control samples have been noticed. The impact of electromagnetic field on protein showed tendency to BSA stabilization under 125, 180, 230 MHz exposition. Changes were the most notable for 230 MHz whereas 125 MHz and 180 were small but significant.

7) **Jauchem and Frei (1997)**: (350 Mhz; 348.7; 0.37%); norm.: 2.800 GHz

Jauchem JR. Exposure to extremely-low-frequency electromagnetic fields and radiofrequency radiation: cardiovascular effects in humans. Int Arch Occup Environ Health 70:9-21; 1997.

8) **Holt JA (1977)**: (434 MHz; 438.36; 0.99%); norm.: 3.472 GHz

Holt JA. Increase in X-Ray Sensitivity of Cancer after Exposure to 434 MHz Electromagnetic Radiation. med. app., J Bioeng 1977; 1 (5-6): 479-485.

9) **Sanders et al. (1980)**: (591 Mhz; 584.5; 1.1%); norm.: 2.364 GHz

Sanders, A.P., Schaefer, D.J. and Joines, W.T., Microwave effects on energy metabolism of rat brain. Bioelectromagnetics 1:171-182, 1980.

10) **Frei et al. (1989):** (700 MHz; 697.4; 0.37%); norm.: 2.800 GHz

Frei MR, Jauchem JR, Padilla JM. Effects of field orientation during 700-MHz radiofrequency irradiation of rats. med./bio.Physiol Chem Phys Med NMR 1989; 21 (1): 65-72.

Heart rate and mean arterial blood pressure significantly increased during exposure; however, alterations between orientations were not different. Respiratory rate significantly increased during exposure in H-, but not in E-orientation.

11) **Daniells et al. (1998)**: (750 Mhz; 737.2; 1.73%); norm.: 3.000 GHz

Daniells, C, Duce, I, Thomas, D, Sewell, P, Tattersall, J, de Pomerai, D, 1998: "Transgenic nematodes as biomonitors of microwave-induced stress". Mutat Res 399: 55-64.

12) **Mashevich et al. (2003):** (830 Mhz; 826.8; 0.38%); norm.: 3.320 GHz

Mashevich M, Folkman D, Kesar A, Barbul A, Korenstein R, Jerby E, Avivi L. Exposure of human peripheral blood lymphocytes to electromagnetic fields associated with cellular phones leads to chromosomal instability. Bioelectromagnetics. 2003 Feb;24(2):82-90.

13**) Reserve**

14) **Maskey et al. (2014)**: (835 Mhz; 826.8; 1.00%); norm.: 3.340 GHz

Maskey D, Kim HG, Suh MW, Roh GS, Kim MJ. Alteration of glycine receptor immunoreactivity in the auditory brainstem of mice following three months of exposure to radiofrequency radiation 835 MHz at SAR 4.0 W/kg. Int J Mol Med. 2014; 34(2): 409-19.

15) **Donnellan et al. (1997)**: (835 Mhz; 826.8; 1.00%); norm.: 3.340 GHz

Donnellan M et al. Effects of exposure to electromagnetic radiation at 835 Mhz on growth, morphology and secretory characteristics of a mast cell analogue RBL-2H3, Cell boil int. 21:427-439, 1997.

16) **Maskey et al. (2010)**: (835 Mhz; 826.8; 1.00%); norm.: 3.340 GHz

Maskey D, Kim M, Aryal B, Pradhan J, Choi IY, Park KS, Son T, Hong SY, Kim SB, Kim HG, Kim MJ. Effect of 835 MHz radiofrequency radiation exposure on calcium binding proteins in the hippocampus of the mouse brain. med./bio.Brain Res 2010; 1313: 232-241. Journal PubMed doi:10.1016/j.brainres.2009.11.079.

Exposure duration: continuous exposure for up to one month; SAR: 4 W/kg average over mass (whole body) (exposure group high energy); SAR: 1.6 W/kg average over mass (whole body) (exposure group low energy). The body weights of the different groups did not change significantly. The data showed an almost complete pyramidal cell loss in the hippocampal CA1 area of mice exposed to electromagnetic fields for one month (group 6). The authors conclude that 835 MHz radiofrequency exposure may be harmful.

17) **Kim et al. (2018):** (835 MHz; 826.8; 1.00%); norm.: 3.340 GHz

Kim JH, Sohn UD, Kim HG, Kim HR. Exposure to 835 MHz RF-EMF decreases the expression of calcium channels, inhibits apoptosis, but induces autophagy in the mouse hippocampus. Korean J Physiol Pharmacol. 2018 May;22(3):277-289. doi: 10.4196/kjpp.2018.22.3.277.

These results suggested that exposure of RF-EMF could alter intracellular calcium homeostasis by decreasing calcium channel expression in the hippocampus; presumably by activating the autophagy pathway, while inhibiting apoptotic regulation as an adaptation process for 835 MHz RF-EMF exposure.

18) **Pavicic I and Trosic I (2006);** (864 Mhz; 876.8; 1.46%); norm.: 3.456 GHz

Pavicic I, Trosic I. Influence of 864 MHz electromagnetic field on growth kinetics of established cell line. med./bio.Biologia 2006; 61 (3): 321-325.

Growth curves of exposed cells showed a significant decrease after 2 and 3 hours of exposure on experimental day 3, respectively, in comparison to sham exposed cells. Both, the colony forming ability and cell viability of exposed cells did not significantly differ from sham exposure condition. In conclusion, under strictly controlled laboratory conditions, applied radiofrequency irradiation significantly affected cell proliferation kinetics but not cell viability or ability of V79 cells to form colonies.

19) **Zmyslony et al. (2004)**; (930 MHz; 930.3; 0.03%); norm.: 3.720 GHz

Zmyslony M, Politanski P, Rajkowska E, et al. Acute exposure to 930 MHz CW electromagnetic radiation in vitro affects reactive oxygen species level in rat lymphocytes treated by iron ions. Bioelectromagnetics 2004; 25: 324–8

5 W/m² unspecified. The data show that acute exposure does not affect the number of produced ROS. If, however, iron ions (FeCl2) with final concentration 10 µg/ml) was added to the lymphocyte suspensions to stimulate ROS production, after both durations of exposure (5 and 15 min), the magnitude of fluorescence (ROS level during the experiment) was significantly greater in the irradiated cells.

20) **Pavicic I and Trosic I (2008);** (935 Mhz; 929.8; 0.56%); norm.: 3.740 GHz

Pavicic I and Trosic I. Impact of 864 MHz or 935 MHz radiofrequency microwave radiation on the basic growth parameters of V79 cell line. Acta Biol Hung 2008; 59 (1): 67-76.

864 MHz, Modulation type: CW; Exposure duration: continuous for 1, 2, and 3 h power density: 0.14 W/m²
935 MHz, Modulation type: CW; Exposure duration: continuous for 1, 2, and 3 h power density: 0.17 W/m^2
Cell growth impact was time-dependent for both fields: The growth of the 864 MHz exposed cells was significant decreased after 2 h and 3 h exposure 72 h after irradiation. A similar effect was observed 72 h after exposure for cells exposed to 935 MHz microwaves for 3 h.

21) **Maes et al. (1997)**; (935.2 MHz; 930.3; 0.5%); norm.: 3.7408 GHz

Maes A, Collier M, Van Gorp U, Vandoninck S, Verschaeve L, Mutat Res Genet Toxicol Environ Mutagen 1997; 393 (1-2): 151-156. Cytogenetic effects of 935.2-MHz (GSM) microwaves alone and in combination with mitomycin C. med./bio.

Exposure duration: continuous for 2 h power: 4.5 W, SAR: 0.4 W/kg (0.3-0.4 W/kg). No direct cytogenetic effect was found. The combined exposure of the cells to the radiofrequency fields followed by their cultivation in the present of mitomycin C revealed a very weak effect when compared to cells exposed to mitomycin alone.

22) **Herrala et al. (2018):** (872 MHz, 876.80; 0.55%); norm.: 3.488 GHz

Herrala M., Ehab Mustafa, Jonne Naarala & Jukka Juutilainen. Assessment of genotoxicity and genomic instability in rat primary astrocytes exposed to 872 MHz radiofrequency radiation and chemicals. International Journal of Radiation Biology
Volume 94, 2018 - Issue 10: Electromagnetic Fields in Biology and Medicine.

Rat primary astrocytes were exposed to 872 MHz GSM-modulated or continuous wave (CW) RF radiation at specific absorption rates of 0.6 or 6.0 W/kg for 24 h. Menadione (MQ) and methyl methanesulfonate (MMS; only in genotoxicity experiments) were used as co-exposures. Results: No IGI was observed from RF radiation alone or combined treatment with MQ. RF radiation alone was not genotoxic. RF radiation combined with chemical exposure showed some statistically significant differences: increased DNA damage at 6.0 W/kg but decreased DNA damage at 0.6 W/kg in cells exposed to GSM-modulated RF radiation and MQ, and increased micronucleus frequency in cells exposed to CW RF radiation at 0.6 W/kg and MMS. Conclusions: Exposure to GSM modulated RF radiation at levels up to 6.0 W/kg did not induce or enhance genomic instability in rat primary astrocytes. Lack of genotoxicity from RF radiation alone was convincingly shown in multiple experiments. Co-genotoxicity of RF radiation and genotoxic chemicals was not consistently supported by the results.

23) **Luukkonen et al. (2009): (**872 Mhz; 876.7; 0.55%); norm.: 3.488 GHz

Luukkonen J, Hakulinen P, Maki-Paakkanen J, et al. Enhancement of chemically induced reactive oxygen species production and DNA damage in human SH-SY5Y neuroblastoma cells by 872 MHz radiofrequency radiation. Mutat Res 2009; 662: 54–8.

24) **Hao et al. (2012)**: (916 Mhz; 930.28; 1.5%); norm.: 3.664 GHz

Hao, Dongmei, Lei Yang,1 Su Chen,2 Yonghao Tian,2 and Shuicai Wu1, 916 MHz electromagnetic field exposure affects rat behavior and hippocampal neuronal discharge☆ Neural Regen Res. 2012 Jul 5; 7(19): 1488–1492.

25) **Yang, L. et al. (2012)**: (916 Mhz; 930.28; 1.5%); norm.: 3.664 GHz

Yang L, Hao D, Wang M, Zeng Y, Wu S, Zeng Y. Cellular neoplastic transformation induced by 916 MHz microwave radiation. med./bio. Cell Mol Neurobiol 2012; 32 (6): 1039-1046.

The data showed that cell morphology (loss of contact inhibition) and cell proliferation were changed after 5-8 weeks of exposure: The cells of the exposed groups formed colonies in the soft agar plates, whereas the control cells did not. In the carcinogenesis assay, tumors developed on the back of mice inoculated with the exposed cells after 5-7 weeks. Tumors also developed in the additional two mice injected with the mashed tumor tissue (after 4 weeks). All effects were time and dose dependent. In conclusion, the results indicate that microwave exposure can promote neoplastic transformation of NIH3T3 cells.

26) **Johnson and Guy (1972)**: (918 Mhz; 929.9; 1.3%); norm.: 3.672 GHz

Johnson C.C. and Guy, A.W., Nonionizing electromagnetic wave effect in biological materials and systems. Proc IEEE 60:692-718, 1972.

27) **Zmyslony et al. (2004)**: (930 Mhz; 929.9; 0.01%); norm.: 3.720 GHz

Zmyslony M, Politanski P, Rajkowska E, et al. Acute exposure to 930 MHz CW electromagnetic radiation in vitro affects reactive oxygen species level in rat lymphocytes treated by iron ions. Bioelectromagnetics 2004; 25: 324–8.

28) **Maes et al. (1997)**: (935.2 Mhz; 929.9; 0.57%); norm.: 3.741 GHz

Maes A, Collier M, Van Gorp U, Vandoninck S, Verschaeve L, 1997: Cytogenetic effects of 935.2-MHz (GSM) microwaves alone and in combination with mitomycin C. Mutat Res 393(1-2): 151-156.

29) **Jauchem and Frei (2000)**: (1000 Mhz; 986.3; 1.4%); norm.: 4.000 GHz

Jauchem et al 2000 Colonic and sub-cutaneous temperatures, heart rate, respiratory rate, mean arterial blood pressure in anesthetized rats 1 GHz and/or 10 GHz at whole-body SARs of 12 W kg-1 until death.

30) **De Pomerai et al. (2003)**: (1000 Mhz; 986.3; 1.4%); norm.: 4.000 GHz

De Pomerai DI, Smith B, Dawe A, North K, Smith T, Archer DB, Duce IR, Jones D, Candido EP. Microwave radiation can alter protein conformation without bulk heating. FEBS Lett 543:93-97; 2003.

31) **Todorova et al. (2020):** (1.0 GHz, 0.9863 GHz; 1.39%); norm.: 4.000 GHz

32) (2.5 GHz, 2.480, 0.82%); norm.: 2.500 GHz

33) (5.0 GHz, 4.9594; 0.82%); norm.: 2.500 GHz

Estimated decoherent states of EM field induced peptide conformations. All the simulated frequencies at low strength fields (0.007–0.0007 V/nmrms) resulted in the formation of amyloid-prone hairpin conformations similar to those formed under the weak static electric field and ambient conditions.

Todorova, N., A. Bentvelzen, and I. Yarovsky. Electromagnetic field modulates aggregation propensity of amyloid peptides. J. Chem. Phys. 152, 035104 (2020); https://doi.org/10.1063/1.5126367.

34) **Lu et al. (1992)**: (1250 MHz; 1239.8; 0.82%); norm.: 2.500 GHz

Lu, S.T., Brown, DO., Johnson, CE, Mathur, SP, Elson EC. Abnormal cardiovascular responses induced by localized high-power microwave exposure, IEEE Transactions on Biomedical engineering, 1992.

35) **Oscar and Hawkins (1977)**: (1300 MHz; 1315.0; 1.1%) norm.: 2.600 GHz

Oscar, K.J. and Hawkins, T.D., Microwave alteration of the blood-brain-barrier system of rats. Brain Res 126:281-293, 1977.

36) **Schirmacher et al. (1999)**: (1750 MHz; 1753.5; 0.20%); norm.: 2.500 GHz

Schirmacher, A, Bahr, A, Kullnick, U, Stoegbauer, F, 1999: Electromagnetic fields (1.75 GHz) influence the permeability of the blood-brain barrier in cell culture model. Presented at the Twentieth Annual Meeting of the Bioelectromagnetics Society, St. Pete Beach.

37) **Mancinelli et al. (2004)**: (1950 MHz; 1972.6; 1.15%); norm.: 3.900 GHz

Mancinelli F, Caraglia M, Abbruzzese A, d'Ambrosio G, Massa R, Bismuto E. Non-thermal effects of electromagnetic fields at mobile phone frequency on the refolding of an intracellular protein: myoglobin. Published in: J Cell Biochem 2004; 93 (1): 188-196. To study possible nonthermal effects of microwaves on the refolding of myoglobin as model protein.

38) **Miyakoshi et al. (2005):** (1950 MHz; 1972.6; 1.15%); norm.: 3.900 GHz

Miyakoshi J, Takemasa K, Takashima Y, Ding GR, Hirose H, Koyama S. Effects of exposure to a 1950 MHz radio frequency field on expression of Hsp70 and Hsp27 in human glioma cells. med./bio.Bioelectromagnetics 2005; 26 (4): 251-257

Sham-exposed and exposed cells demonstrated a similar growth pattern up to 4 days after exposure. Exposure at both 2 and 10 W/kg did not affect the growth of the cells. In addition, there were no significant differences in protein expression of HSP27 and HSP70 between sham-exposed and exposed cells at a SAR of 1, 2, or 10 W/kg for 1 and 2 h. However, exposure at a SAR of 10 W/kg for 1 and 2 h decreased the protein level of phosphorylated Hsp27 significantly. The data suggest that although exposure to a 1950 MHz radiofrequency field has no effect on cell proliferation and expression of HSP27 and HSP70, it may inhibit the phosphorylation of HSP27 at serine 78 in MO54 cells (HSP27 is phosphorylated at three phosphorylation sites (serine 15, serine 78, and serine 82) by protein kinases. In this investigation, an anti-HSP27 antibody that is specific for phosphorylated HSP27 (serine 78) was used).

39) **Iyama et al. (2004)**: (2000 MHz; 1972.6; 1.4%); norm.: 4.000 GHz

Iyama T, Ebara H, Tarusawa Y, Uebayashi S, Sekijima M, Nojima T, Miyakoshi J. Large scale in vitro experiment system for 2 GHz exposure. Bioelectromagnetics 25:599-606; 2004.

40) **Senavirathna et al. (2014)**: (2000; 1972.6; 1.4%); norm.: 4.000 GHz

Senavirathna Mudalige, Don Hiranya Jayasanka, Takashi Asaeda, Bodhipaksha Lalith Sanjaya Thilakarathne, Hirofumi Kadonoa, Nanometer-scale elongation rate fluctuations in the Myriophyllum aquaticum (Parrot feather) stem were altered by radio-frequency electromagnetic radiation (plants), 2014.

41) **Esmekaya et al. (2013)**: (2100 MHz; 2092.2; 0.37%); norm.: 2.100 GHz

Esmekaya MA, Seyhan N, Kayhan H, Tuysuz MZ, Kursun AC, Yagci M. Investigation of the effects of 2.1 GHz microwave radiation on mitochondrial membrane potential (DeltaPsim), apoptotic activity and cell viability in human breast fibroblast cells. Cell Biochem Biophys 2013; 67 (3): 1371-1378.

In the exposed cell cultures, the cell viability was significantly decreased compared to the corresponding sham exposure. Annexin V and propidium iodide staining showed a significantly increased apoptosis rate in exposed cell cultures in comparison to the sham exposed cell cultures.The mitochondrial membrane potential was significantly decreased in exposed cell cultures compared to sham exposure. The data indicate that exposure at 0.142 mW/cm² of human breast fibroblasts to a W-CDMA signal could reduce the cell viability and induce apoptosis via a mitochondrial pathway.

42) **Esmekaya et al. (2017)**: (2100 MHz; 2092.2; 0.37%); norm.: 2.100 GHz

Esmekaya MA, Canseven AG, Kayhan H, Tuysuz MZ, Sirav B, Seyhan N. Mitochondrial hyperpolarization and cytochrome-c release in microwave-exposed MCF-7 cells. Gen Physiol Biophys 2017; 36: 211-218.

Cells exposed to the electromagnetic field at 0.12 mW/cm² for 4 hours (group 1) or 24 hours (group 2) showed a significantly decreased cell viability compared to sham exposed cells. The percentage of apoptotic cells, level of cytochrome-c and the mitochondrial membrane potential were significantly higher in exposed cells (groups 1 and 2) compared to sham exposed cells. The authors conclude that exposure of breast cancer cells to a 2.1 GHz electromagnetic field might cause hyperpolarization of mitochondria which in turn could induce apoptosis.

43) **Bedir et al. (2015)**: (2100 MHz; 2092.2; 0.37%); norm.: 2.100 GHz

Bedir R, Tumkaya L, Mercantepe T, Yilmaz A. Pathological Findings Observed in the Kidneys of Postnatal Male Rats Exposed to the 2100 MHz Electromagnetic Field. Published in: Arch Med Res 2018; 49 (7): 432-440

Twenty-four Sprague Dawley rats were divided into a control group (n 5 8, no EMF exposure), a group exposed to 2100 MHz for 6 h for 30 d (n 5 8), and a group exposed to 2100 MHz for12 h for 30 d (n 5 8). Deterioration was observed in the brush border in renal tubules of the EMF groups. The results of the immunohistochemical analysis revealed a greater number of
positively stained renal tubular epithelial cells in the EMF groups as compared with that in the control group. In the EMF groups, renal MDA levels increased, and renal GSH levels decreased compared with those in the control group, as shown by a biochemical examination (p 5 0.00 and p 5 0.00, respectively). Conclusion. The findings showed that exposure to 2100 MHz for 6 and 12 h induced oxidative stress-mediated acute renal injury, depending on the length of exposure and dosage.

44) **Sahin et al. (2016)**: (2100 MHz; 2092.2; 0.37%); norm.: 2.100 GHz

Sahin D, Ozgur E, Guler G, Tomruk A, Unlu I, Sepici-Dincel A, Seyhan N. The 2100 MHz radiofrequency radiation of a 3G-mobile phone and the DNA oxidative damage in brain. med./bio.J Chem Neuroanat 2016; 75 Pt B: 94-98.

Exposure duration: 6 h/day on 5 consecutive days/week for 2 weeks; acute exposure electric field strength: 16 V/m
SAR: 0.4 W/kg. The amount of oxidative DNA damage was significantly increased after two weeks of exposure (group 1) compared to the control group (group 2), whereas no differences were found in lipid peroxidation.
After 8 weeks of exposure (group 3), oxidative DNA damage as well as lipid peroxidation were significantly reduced compared to the control group (group 4). The authors conclude that an acute exposure of rats to a 2100 MHz electromagnetic field could cause oxidative DNA damage in the brain. However, chronic exposure could also lead to the adaptation and stimulation of DNA repair mechanisms.

45) **Gokcek-Sarac et al. (2017):** (2100 MHz; 2092.2; 0.37%); norm.: 2.100 GHz

Gokek-Sarac C., Hakan Er, Ceren Kencebay Manas, Deniz Kantar Gok, Sukru Ozen and Narin Derin. Effects of acute and chronic exposure to both 900 MHz and 2100 MHz electromagnetic radiation on glutamate receptor signaling pathway. INTERNATIONAL JOURNAL OF RADIATION BIOLOGY, 2017. https://doi.org/10.1080/09553002.2017.1337279

The obtained results revealed that the hippocampal level/activity of selected enzymes was significantly higher in the chronic groups as compared to the acute groups at both 900 and 2100 MHz RF-EMR exposure. In addition, hippocampal level/activity of selected enzymes was significantly higher at 2100MHz RF-EMR than 900 MHz RF-EMR in both acute and chronic groups.

46) **Jong Jin Oh et al. (2018):** (2104 MHz; 2092.2; 0.37%); norm.: 2.100 GHz

Jong Jin Oh, Seok-Soo Byun, Sang Eun Lee, Gheeyoung Choe, and Sung KyuHong. Effect of Electromagnetic Waves from Mobile Phones on Spermatogenesis in the Era of 4G-LTE. Hindawi BioMed Research International
Volume 2018, Article ID 1801798, 8 pages https://doi.org/10.1155/2018/1801798.

To investigate the effect of long duration exposure to electromagnetic field from mobile phones on spermatogenesis in rats using 4G-LTE. The power was generated by a specific generator (Korea E3 Test Institute) operating at 2.104 GHz continuously. For rats weighing between 150 and 200 g, whole-body averaged specific absorption rate (SAR) was determined to be 3.0 W/kg. Methods. Twenty Sprague-Dawley male rats were placed into 4 groups according to the intensity and exposure duration: Group 1 (sham procedure), Group 2 (3 cm distance + 6 h exposure daily), Group 3 (10 cm distance + 18 h exposure daily), and Group 4 (3 cm distance + 18 h exposure daily). After 1 month, we compared sperm parameters and histopathological findings of the testis. Results. The mean spermatid count (×106/ml) was 398.6 in Group 1, 365.40 in Group 2, 354.60 in Group 3, and 298.60 in Group 4 (p = 0.041). In the second review, the mean count of spermatogonia in Group 4 (43.00) was significantly lower than in Group 1 (57.00) and Group 2 (53.40) (p < 0.001 and p = 0.010, resp.). The sum of the germ cell counts was decreased in Group 4 compared to Groups 1, 2, and 3 (p = 0.032). The mean Leydig cell count was significantly decreased in Group 4 (p < 0.001). Conclusions. The longer exposure duration of electromagnetic field decreased the spermatogenesis. Our findings warrant further investigations on the potential effects of EMF from mobile phones on male fertility.
47) **Kesari et al. (2014):** (2115 MHz; 2092.2; 1.09%); norm.: 2.115 GHz

Kesari KK, Meena R, Nirala J, Kumar J, Verma HN. Effect of 3G Cell Phone Exposure with Computer Controlled 2-D Stepper Motor on Non-thermal Activation of the hsp27/p38MAPK Stress Pathway in Rat Brain. Published in: Cell Biochem Biophys 2014; 68 (2): 347-358.

2,115 MHz, exposure duration: continuous for 2 hours/day for 60 days, SAR: 0.9 W/kg mean (according to manufacturer's instruction), SAR: 0.26 W/kg. In the exposed group, the level of reactive oxygen species, DNA damage, protein expression of all examined proteins and the apoptosis rate were significantly increased compared to the sham exposure group. No significant changes occurred between the sham exposure group and the cage control. The authors conclude that exposure to a radiofrequency electromagnetic field emitted by a 3G mobile phone could have a deleterious effect on the brain of young rats.

48) **Chandel et al. (2019)**: (2350 MHz; 2337.9; 0.52%); norm.: 2.350 GHz

Chandel S, Kaur S, Issa M, Singh HP, Batish DR, Kohli RK. Exposure to mobile phone radiations at 2350 MHz incites cyto- and genotoxic effects in root meristems of Allium cepa. [med./bio.], J Environ Health Sci Eng 2019; 17 (1): 97-104

The results manifested a significant increase of MI and chromosomal aberrations (%) upon 4 h, and ≥ 2 h of exposure, respectively, as compared to the control. No specific changes in phase index in response to EMF-r exposure were observed. Theb % HDNA and % TDNA values exhibited significant changes in contrast to that of control upon 2 h and 4 h of exposure,
respectively. However, TM and OTM did not change significantly. Conclusions Our results infer that continuous exposures of radiofrequency EMF-r (2350 MHz) for long durations have a potential of inciting cyto- and genotoxic effects in onion root meristems.

49) **Shandalal et al. (1979)**: (2375 MHz; 2337.9; 1.6%); norm.: 2.375 GHz

Shandala, M.G., Dumanski, U.D., Rudnev, M.I., Ershova, L.K. and Los, I.P., Study of nonionizing microwave radiation effects upon the central nervous system and behavior reaction. Environ Health Perspect 30:115-121, 1979.

50) **Lai et al. (1987, 1988):** (2450 MHz; 2479.6; 1.2%); norm.: 2.450 GHz

Lai, H., Horita, A., Chou, C.K. and Guy, A.W., Low-level microwave irradiation affects central cholinergic activity in the rat. J Neurochem 48:40-45, 1987.

51) **Deshmukh et al. (2015)**: (2450 MHz; 2479.6; 1.2%); norm.: 2.450 GHz

Deshmukh P.S. et al., 2015. Cognitive impairment and neurogenotoxic effects in rats exposed to low-intensity microwave radiation. Int J Toxicol. 34(3): 284-290.

52) **D'Andrea et al. (1986)**: (2450 MHz; 2479.6; 1.2%); norm.: 2.450 GHz

D'Andrea JA, DeWitt JR, Gandhi OP, Stensaas S, Lords JL, Nielson HC. Behavioral and physiological effects of chronic 2,450-MHz microwave irradiation of the rat at 0.5 mW/cm2. med./bio.Published in: Bioelectromagnetics 1986; 7 (1): 45-56.

2.45 GHz Modulation type: CW, Exposure duration: 630 h altogather (7 h/d, 7 d/wk)
power density: 5 W/m² mean, SAR: 140 µW/g mean (partial body) (0.11 to 0.18 W/kg; determined by twin well calorimetry method). Daily measures of body mass and food and water intake indicated no statistically significant effects of microwave irradiation. Monthly assessment of reactivity to electric footshock, levels of cholinesterase and sulfhydryl groups in blood, and 17-ketosteroids in urine revealed no reliable differences between sham-exposed and microwave-exposed animals. After the 90 days of irradiation, rats from each group were assessed for open field behavior, shuttlebox performance, and schedule-controlled lever pressing for food pellets. Statistically significant differences between microwave-exposed and sham-exposed animals were found in shuttlebox performances and lever pressing. Post mortem measures of mass of several organs and microscopic examination of adrenal tissue revealed no differences between the two groups of rats. In summary, the results of chronic intermittent irradiation of rats to 0.5 mW/cm² appear to be minor or of little biological significance.

53) **Switzer and Mitchell (1977)**: (2450 MHz; 2479.6; 1.2%); norm.: 2.450 GHz

Switzer, W.G. and Mitchell, D.S., Long-term effects of 2.45 GHz radiation on the ultrastructure of the cerebral cortex and hematologic profiles of rats. Radio Sci 12:287-293, 1977.

54) **Meena et al., (2014)**: (2450 MHz; 2479.6; 1.2%); norm.: 2.450 GHz

Meena et al., 0.14W/Kg Wistar rats (Melatonin 2 mg/kg bw/day) 2 h/day, 7 days/week, 45 days 6/group Increased XO, DNA fragmentation and protein carbonyl content, decreased sperm count and testosterone level in testicular cells ($p < 0.05$).

Meena, R.; Kumari, K.; Kumar, J.; Rajamani, P.; Verma, H.N.; Kesari, K.K. Therapeutic approaches of melatonin in microwave radiations-induced oxidative stress-mediated toxicity on male fertility pattern of Wistar rats. Electromagn. Biol. Med. 2014, 33, 81–91.

55) **Szmigielski et al. (1982)**: (2450 MHz, 2479.6; 1.2%); norm.: 2.450 GHz

Szmigielski, C3H/HeA (breast cancer-prone) and Balb/c mice 12 months (M, F) 50, 150W/m2 Balb/c mice also treated with 3, 4-benzopyrene (BP) 2 h/day, 6 days/week NR Acceleration of breast tumor developed in C3H/HeA mice Acceleration of BP-induced skin cancer in Balb/c mice ($p < 0.05$).

Szmigielski, S.; Szudzinski, A.; Pietraszek, A.; Bielec, M.; Janiak, M.; Wrembel, J.K. Accelerated development of spontaneous and benzopyrene-induced skin cancer in mice exposed to 2450-MHz microwave radiation. Bioelectromagnetics 1982, 3, 179–191.

56) **Kesari et al. (2010)**: (2450 Mhz; 2479.6; 1.2%); norm.: 2.450 GHz

Kesari KK, Behari J, Microwave exposure affecting reproductive system in male rats. Appl Biochem Biotechnol. 2010 Sep;162(2):416-28. doi: 10.1007/s12010-009-8722-9. Epub 2009 Sep 19.

57) **Shokri S. et al. (2015)**: (2450 MHz; 2479.6; 1.2%); norm.: 2.450 GHz

Shokri S, Soltani A, Kazemi M, Sardari MD, Mofrad FB. Effects of Wi-Fi (2.45 GHz), Exposure on Apoptosis, Sperm Parameters and Testicular Histomorphometry in Rats: A Time Course Study. Cell J. 2015; 17(2): 322–331.

58) **Marcickiewicz et al. (1986)**: (2,45 GHz; 2.480, 1.2%); norm.: 2.450 GHz

Marcickiewicz J, Chazan B, Niemiec T, Sokolska G, Troszyński M, Luczak M, Szmigielski S. Microwave radiation enhances teratogenic effect of cytosine arabinoside in mice. Biol Neonate. 1986; 50(2):75-82.

59) **Roszkowski et al. (1980b)**: (2.45 GHz; 2.480 GHz, 1.2%); norm.: 2.450 GHz

Roszkowski, W., WREMBEL, J. K., ROSZKOWSKI, K., JANIAK, M. & SZMIGIELSKI, S. (1980b). Does whole-body hyperthermia therapy involve participation of the immune system? Int. J. Cancer, 25, 289.

60) **Szudzinski et al. (1982)**: (cocarcinogenic 2.45 GHz; 2.480 GHz, 1.2%); norm.: 2.450 GHz

Szudziński A, Pietraszek A, Janiak M, Wrembel J, Kałczak M, Szmigielski S. Acceleration of the development of benzopyrene-induced skin cancer in mice by microwave radiation. Arch Dermatol Res. 1982; 274(3-4):303-12.

61) **Usikalu et al. (2013):** (2.45 GHz; 2.480 GHz, 1.2%); norm.: 2.450 GHz

Usikalu, M. R., Obembe, O. O., Akinyemi, M. L. and Zhu, J. Short-duration exposure to 2.45 GHz microwave radiation induces DNA damage in Sprague Dawley rat's reproductive systems. African Journal of Biotechnology Vol. 12(2), pp. 115-122, 9 January, 2013, DOI: 10.5897/AJB12.2360, ISSN 1684–5315 ©2013 Academic Journals

The genotoxic effects of 2.45 GHz microwave (MW) radiation on the testis and ovary of Sprague Dawley rats was investigated. The animals were exposed to varying levels of specific absorption rate (SAR) of 0 (control), 0.48, 0.95, 1.43, 1.91, 2.39, 2.90, 3.40, 3.80 and 4.30 Wkg-1, for 10 min. The induction of DNA damages was assessed using DNA direct amplification of length polymorphisms (DALP) and validated with single cell gel electrophoresis (SCGE) comet assay for same cells at SAR 2.39 Wkg-1. Potential damage at the organ level was assessed by histopathological study. The results show significant differences in the Olive moment and % DNA in the blood of the exposed animals when compared with the control ($p < 0.05$). Hyperchromasia was observed in the ovary of the animals exposed to MW radiation. Also, there was reduction in the number of germ cells and cell disorganization in the testis of exposed group with increasing SARs. These results suggest that MW radiation has the potential to affect both male and female fertility adversely. Alteration in DNA bands pattern, single strand break and reduction in the number of male germ cells of Sprague Dawley rats as a result of exposure to 2.45 GHz microwave for just 10 min without change in body temperature. Our findings reveal that exposure to microwave radiation of 0.48 Wkg-1 and above produces genotoxic effects on testis and ovary as observed from the genomic result, comet assay and the histopathology results. Thus, there is high possibility of compromising the fertility in the exposed rats. Although, rats are known to be more metabolically active than humans, however, these results give an indication of possible long-term effects that may be expected on the reproductive organs in humans when exposed at similar microwave radiation for a considerable period of time

62) **Megha et al. (2015):** (2.45 GHz; 2.480 GHz, 1.2%); norm.: 2.450 GHz)

Megha K., Pravin Suryakantrao Deshmukh, Basu Dev Banerjee, Ashok Kumar Tripathi, Rafat Ahmed, Mahesh Pandurang Abegaonkar. Low intensity microwave radiation induced oxidative stress, inflammatory response and DNA damage in rat brain. NeuroToxicology 51 (2015) 158–165.

The group of rats consisted of sham exposed (control) rats, group II–IV consisted of rats exposed to microwave radiation at frequencies 900, 1800 and 2450 MHz, specific absorption rates (SARs) 0.59, 0.58 and 0.66 mW/kg, respectively in gigahertz transverse electromagnetic (GTEM) cell for 60 days (2 h/day, 5 days/week). Rats were sacrificed and decapitated to isolate hippocampus at the end of the exposure duration. In conclusion, the present study suggests that low intensity microwave radiation induces oxidative stress, inflammatory response and DNA damage in brain by exerting a frequency dependent effect. The study also indicates that increased oxidative stress and inflammatory response might be the factors involved in DNA damage following low intensity microwave exposure. In the present study, among all the different microwave exposed frequencies, the effects of exposure to 2450 MHz microwave radiation was found to be most effective in all aspects.

63) **Karimi et al. (2018):** (2.45 GHz; 2.480 GHz, 1.2%); norm.: 2.450 GHz

Karimi N, Bayat M, Haghani M, Saadi H, Ghazipour GR. 2.45 GHz microwave radiation impairs learning, memory, and hippocampal synaptic plasticity in the rat. Toxicol Ind Health. 2018 Oct 21:748233718798976. doi: 10.1177/0748233718798976.

2.45 GHz microwave radiation impairs learning, memory, and hippocampal synaptic plasticity in the rat. The rats were exposed to 2.45 GHz MW radiation (continuous wave with overall average power density of 0.016 mW/cm2 and overall average whole-body specific absorption rate value of 0.017 W/kg) for 2 h/day over a period of 40 days. The evaluation of hippocampal morphology indicated that the neuronal density in the hippocampal CA1 area was significantly decreased by MW.

64) **Varghese et al. (2018**): (2.45 GHz; 2.480 GHz, 1.2%); norm.: 2.450 GHz

Varghese R., Anuradha Majumdar, Girish Kumar, Amit Shukla. Rats exposed to 2.45 GHz of non-ionizing radiation exhibit behavioral changes with increased brain expression of apoptotic caspase 3. Rats exposed to 2.45 GHz of non-ionizing radiation exhibit behavioral changes with increased brain expression of apoptotic caspase 3. Pathophysiology. 25(1):19-30. March 2018. https://doi.org/10.1016/j.pathophys.2017.11.001.

Analysis of dendritic arborization of neurons showcased reduction in number of dendritic branching and intersections which corresponds to alteration in dendritic structure of neurons, affecting neuronal signaling. The study clearly indicates that exposure of rats to microwave radiation of 2.45 GHz at a power density of 7.88 W/m2 leads to detrimental changes in brain leading to lowering of learning and memory and expression of anxiety behavior in rats along with fall in brain antioxidant enzyme systems.

65) **Topsakal et al. (2017):** 2.45GHz, 217 Hz coherently pulsed (2.45 GHz; 2.480 GHz, 1.2%); norm.: 2.450 GHz

Topsakal S., Ozlem Ozmen, Ekrem Cicek , Selcuk Comlekci. The ameliorative effect of gallic acid on pancreas lesions induced by 2.45 GHz electromagnetic radiation (Wi-Fi) in young rats. Journal of Radiation Research and Applied Sciences 10 (2017) 233e240.

The aim of this study was to investigate the effects of electromagnetic radiation (EMR) on the pancreas tissue of young rats and the ameliorative effect of Gallic acid (GA). 2.45 GHz RF emission, pulsed with 217 Hz. Six-week-old, 48 male rats were equally divided into four groups: Sham group, EMR group(2.45GHz), EMR (2.45 GHz) þGA group (30 mg/ kg/daily) orally and GA group (30 mg/kg/daily). After 30 days, serum and pancreatic tissue samples were harvested for biochemical, histopathological and immunohistochemical analysis. Serum amylase, lipase, glucose, and tissue malondialdehyde, total oxidant status and oxidative stress index were increased, whereas total antioxidant status decreased in the EMR group. The histopathological examination of the pancreases indicated slight degenerative changes in some pancreatic endocrine and exocrine cells and slight inflammatory cell infiltrations in the EMR group. At the immunohistochemical examination, marked increase was observed in calcitonin gene related protein and Prostaglandin E2 expressions in pancreatic cells in this group. There were no changes in interleukin-6 expirations. GA ameliorated biochemical and pathological findings in the EMRþGA group. These findings clearly demonstrate that EMR can cause degenerative changes in both endocrine and exocrine pancreas cells in rats during the developmental period and GA has an ameliorative effect.

66) **Figueiredo et al. (2004)**: (2500 MHz; 2479.7; 0.8%); norm.: 2.500 GHz

Figueiredo ABS, Alves RN, Ramalho AT. Genet Mol Biol 2004; 27 (3): 460-466. Cytogenetic analysis of the effects of 2.5 and 10.5 GHz microwaves on human lymphocytes. med./bio.

67) **Liburdy R. (1979)**: (2.6 GHz; 2.630; 1.14%); norm. 2.600 GHz

Liburdy R. P. Radiofrequency radiation alters the immune system: modulation of T- and B-lymphocyte levels and cell-mediated immune competence by hyperthermic radiation. [med./bio.], Radiat Res 1979; 77 (1): 34-46.

2.6 GHz exposure at 25 Mw/cm2, (3.8 W/kg) for 1 hr, measured reduction of lymphocytes.

68) **Thomas et al. (1982)**: (2800 MHz; 2789.6; 0.37%); norm.: 2.800 GHz

Thomas JR, Schrot J, Banvard RA (1982). Comparative effects of pulsed and continuous-wave 2.8-GHz microwaves on 1564 temporally defined behavior. Bioelectromagnetics, 3(2):227-235.

69) **Albert et al. (1977)**: (2800 MHz; 2789.6; 0.37%); norm.: 2.800 GHz

Albert, E.N., Light and electron microscopic observations on the blood-brain-barrier after microwave irradiation, in: "Symposium on Biological Effects and Measurement of Radio Frequency Microwaves," D.G. Hazzard, ed., HEW Publication (FDA) 77-8026, Rockville, MD, 1977.

70) **Frei and Jauchem (1989)**: (2800 MHz; 2789.6; 0.37%); norm.: 2.800 GHz

Frei, MR, J. R. Jauchem Effects of 2.8-GHz microwaves on restrained and ketamine-anesthetized rats; Radiation and Environmental Biophysics June 1989, Volume 28, Issue 2, pp 155-164.

71) **Gandhi et al. (1989)**: (2800 MHz; 2789.6; 0.37%); norm.: 2.800 GHz

Gandhi, C.R. and Ross, D.H., Microwave induced stimulation of 32 Pi- incorporation into phosphoinositides of rat brain synaptosomes. Radiat Environ Biophys 28:223-234, 1989.

72) **Hai-juan Li et al. (2015):** (2.856 GHz; 2789.6; 0.23%); norm.: 2.856 GHz

Li, Hai-juan, Rui-yun Peng, Xiang-jun Hu et al. Alterations of cognitive function and 5-HT system in rats after long term microwave exposure. Physiology & Behavior Volume 140, 1 March 2015, Pages 236-246

This is an animal study investigating the long-term effects of chronic microwave radiation on cognitive function. Rats were either exposed or sham to 2.856 gigahertz (GHz) microwaves with the average power density level of 5, 10, 20 or 30 milliwatts per square centimetre (mW/cm2) for 6 minutes, three times a week for up to 6 weeks. The authors suggested that in the long-term, chronic microwave exposure could induce dose dependent deficit of spatial learning and memory in rats.

73) **Zuo H. et al. (2014):** (2.856 GHz; 2789.6; 0.23%); norm.: 2.856 GHz

Zuo H, Lin T, Wang D, Peng R, Wang S, Gao Y, Xu X, Zhao L, Wang S, Su Z. Mol Neurobiol. 2015;51(3):1520-9. doi: 10.1007/s12035-014-8831. RKIP Regulates Neural Cell Apoptosis Induced by Exposure to Microwave Radiation Partly Through the MEK/ERK/CREB Pathway.

73.1) **Hui Wang et al. (2017):** (2.856 GHz; 2789.6; 0.23%); norm.: 2.856 GHz

Wang Hui, Shengzhi Tan, Xinping Xu, LiZhao, Jing Zhang, Binwei Yao, Yabing Gao, Hongmei Zhou, RuiyunPeng. Long term impairment of cognitive functions and alterations of NMDAR subunits after continuous microwave exposure. Physiology & Behavior Volume 181, 1 November 2017, Pages 1-9

In this study, 220 male Wistar rats were exposed by a 2.856 GHz radiation source with the average power density of 0, 2.5, 5 and 10 mW/cm2 for 6 min/day, 5 days/week and up to 6 weeks. The MWM task, the EEG analysis, the hippocampus structure observation and the western blot were applied until the 12 months after microwave exposure to detect the spatial learning and memory abilities, the cortical electrical activity, changes of hippocampal structure and the NMDAR subunits expressions.
Results found that the rats in the 10 mW/cm2 group showed the decline of spatial learning and memory abilities and EEG disorders (the decrease of EEG frequencies, and increase of EEG amplitudes and delta wave powers). Moreover, changes of basic structure and ultrastructure of hippocampus also found in the 10 and 5 mW/cm2 groups. The decrease of NR 2A, 2B and p-NR2B might contribute to the impairment of cognitive functions. The findings suggested that the continuous microwave exposure could cause the dose-dependent long-term impairment of spatial learning and memory, the abnormalities of EEG and the hippocampal structure injuries. The decrease of NMDAR key subunits and phosphorylation of NR 2B might contribute to the cognitive impairment.

74) **Siekierzynski et al. (1972)**: (2950 MHz; 2948.9; 0.37%); norm.: 2.950 GHz

Siekierzynski. Decreased erythrocyte production in rabbits; pulsed exposure more effective (1972).

75) **Pu et al. (1997)**: (3000 MHz; 2948.9; 1.7%); norm.: 3.000 GHz

Pu et al 1997 Electrical activity recorded in mouse brain during exposure on 7th day.

76) **D'Ándrea et al., (1994)**: (5600 MHz; 5579.3; 0.37%); norm.: 2.800 GHz

D'Andrea JA, Thomas A, Hatcher DJ. 1994. Rhesus monkey behavior during exposure to high-peak-power 5.62-GHz microwave pulses. Bioelectromagnetics 15:163–176.

77) **Jensh et al. (1984)**: (6000 MHz; 5897.7; 1.7%); norm.: 3.000 GHz

Jensh RP. Studies of the teratogenic potential of exposure of rats to 6000-MHz microwave radiation. Postnatal psychophysiologic evaluations. Radiat Res 97:282-301; 1984b.

78) **Goldstein and Sisko et al. (1974)**: (9300 MHz, 9351.7; 0.55%); norm.: 2.325 GHz

Goldstein, L. and Sisko, Z., A quantitative electro-encephalographic study of the acute effect of X-band microwaves in rabbits, in: "Biological Effects and Health Hazards of Microwave Radiation: Proceedings of an International Symposium," P. Czerski, et al., eds., Polish Medical Publishers, Warsaw, 1974.

79) **Zhang Y et al. (2014)**: (9417 MHz; 9351.7; 0.70%); norm.: 2.354 GHz

Zhang Y, Li Z, Gao Y, Zhang C., Effects of fetal microwave radiation exposure on offspring behavior in mice, 2014. J Radiat Res. 2015 Mar;56(2):261-8. doi: 10.1093/jrr/rru097. Epub 2014 Oct 30.

80) **Sharma et al. (2014)**: (10.0 GHz; 9.92; 0.8%); norm.: 2.500 GHz

Sharma A, Rashmi Sisodia, Deepak Bhatnaga, 10 Ghz Microwaves Induced Biochemical, Learning and Memory Alterations in Swiss Albino Mice Brain, 2014.

81) **Millenbaugh et al. (2008**): (35 GHz; 35.26; 0.72%); norm.: 2.1875 GHz

Millenbaugh NJ, Roth C, Sypniewska R, Chan V, Eggers JS, Kiel JL, Blystone RV, Mason PA. Gene Expression Changes in the Skin of Rats Induced by Prolonged 35 GHz Millimeter-Wave Exposure. med./bio. Radiat Res 2008; 169 (3): 288-300.

The authors identified significant microscopic changes in skin induced by millimeter wave exposure and thus demonstrated that the detected changes in gene transcription may be associated with observable alterations in cell behavior and tissue structure. The data are indicative of thermally induced injury to skin tissue. The observed responses to millimeter wave exposure differ significantly from those induced by warm air and from the sham exposure.

82) **Sypniewska et al. (2008**): (35 GHz; 35.26; 0.72%); norm.: 2.1875 GHz

Sypniewska, R. K., Millenbaugh, N. J., Kiel, J. L., Blystone, R. V., Ringham, H. N., Mason, P. A., Witzmann, F. A., 2010. Protein changes in macrophages induced by plasma from rats exposed to 35 GHz millimeter waves. Bioelectromagnetics 3, 656-663. doi:0.1002/bem.20598.

A macrophage assay and proteomic screening were used to investigate the biological activity of soluble factors in the plasma of millimeter wave-exposed rats. NR8383 rat macrophages were incubated for 24 h with 10% plasma from male Sprague-Dawley rats that had been exposed to sham conditions, or exposed to 42 °C environmental heat or 35 GHz millimeter waves at 75 mW/cm² until core temperature reached 41.0 °C. Two-dimensional polyacrylamide gel electrophoresis, image analysis, and Western blotting were used to analyze approximately 600 protein spots in the cell lysates for changes in protein abundance and levels of 3-nitrotyrosine, a marker of macrophage stimulation. Proteins of interest were identified using peptide mass fingerprinting. Compared to plasma from sham-exposed rats, plasma from environmental heat- or millimeter wave-exposed rats increased the expression of 11 proteins, and levels of 3-nitrotyrosine in seven proteins, in the NR8383 cells. These altered proteins are associated with inflammation, oxidative

stress, and energy metabolism. Findings of this study indicate both environmental heat and 35 GHz millimeter wave exposure elicit the release of macrophage-activating mediators into the plasma of rats.

83) **Foster et al. (2008**): (35 GHz; 35.26; 0.72%); norm.: 2.1875 GHz

Foster KR, D'Andrea JA, Chalfin, S, and Hatcher, DJ (2003). Thermal Modeling of Millimeter Wave Damage to the primate cornea at 35 GHz and 94 GHz. Health Physics, 84(6): 764-769.

Chaflin et al. (2002) reported thresholds for millimeterwave (35 and 94 GHz) induced lesions to the primate cornea. In those studies, which were conducted on five juvenile rhesus monkeys (Macaca mulatta), the mean fluence F required to produce a threshold corneal lesion (faint epithelial edema and fluorescein staining) was 7.5 J cm_2 at 35 GHz and 5 J cm_2. The thresholds for damage to the cornea (staining of the corneal epithelium by fluorescein and corneal edema) correspond to temperature increases of about 20°C at both irradiation frequencies.

84) **Makar et al. (2005**): (42.2 GHz; 42.1; 0.28%); norm.: 2.638 GHz

Makar, V.R., Logani, M.K., Bhanushali, A., Kataoka, M., Ziskin, M.C., 2005. Effect of millimeter waves on natural killer cell activation. Bioelectromagnetics 26 (1), 10–19.http://dx.doi.org/10.1002/bem.20046. ⟨https://www.ncbi.nlm.nih.gov/pubmed/15605409⟩.

Tumor suppression. Makar et al. (2005) showed that MMW irradiation at 42.2 GHz can up-regulate natural killer (NK) cell functions with short exposures. An increase in TNF-alpha was also identified.

84.2) **Gapeyev et al. (2011):** (42.2 GHz; 42.1; 0.28%); norm.: 2.638 GHz

Gapeyev, A.B.; Kulagina, T.P.; Aripovsky, A.V.; Chemeris, N.K. The role of fatty acids in anti-inflammatory effects of low-intensity extremely high-frequency electromagnetic radiation. Bioelectromagnetics 2011, 32, 388–395. [CrossRef]

Exposure 1: 42.2 GHz, Modulation type: CW, Exposure duration: continuous for 20 min, power: 8 mW power density: 0.1 mW/cm², SAR: 1.5 W/kg (at the container's surface). Using the inflammation model, it was shown that the exposure of mice significantly increased the content of polyunsaturated fatty acids (dihomo-gamma-linolenic acid, arachidonic acid, eicosapentaenoic, docosapentaenoic, and docosahexaenoic) and reduced the content of monounsaturated fatty acids (palmitoleic acid and oleic acid) in thymic cells.
Changes in the fatty acid composition in the blood plasma were less pronounced and became manifest in an increase in the level of saturated fatty acids during the inflammation. The authors conclude that the changes of fatty acid composition induced by low-intensity extremely high frequency electromagnetic radiation may be considered as a key element in the mechanisms of biological effects of radiation.

85) **Lushnikov et al. (2003**): (42.0 GHz; 42.1; 0.24%); norm.: 2.625 GHz

Lushnikov, K.V., Gapeedv, A.V., Shumilina, Iu.V., Shibaev, N.V., Sadovnikov, V.B., Chmeris, N.K., 2003. Decrease in the intensity of the cellular immune response and nonspecific inflammation upon exposure to extremely high frequency electromagnetic radiation. Biofizika 48 (5), 918–925. ⟨https://www.ncbi.nlm.nih.gov/pubmed/14582420⟩.

Lushnikov et al. (2003) investigated cell-mediated immunity and nonspecific inflammatory response in mice exposed to low-intensity extremely high-frequency electromagnetic radiation (EHF EMR, 42.0 GHz, 0.1 mW/cm2, 20 min daily). They found that MMW radiation reduced both immune and nonspecific inflammatory responses.

86) **Gapeev et al. (2003**): (42.0 GHz; 42.1; 0.24%); norm.: 2.625 GHz

Gapeev, A.B., Lushnikov, K.V., Shumilina, Iu.V., Sirota, N.P., Sadovnikov, V.B., Chemeris, N.K., 2003. Effects of low-intensity extremely high frequency electromagnetic radiation on chromatin structure of lymphoid cells in vivo and in vitro. Radiats Biol. Radioecol. (1), 87–92. ⟨https://www.ncbi.nlm.nih.gov/pubmed/12677665⟩.

Gapeev et al. (2003) showed that low-intensity extremely high-frequency MMH electromagnetic radiation in vivo causes effects on spatial organization of chromatin in cells of lymphoid organs. Chromatin is a complex of DNA and proteins that forms chromosomes within the nucleus of eukaryotic cells. He exposed mice to a single whole-body exposure for 20 min at 42.0 GHz and 0.15 mW/cm2. He suggests that the effects were due to involvement of the neuroendocrine and central nervous systems.

87) **Frei et al. (1995**): (35 GHz; 35.26; 0.72%); norm.: 2.1875 GHz

Frei MR, Ryan KL, Berger RE, Jauchem JR. Sustained 35-GHz radiofrequency irradiation induces circulatory failure. Shock 4:289-293; 1995.

88) **Kesari et al.** (2009); (50 GHz; 50.05, 0.09%); norm.: 3.125 GHz

Kesari KK, Behari J. Appl Biochem Biotechnol 2009; 158 (1): 126-139, Journal PubMed doi:10.1007/s12010-008-8469-8.

The data showed that the chronic exposure to these microwaves caused DNA double-strand breaks and a significant decrease in glutathione peroxidase and superoxide dismutase enzyme activities in brain cells, whereas catalase enzyme activity significantly increased in the brain samples of the exposed group compared with controls. Additionally, protein kinase C level significantly decreased in whole brain and hippocampus. The authors conclude that prolonged exposure to 50 GHz microwave exposure may decrease the level of protein kinase C, cause DNA double-strand breaks and changes in antioxidant enzyme activities in the neurological system of male rats due to free radicals formation. The possible site of action of such irradiation seems to be the hippocampus.

89) **Albini et al. (2014):** (53.37 GHz; 52.90; delta 0.89%); norm.: 3.125 GHz

Albini M., Simone Dinarelli, Francesco Pennella, Stefania Romeo, Emiliano Zampetti, Marco Girasole, Umberto Morbiducci, RitaMassa, Alfonsina Ramundo-Orlando. Induced movements of giant vesicles by millimeter wave radiation. Biochimica et Biophysica Acta 1838 (2014) 1710–1718.

90) **D'Agostino et al. (2018**): (53.37 GHz; 52.90; delta 0.89%); norm.: 3.336 GHz

Simona D'Agostino, Chiara Della Monica, Eleonora Palizzi, Fabio Di Pietrantonio, Massimiliano Benetti, Domenico Cannatà, Marta Cavagnaro, Dariush Sardari, Pasquale Stano & Alfonsina Ramundo-Orlando. Extremely High Frequency Electromagnetic Fields Facilitate Electrical Signal Propagation by Increasing Transmembrane Potassium Efflux in an Artificial Axon Model. SCIENTIfIC REPORS | (2018) 8:9299 | DOI:10.1038/s41598-018-27630-8.

91) **Habauzit et al. (2018**): (60 GHz; 59.51; delta 0.82%); norm.: 3.750 GHz

Habauzit et al. (2014) looked at gene expression in keratinocytes with 60 GHz exposure at the upper limit of current guidelines and concluded, "In our experimental design, the high number of modified genes (665) shows that the ICNIRP current limit is probably too permissive to prevent biological response."

Habauzit, D., Quément, C.L., Zhadobov, M., Martin, C., Aubry, M., Sauleau, R., Dréan, Y.L., 2014. Transcriptome analysis reveals the contribution of thermal and the specificeffects in cellular response to millimeter wave exposure. PLoS One. http://dx.doi.org/10.1371/journal.pone.0109435.

91.2) **Bellossi et al. (2018**): (60 GHz; 59.51; delta 0.82%); norm.: 3.750 GHz

Bellossi, A.; Dubost, G.; Moulinoux, J.P.; Himdi, M.; Ruelloux, M.; Rocher, C. Biological E↵ects of Millimeter-Wave Irradiation on Mice—Preliminary Results. IEEE Trans. Microw. Theory Tech. 2000, 48, 2104–2110.

Specific absorption rate and internal fields have been computed for a mouse irradiated at 60 GHz. The measured power flux in free space at the irradiation area is close to 0.5 mW/cm2, this probably produces some subtle biological effects. To look for possible biological effects, the authors exposed DBA2 mice grafted either with L1210 cells or with Lewis tumor cells and healthy Swiss mice. There were four obvious observations: there is an individual sensitiveness to 60 GHz

waves; the survival of mice grafted with L1210 cells could be increased; the growth of Lewis tumor was enhanced; and the activity of Swiss mice was increased. In any way, those effects have to be taken into account, and the authors suggest prudence before using a 60-GHz waves for indoor communications.

92) **Le Quément et al. (2014)**: (60.4 GHz; 59.51; 1.50%); norm.: 3.775 GHz

Le Quément, C., Christophe Nicolas Nicolaz Denis Habauzit Maxim Zhadobov Ronan Sauleau Yves Le Dréan. Impact of 60-GHz millimeter waves and corresponding heat effect on endoplasmic reticulum stress sensor gene expression. Volume35, Issue6 September 2014, Pages 444-451.

93) **Mahamoud et al. (2019**): (60.4 GHz; 59.51; 1.50%); norm.: 3.775 GHz

Mahamoud YS., Meziane Aite, Catherine Martin, Maxim Zhadobov, Ronan Sauleau, Yves Le Dréan, Denis Habauzit Published: August 16, 2016, https://doi.org/10.1371/journal.pone.0160810. Additive Effects of Millimeter Waves and 2-Deoxyglucose Co-Exposure on the Human Keratinocyte Transcriptome.

Using a microarray-based approach, modifications to the whole genome of a human keratinocyte model have been analysed that was exposed at 60.4 GHz-MMW at an incident power density (IPD) of 20 mW/cm2 for 3 hours in athermic conditions. The MMW/2dG co-treatment did not alter the keratinocyte ATP content, but it did slightly alter the transcriptome, which reflected the capacity of MMW to interfere with the bioenergetic stress response. The RT-PCR-based validation confirmed 6 MMW-sensitive genes (SOCS3, SPRY2, TRIB1, FAM46A, CSRNP1 and PPP1R15A) during the 2dG treatment. These 6 genes encoded transcription factors or inhibitors of cytokine pathways, which raised questions regarding the potential impact of long-term or chronic MMW exposure on metabolically stressed cells.

94) **Le Pogam et al. (2019**): (60.4 GHz; 59.51; 1.50%); norm.: 3.775 GHz

Le Pogam P, Le Page Y, Habauzit D, Doué M, Zhadobov M, Sauleau R, Le Dréan Y, Rondeau D. Untargeted metabolomics unveil alterations of biomembranes permeability in human HaCaT keratinocytes upon 60 GHz millimeter-wave exposure. Sci Rep. 2019 Jun 27;9(1):9343. doi: 10.1038/s41598-019-45662-6.

Untargeted metabolomics unveil alterations of biomembranes permeability in human HaCaT keratinocytes upon 60 GHz millimeter-wave exposure. (HaCaT human keratinocytes were exposed at 60.4 GHz with an incident power density of 20 mW/cm^2).

95) **Foster et al. (2003)**; (94 GHz; 94.32; 0.34%); norm.: 2.9375 GHz

Foster KR, D'Andrea JA, Chalfin, S, and Hatcher, DJ (2003). Thermal Modeling of Millimeter Wave Damage to the primate cornea at 35 GHz and 94 GHz. Health Physics, 84(6): 764-769.

Chaflin et al. (2002) reported thresholds for millimeterwave (35 and 94 GHz) induced lesions to the primate cornea. In those studies, which were conducted on five juvenile rhesus monkeys (Macaca mulatta), the mean fluence F required to produce a threshold corneal lesion (faint epithelial edema and fluorescein staining) was 7.5 J cm_2 at 35 GHz and 5 J cm_2. The thresholds for damage to the cornea (staining of the corneal epithelium by fluorescein and corneal edema) correspond to temperature increases of about 20°C at both irradiation frequencies.

96) **Homenko et al. (2009):** (100 GHz; 100.09; 0.09%); norm.: 3.125 GHz

Homenko A, Kapilevich B, Kornstein R, Firer MA. Published in: Bioelectromagnetics 2009; 30 (3): 167-175.

Exposure of enzyme either prior to addition of substrate or during the enzymatic reaction resulted in small but significant reductions in enzyme activity. These differences were not found if the enzyme had previously been immobilized onto plastic micro-wells. Irradiation of immobilized antigen did not influence the ability of the antigen to interact with antibody. However, irradiation appeared to decrease the stability of previously formed antigen-antibody complexes. The data suggest that 100 GHz exposure can induce small but statistically significant alterations in the characteristics of these two types of biomolecular interactions.

97) **Tafforeau et al. (2004**): (105 GHz; 105.85; 0.80%); norm.: 3.281 GHz

Plant sensitivity to low intensity 105 GHz electromagnetic radiation September 2004, Bioelectromagnetics 25(6):403-7

98) **Sheng Zhi Tan et al. (2019)** (0.16 THz; 0.1587; 0.82%); norm.: 2.500 GHz

99) **Sheng Zhi Tan et al. (2019)** (0.17 THz; 0.1683; 1.01%); norm.: 2.656 GHz

Sheng Zhi, T., TAN Peng Cheng, LUO Lan Qing, CHI Yun Liang, YANG Zi Long, ZHAO Xue Long, ZHAO Li, DONG Ji, ZHANG Jing, YAO Bin Wei, XU Xin Ping, TIAN Guang, CHEN Jian Kui, WANG Hui, and PENG Rui Yun. Exposure Effects of Terahertz Waves on Primary Neurons and Neuron-like Cells Under Nonthermal Conditions. Published 2019, DOI:10.3967/bes2019.094

This study aimed to explore the potential effects of terahertz (THz) waves on primary cultured neurons from 4 rat brain regions (hippocampus, cerebral cortex, cerebellum, and brainstem) and 3 kinds of neuron-like cells (MN9D, PC12, and HT22 cells) under nonthermal conditions. THz waves with an output power of 50 (0.16 THz) and 10 (0.17 THz) mW with exposure times of 6 and 60 min were used in this study. Analysis of temperature change, neurite growth, cell membrane roughness, micromorphology, neurotransmitters and synaptic-related proteins (SYN and PSD95) was used to evaluate the potential effects. Temperature increase caused by the THz wave was negligible. THz waves induced significant neurotransmitter changes in primary hippocampal, cerebellar, and brainstem neurons and in MN9D and PC12 cells. THz wave downregulated SYN expression in primary hippocampal neurons and downregulated PSD95 expression in primary cortical neurons. Different types of cells responded differently after THz wave exposure, and primary hippocampal and cortical neurons and MN9D cells were relatively sensitive to the THz waves. The biological effects were positively correlated with the exposure time of the THz waves.

100) **Ahlberg Gagnér et al. (2019)**: (0.5 THz, 0.505 THz; 0.99%); norm.: 2.656 GHz

Ahlberg Gagnér,V., Ida Lundholm, Maria-Jose Garcia-Bonete, Helena Rodilla,Ran Friedman, Vitali Zhaunerchyk, Gleb Bourenkov, Thomas Schneider, Jan Stake, Gergely Katona. Clustering of atomic displacement parameters in bovine trypsin
reveals a distributed lattice of atoms with shared chemical properties. Scientific Reports | (2019) 9:19281 | https://doi.org/10.1038/s41598-019-55777-5.

101) **Wilmink et al. (2010)**: (2.52 THz; 2.54; 0.78%); norm.: 2.4609 GHz

Wilmink GJ. & Jessica E. Grundt, Invited Review Article: Current State of Research on Biological Effects of Terahertz Radiation, J Infrared Milli Terahz Waves (2011) 32:1074–1122

102) **Ol'shevskaia et al. (2009):** (85.1 THz; 86.18; 1.26%); norm.: 2.597 GHz

Ol'shevskaia Iu S, Kozlov AS, Petrov AK, et al. Influence of terahertz (submillimeter) laser radiation on neurons in vitro. Zh Vyssh Nerv Deiat Im I P Pavlova, 2009; 59, 353−9.

Ol'shevskaia et al. used a THz wave of 85.1 THz and 0.3-30 mW/cm2 to irradiate isolated rat brain slices for 20-40 min and showed neuronal cell membrane bulging, synaptic growth disorders and decreased membrane potential.

2.2 Frequencies that are proposed healthy, related to coherent frequency patterns at MHz and GHz, that fit in the algorithm

Name, (year): (applied frequency, calculated coherent pointer frequency; difference between applied frequency and pointer frequency); calculated normalized applied frequency.

103) **Kyung Shin Kang et al. (2013)**: (0.500 MHz; 0.4975; 0.50%); norm.: 4.0960 GHz

104) **Kyung Shin Kang et al. (2013)**: (1.000 Mhz; 0.995; 0.50%); norm.: 4.0960 GHz

Kyung Shin Kang, Jung Min Hong, PhD, Jo A. Kang, MS, Jong-Won Rhie, MD, PhD, Dong-Woo Cho, PhD; Osteogenic Differentiation of Human Adipose-Derived Stem Cells Can Be Accelerated by Controlling the Frequency of Continuous, ultrasound, 2013; doi: 10.7863/ultra.32.8.1461.

105) **Takebe et al. (2013)**: (1.000 Mhz; 0.995; 0.50%); norm.: 4.0960 GHz

Takebe H, Nakanishi Y, Hirose Y, Ochi M. Effect of low intensity pulsed ultrasound stimulation on sinus augmentation in rabbits. Clin Oral Implants Res 2014; 25(6): 735-41.

106) **Bandyopadhyay et al. (2014)**: (1.000 Mhz; 0.995; 0.50%); norm.: 4.0960 GHz

Sahu S., Subrata Ghosh, Daisuke Fujita & Anirban Bandyopadhyay; 2014. Live visualizations of single isolated tubulin protein self-assembly via tunneling current: effect of electromagnetic pumping during spontaneous growth of microtubule, Scientific Reports, volume 4, Article number: 7303.

107) **Usselman et al. (2016)**: (1.4 MHz, 1.398, 0.18%); norm.: 2.8672 GHz

Usselman RJ., Cristina Chavarriaga, Pablo R. Castello, Maria Procopio, Thorsten Ritz, Edward A. Dratz, David J. Singel & Carlos F. Martino. The Quantum Biology of Reactive Oxygen Species Partitioning Impacts Cellular Bioenergetics, Scientific Reports, November 2016| 6:38543 | DOI: 10.1038/srep38543.

108) **Kyung Shin Kang et al. (2013)**: (1.5 Mhz; 1.4829; 1.15%); norm.: 3.0720 GHz

Kyung Shin Kang, Jung Min Hong, PhD, Jo A. Kang, MS, Jong-Won Rhie, MD, PhD, Dong-Woo Cho, PhD; Osteogenic Differentiation of Human Adipose-Derived Stem Cells Can Be Accelerated by Controlling the Frequency of Continuous, ultrasound, 2013; doi: 10.7863/ultra.32.8.1461.

109) **Takebe et al. (2013)**: (3.000 MHz; 2.9658; 1.15 %); norm.: 3.0720 GHz

Takebe H, Nakanishi Y, Hirose Y, Ochi M. Effect of low intensity pulsed ultrasound stimulation on sinus augmentation in rabbits. Clin Oral Implants Res 2014; 25(6): 735-41.

110) **Agulan et al. (2015)**: (pulsed 3.3 MHz; 3.31; 0.49%); (656, 648; 1.24%); norm.: 3.389 GHz

Agulan RTV., Edcy Marie F. Capule, and Romeric F. Pobre. Effect of Pulsed Electromagnetic Fields on Colon Cancer Cell Lines (HCT 116) Through Cytotoxicity Test, Presented at the DLSU Research Congress 2015 De La Salle University, Manila, Philippines.

111) **Bandyopadhyay et al. (2014)**: (3.770 Mhz; 3.728; +1.07%); norm.: 3.8605 GHz;

Satyajit Sahu, Subrata Ghosh, Daisuke Fujita & Anirban Bandyopadhyay; 2014. Live visualizations of single isolated tubulin protein self-assembly via tunneling current: effect of electromagnetic pumping during spontaneous growth of microtubule. Scientific Reports, volume 4, Article number: 7303.

112) **Zou et al. (2007)**: (5.000 MHz; 4.971; 0.60%); norm.: 2.560 GHz

Zou H, Mellon S, Syms RR, Tanner KE. 2-Dimensional MEMS dielectrophoresis device for osteoblast cell stimulation. Biomed. Microdev. 2006; 8: 353–359.

113) **Pokorny et al. (2009)**: (8.000 MHz; 7.962; 0.50%); norm.: 4.096 GHz

Pokorny, Jelínek F, Cifra M, Pokorný J, Vanis J, Simsa J, Hasek J, Frýdlová I. Measurement of electrical oscillations and mechanical vibrations of yeast cells membrane around 1 kHz. Electromagn Biol Med. 2009; 28(2): 223-32.

114) **Chen X. et al. (2012, 2014)**: (10 MHz, 9.94 MHz; 0.71%); norm.: 2.560 GHz; (33.3 MHz, 33.5 MHz; 0.63%); (0.5 Hz, 0.5 Hz; 0.0 %); (1.0 Hz, 1.0 Hz; 0.0%)

Chen, X., Swanson, J. R., Kolb, J.F., Nuccitelli, R., Schoenbach K.H. (2009) Histopathology of Normal Skin and Melanomas after Nanosecond Pulsed Electric Field Treatment. Melanoma Research, 19, 361-371.

115) **Bandyopadhyay et al. (2014)**: (20.00 MHz; 19.90; 0.50%); norm.: 2.560 GHz

Satyajit Sahu, Subrata Ghosh, Daisuke Fujita & Anirban Bandyopadhyay; 2014. Live visualizations of single isolated tubulin protein self-assembly via tunneling current: effect of electromagnetic pumping during spontaneous growth of microtubule. Scientific Reports, volume 4, Article number: 7303.

116) **Stolfa et al. (2007)**: (21.20 MHz; 21.23; 0.19%); norm.: 2.7136 GHz

Stolfa S, Skorvánek M, Stolfa P, Rosocha J, Vasko G, Sabo J. Effects of static magnetic field and pulsed electromagnetic field on viability of human chondrocytes in vitro. Physiol Res 2007; 56 Suppl 1:S45-9.

117) **Garon et al. (2007)**: (50 MHz; 50.34; 0.68%); norm.: 3.200 GHz

Garon, E.B.; Sawcer, D.; Vernier, P.T.; Tang, T.; Sun, Y.; Marcu, L.; Gundersen, M.A.; Koeffler, H.P. In vitro and in vivo evaluation and a case report of intense nanosecond pulsed electric field as a local therapy for human malignancies. Int. J. Cancer 2007, 121, 675–682

118) **Lary et al., (1983):** (100 MHz; 100.7; 0.70%); norm.: 3.200 GHz

Lary et al., Sprague-Dawley rats (F) 0.4 W/kg 6 h 40 min/day, 6 days 3-10/group Viable litter size/live birth index, neonatal growth, neonatal survival indices, prenatal mortality Not any statistically significant alteration (NS). Lary J.M.; Conover, D.L.; Johnson, P.H. Absence of embryotoxic effects from low-level (nonthermal) exposure of rats to 100 MHz radiofrequency radiation. Scand. J. Work Environ. Health 1983, 9, 120–127.

119) **Alessio et al. (2019)**: (169 MHz; 169.9; 0.51%); norm.: 2.7040 GHz

Alessio N., Elisa Santoro, Tiziana Squillaro, Domenico Aprile, Massimo Briccola, Paolo Giubbini, Raffaella Marchesani, Maria Rosaria Muoio, Monica Lamberti.

Low-Level Radiofrequency Exposure Does Not Induce Changes in MSC Biology: An in vitro Study for the Prevention of NIR-Related Damage. Stem Cells and Cloning: Advances and Applications downloaded from https://www.dovepress.com/ by 184.174.118.20 on 18-Dec-2019.

120) **Roti et al. (2001)**: (835.62 Mhz; 848.42; 1.51%); norm.: 3.3425 GHz

Roti Roti JL, Malyapa RS, Bisht KS, Ahern EW, Moros EG, Pickard WF, Straube WL. Neoplastic transformation in C3H 10T(1/2) cells after exposure to 835.62 MHz FDMA and 847.74 MHz CDMA radiations. Radiat Res 2001; 155 (1) Pt 2: 239-247.

After both exposures (7 days RF exposure (835.62 MHz FDMA or 847.74 MHz CDMA) and 42 days exposure after X-ray irradiation) no statistically significant differences in the neoplastic transformation frequencies were observed.

121) **LaRegina et al. (2003)**: (835.62 Mhz; 848.42; 1.51%); norm.: 3.3425 GHz

LaRegina MC, Moros EG, Pickard WF, Straube WL, Baty J, Roti Roti JL. The Effect of Chronic Exposure to 835.62 MHz FDMA or 847.74 MHz CDMA Radiofrequency Radiation on the Incidence of Spontaneous Tumors in Rats. Radiat Res 2003; 160 (2): 143-151.

Exposure 1: 835.62 MHz, Exposure duration: repeated daily exposure, 4 h/day, 5 days/week, over two years power: 1.5 W average over time (± 0.25 W), SAR: 1.3 W/kg average over time (brain) (± 0.5 W/kg). There were no significant differences among final survival days or body weights for either males or females in any group. No significant differences were found between treated and sham-exposed rats for any tumor in any organ. The authors conclude that chronic exposure to FDMA or CDMA radiofrequency radiation had no significant effect on the incidence of spontaneous tumors in rats.

122) **Roti et al. (2001)**: (847.74 MHz; 848.42; 0.08%); norm.: 3.3910 GHz

Roti Roti JL, Malyapa RS, Bisht KS, Ahern EW, Moros EG, Pickard WF, Straube WL. Neoplastic transformation in C3H 10T(1/2) cells after exposure to 835.62 MHz FDMA and 847.74 MHz CDMA radiations. Radiat Res 2001; 155 (1) Pt 2: 239-247.

After both exposures (7 days RF exposure (835.62 MHz FDMA or 847.74 MHz CDMA) and 42 days exposure after X-ray irradiation) no statistically significant differences in the neoplastic transformation frequencies were observed.

123) **LaRegina, (2003)**: (847.74 MHz; 848.42; 0.08%); norm.: 3.3910 GHz

LaRegina MC, Moros EG, Pickard WF, Straube WL, Baty J, Roti Roti JL. The Effect of Chronic Exposure to 835.62 MHz FDMA or 847.74 MHz CDMA Radiofrequency Radiation on the Incidence of Spontaneous Tumors in Rats. Radiat Res 2003; 160 (2): 143-151.

847.74 MHz Exposure duration: repeated daily exposure, 4 h/day, 5 days/week, over two years power: 1.5 W average over time (± 0.25 W) SAR: 1.3 W/kg average over time (brain) (± 0.5 W/kg). The Effect of Chronic Exposure to 847.74 MHz CDMA Radiofrequency Radiation on the Incidence of Spontaneous Tumors in Rats. Radiat Res 2003; 160 (2): 143-151. There were no significant differences among final survival days or body weights for either males or females in any group. No significant differences were found between treated and sham-exposed rats for any tumor in any organ. The authors conclude that chronic exposure to FDMA or CDMA radiofrequency radiation had no significant effect on the incidence of spontaneous tumors in rats.

124) **Lee et al., (2010)**: 848.5 MHz; 848.5; 0%); norm.: 3.394 GHz

Lee et al. Sprague-Dawley rats 2.0 W/kg (CDMA) 90 min/day, 5 days/week, 12 weeks 20/group Not any statistically significant alteration (NS) > highly coherent. Lee et al., (2012) Sprague-Dawley rats 848.5MHz (CDMA), 1950 MHz (WCDMA) 4.0W/kg 45 min/day, 5 days/week, 12 weeks 20/group (cage control group: 5) Not any statistically significant alteration (NS).

Lee, H.J.; Jin, Y.B.; Lee, J.S.; Choi, S.Y.; Kim, T.H.; Pack, J.K.; Choi, H.D.; Kim, N.; Lee, Y.S. Lymphoma development of simultaneously combined exposure to two radiofrequency signals in AKR/J mice. Bioelectromagnetics 2011, 32, 485–492.

125) **Kim et al., (2010)**: 848.5 MHz; 848.5; 0%); norm.: 3.394 GHz

Kim HS, Kim YJ, Lee YH, Lee YS, Choi HD, Pack JK, Kim N, Ahn YH. Effect of whole-body exposure to the 848.5 MHz code division multiple access (CDMA) electromagnetic field on adult neurogenesis in the young, healthy rat brain. med./bio. Int J Radiat Biol 2015; 91 (4): 354-359.

No significant differences in cell proliferation were found between the exposure groups (5 and 6) and the corresponding sham exposure groups (3 and 4) and cage control groups (1 and 2) in the investigated brain areas. The authors conclude that they could not find any effect of an acute whole-body exposure of rats to 848.5 MHz electromagnetic field on the neurogenesis in the adult brain Exposure duration: continuous for 1 h daily, 5 days per week, for 2 weeks, SAR: 2 W/kg mean (whole body).

126) **Keleş et al. (2018, 2019):** (900 Mhz; 905.9; 0.66%); norm.: 3.600 GHz

Keleş A, Yıldırım M, Gedikli Ö, Çolakoğlu S, Kaya H, Baş O, Sönmez OF, Odacı E. The effects of a continuous 1-h a day 900-MHz electromagnetic field applied throughout early and mid-adolescence on hippocampus morphology and learning behavior in late adolescent male rats. J Chem Neuroanat. 2018 Dec; 94:46-53. doi: 10.1016/j.jchemneu.2018.08.006.

Effects of continuous 1-h a day 900-MHz EMF applied through early & mid-adolescence on hippocampus morphology & learning behavior in late adolescent male rats. No significant change was observed in learning, memory or locomotor

behavior in any group. In conclusion, 900-MHz EMF applied in early and mid-adolescence causes no changes in learning, memory or locomotor behaviour.

Keleş Aİ, Nyengaard JR, Odacı E. Changes in pyramidal and granular neuron numbers in the rat hippocampus 7 days after exposure to a continuous 900-MHz electromagnetic field during early and mid-adolescence. J Chem Neuroanat. 2019 Aug 26:101681. doi: 10.1016/j.jchemneu.2019.101681. Remark (Geesink): but changes in pyramidal and granular neuron numbers in the rat hippocampus have been found.

127) **Surducan et al.** (2020) (915 MHz; 905.9; 1.01%); norm.: 3.660 GHz

Surducan V., Emanoil Surducan, Camelia Neamtu, Augustin C. Mot, Alexandra Ciorîță. Effects of Long-Term Exposure to Low-Power 915 MHz Unmodulated Radiation on Phaseolus vulgaris. 06 February 2020 https://doi.org/10.1002/bem.22253.

The morphophysiological response of Phaseolus vulgaris L. to low-power electromagnetic radiation was investigated in order to assess the potential harmful effects of long-term continuous exposure. The plants were grown in two separate electromagnetic field (EMF) shielded rooms, in a controlled, greenhouse-like environment. An unmodulated signal at 915 MHz (the central frequency between the uplink and downlink of the GSM900 mobile communications band) was used, with a maximum power density of 10 mW/m2 measured near the plants. The irradiated batch grew higher (19% increase in plant height, 20% increase in stem and leaves' dry mass), with 18% fewer inflorescences, and extremely long roots (34% increase in dry mass). The ultrastructure of the irradiated leaves showed irregular cells and a higher content of plastoglobules in the chloroplasts.

128) **D'Andrea et al.** (2000) (915 MHz; 905.9; 1.01%); norm.: 3.660 GHz

D'Andrea JA, Gandhi OP, Lords JL, Durney CH, Astle L, Stensaas LJ, Schoenberg AA. Physiological and behavioral effects of prolonged exposure to 915 MHz microwaves. med./bio.Published in: J Microw Power 1980; 15 (2): 123-135

915 MHz Modulation type: CW; Exposure duration: 640 h total (8 hr/day, 5 days/week, 16 weeks)
power density: 50 W/m² average over time, SAR: 2.46 mW/g average over mass (whole body).

Daily measures of body mass and of food and water intake indicated no statistically significant effects of microwave exposure. Measures by activity wheels and stabilimetric platforms of spontaneous locomotion indicate that mean activity levels increased about 25% after microwave irradiation, but the statistical significance of the findings are doubtful. Studies of blood sampled after 2, 6, 10, and 14 weeks of irradiation showed alterations of free sulfhydryls. Measures of levels of urinary 17-ketosteroids at weeks 1, 5, 9, and 12 of irradiation, and measures of brain hypothalamic tissue, and of mass of adrenals, heart, and liver at the end of the 16-week period, revealed no significant differences between exposed and control rats. Cortical EEGs sampled after conclusion of microwave exposures also showed no significant differences.

129) **Masuda al. (2009)**: (915 MHz; 905.9; 1.01%); norm.: 3.660 GHz

Masuda H, Ushiyama A, Takahashi M, Wang J, Fujiwara O, Hikage T, Nojima T, Fujita K, Kudo M, Ohkubo C. Effects of 915 MHz electromagnetic-field radiation in TEM cell on the blood-brain barrier and neurons in the rat brain. med./bio. Radiat Res 2009; 172 (1): 66-73, Journal PubMed doi:10.1667/RR1542.1

Exposure 1: 915 MHz, Exposure duration: continuous for 2 h SAR: 0.02 W/kg average over mass (whole body), SAR: 0.2 W/kg average over mass (whole body), SAR: 2 W/kg average over mass (whole body). Neither albumin leakage nor dark neurons were found in any rat brains after radiofrequency electromagnetic field exposure at levels up to 2.0 W/kg whole body SAR, which is 10-fold higher than the SARs Salford et al. used. Therefore, the authors were unable to confirm the results of the previous study of Salford et al. (2003).

130) **Trošic et al., (2013)**: (915 MHz; 906.0; 1.01%); norm.: 3.660 GHz

Trošic et al., Wistar rats 0.6 W/kg 1 h/day, 7 days/week, 2 weeks 9/group Not any statistically significant alteration (NS). Trošic, I.; Matauši´c-Pišl, M.; Pavicic, I.; Marjanovi´c, A.M. Histological and cytological examination of rat reproductive tissue after short-time intermittent radiofrequency exposure. Arh. Hig. Rada. Toksikol. 2013, 64, 513–519.

131) **Furtado-Filho et al., (2015)**: (950 MHz; 954.5; 0.47%); norm.: 3.8 GHz

Furtado-Filho OV, Borba JB, Maraschin T, Souza LM, Henriques JA, Moreira JC, Saffi J. Effects of chronic exposure to 950 MHz ultra-high-frequency electromagnetic radiation on reactive oxygen species metabolism in the right and left cerebral cortex of young rats of different ages. med./bio. Int J Radiat Biol 2015; 91 (11): 891-897.

New born rats from exposed dams had a significantly reduced body weight in comparison to rats from sham exposed dams.
6-day-old exposed rats showed a significantly higher amount of carbonyl proteins in the right cortex and a significantly lower blood glucose level compared to the sham exposure group. All other parameters did not show any significant differences between the exposure groups and the respective sham exposure groups. The authors conclude that a prenatal and postnatal exposure of rats to a 950 MHz electromagnetic field does not seem to induce oxidative damages of DNA, proteins and lipids in the cortex.

132) **Seyednour et al. (2011):** (pulsed 950 MHz; 954.5; 0.47%); norm.: 3.8 GHz

Seyednour R, Chekaniazar V. Effects of Exposure to Cellular Phones 950 MHZ Electromagnetic Fields on Progesterone, Cortisol and Glucose Level in Female Hamsters (Mesocricetus auratus). med./bio. Asian J Anim Vet Adv 2011; 6 (11): 1084-1088.

A statistically significant decrease in the progesterone level and a significant increase in the cortisol level was observed in both exposed groups (short-term and long-term) compared to the control group. The glucose level of the long-term exposed group was significantly increased in comparison to the short-term exposed group and the control group.

133) **Gibot et al. (2019):** (1.5 GHz; 1.519; 1.22%); norm.: 3.0 GHz

134) **Gibot et al. (2019):** (150 MHz, 150.99; 0.66%); norm.: 2.4 GHz

Gibot L., Jelena Kolosnjaj-Tabi, Elisabeth Bellard, Thomas Chretiennot, Quentin Saurin, Alexandre Catrain, Muriel Golzio , René Vézinet & Marie-Pierre Rols. Evaluations of Acute and Sub-Acute Biological Effects of Narrowband and Moderate-Band High Power Electromagnetic Waves on Cellular Spheroids. (2019) 9:15324 | https://doi.org/10.1038/s41598-019-51686-9.

No significant effects were observed, indicating that 1.5 GHz narrowband electromagnetic fields with incident amplitude level of 40 kV/m, and 150 MHz moderate band electric fields with an amplitude of 72.5 to approximately 200 kV/m, do not cause any significant alterations of assessed parameters.

135) **Vijayalaxmi et al. (2003):** (1.6 GHz; 1.61; 0.62%) %); norm.: 3.2 GHz

Vijayalaxmi, Sasser LB, Morris JE, Wilson BW, Anderson LE. Genotoxic potential of 1.6 GHz wireless communication signal: in vivo two-year bioassay, Radiat Res 2003; 159 (4): 558-564.

The data did not indicate a genotoxic potential of chronic exposure to 1.6 GHz radiofrequency (RF) radiation.The extent of genotoxicity (determined from incidence of micronuclei/2000polychromatic erythrocytes) was not significantly different between RF-radiation-exposed rats and sham-exposed controls or cage control rats; power density: 0.33 mW/cm².

136) **Anderson et al., (2004)**: (1600 MHz; 1610.6; 0.66%); norm.: 3.2 GHz

Anderson et al., Fischer 344 rats (M, F) 24 months, iridium signal Prenatal brain SAR (fetuses): 0.16 W/kg, Brain SAR: 0.16W/kg, 1.6 W/kg, 2 h/day, 5 days/week 90/sex/group, Not any increased tumor incidence (NS).

Anderson, L.E.; Sheen, D.M.; Wilson, B.W.; Grumbein, S.L.; Creim, J.A.; Sasser, L.B. Two-year chronic bioassay study of rats exposed to a 1.6 GHz radiofrequency signal. Radiat. Res. 2004, 162, 201–210.

137) **Gurbuz et al., (2014)**: (1800 MHz; 1811.97; 0.66%); norm.: 3.6 GHz

138) **Guler et al., (2016):** (1800 MHz; 1811.97; 0.66%); norm.: 3.6 GHz

Guler, G., et al., Neurodegenerative changes and apoptosis induced by intrauterine and extrauterine exposure of radiofrequency radiation. J Chem Neuroanat, 2016. 75(Pt B): p. 12833.

Guler et al., (2016) investigated the impact of 1800 MHz RFR on the brains of developing rabbits. The endpoints were oxidative DNA damage (8-hydroxy-2'deoxyguanosine determination), lipid peroxidation (malondialdehyde determination) and apoptotic cell formation TUNEL assay). A signal generator with an integrated pulse modulation unit and horn antenna was used to expose the animals. The estimated SAR was 18 mW/kg. 36 female rabbits were exposed for 15 minutes /day for 7 days. 36 males were exposed for 15 minutes / day for 14 days. 36 of the infant rabbits were exposed for 15 minutes / day in the intrauterine gestational period. The authors found that intrauterine and extrauterine 1800 MHz RFR exposure may cause oxidative and DNA damage in the brain tissue of baby rabbits which are exposed while they are fetus and after they are 1-month old. However, there was no evidence of apoptosis in any of the groups.

139) **McNamee et al. (2003)**: (1.9 GHz; 1.909; 0.47%); norm.: 3.8 GHz

McNamee JP, Bellier PV, Gajda GB, Lavallee BF, Marro L, Lemay E, Thansandote A. No evidence for genotoxic effects from 24 h exposure of human leukocytes to 1.9 GHz radiofrequency fields, Radiat Res 2003; 159 (5): 693-697.

No evidence of increased primary DNA damage or micronucleus induction in human leukocytes was detected for any 1.9 GHz RF field (neither CW nor PW) exposed cultures compared to the sham control.

140) **Miyakoshi et al. (2019):** (5.8 GHz; 5.73; 1.28%); norm.: 2.9 GHz

Miyakoshi J, Tonomura H, Koyama S, Narita E, Shinohara N. Effects of Exposure to 5.8 GHz Electromagnetic Field on Micronucleus Formation, DNA strand breaks, and Heat Shock Protein Expressions in Cells Derived from Human Eye. IEEE Trans Nanobioscience. 2019 Mar 15. doi: 10.1109/TNB.2019.2905491.

In the near future, electrification will be introduced to heavy-duty vehicles and passenger cars. However, wireless power transfer (WPT) requires high energy levels, and the suitability of various types of WPT systems must be assessed. This paper describes a method for solving technical and safety issues associated with this technology. We exposed human corneal epithelial (HCE-T) cells derived from the human eye to 5.8-GHz electromagnetic fields for 24 h. We observed no statistically significant increase in micronucleus (MN) frequency in cells exposed to a 5.8-GHz field at 1 mW/cm2(the general public level in ICNIRP) relative to sham-exposed or incubator controls. Similarly, DNA strand breaks, and expression of heat shock protein (Hsp) Hsp27, Hsp70, and Hsp90α exhibited no statistically significant effects as a result of exposure. These results indicate that exposure to 5.8-GHz electromagnetic fields at 1 mW/cm2 for 24 h has little or no effect on micronucleus formation, DNA strand breaks, and Hsp expression in human eye cells.

141) **Hansteen et al. (2009):** (16.5 GHz; 16.3; 1.18%); norm.: 4.125 GHz

142) **Hansteen et al. (2009):** (18.0 GHz; 18.1; 0.54%); norm.: 2.250 GHz

Hansteen IL, Lageide L, Clausen KO, Haugan V, Svendsen M, Eriksen JG, Skiaker R, Hauger E, Vistnes AI, Kure EH. Cytogenetic effects of 18.0 and 16.5 GHz microwave radiation on human lymphocytes in vitro. Anticancer Res 2009; 29 (8): 2885-2892.

The authors conclude, that neither 18.0 GHz continuous wave nor 16.5 GHz pulsed wave exposure of human lymphocytes induced statistically significant increases in chromosome aberration frequencies. 18.0 GHz and 1 W/m^2; 16.5 GHz, modulation type: pulsed exposure duration: continuous for 53 hr, 10 W/m^2. 16.5 GHz pulsed wave exposure requires further studies before a true negative conclusion can be drawn.

143) **Beneduci et al. (2005)**: (46.00 GHz; 45.81; 0.46%) %); norm.: 2.875 GHz

Beneduci A, Chidichimo G, De Rose R, Filippelli L, Straface SV, Venuta S. Frequency and irradiation time-dependant antiproliferative effect of low-power millimeter waves on RPMI 7932 human melanoma cell line. Anticancer Res. 2005.

143.2) **Samoilov et al. (2015)**: (54 GHz; 54.30; delta 0.89%); norm.: 3.375 GHz

Samoilov, V.O.; Shadrin, E.B.; Filippova, E.B.; Katsnelson, Y.; Backho↵, H.; Eventov, M. The effect of transcranial electromagnetic brain stimulation on the acquisition of the conditioned response in rats. Biophysics 2015, 60, 303–308.

In rats, the influence of 54 GHz, 150 mW/cm2, on an area of approximately 2 cm2 on the head was examined. This transcranial electromagnetic brain stimulation induced pain prevention and prevented the conditioned avoidance response to a pain stimulus in 50% of the animals. However, no changes were detected when serotonin inhibitors were previously administered. Therefore, the authors concluded that transcranial electromagnetic brain stimulation promotes the synthesis of serotonin, a transmitter that changes the animals' pain threshold.

144) **Nicolaz et al. 2009**: (60.4 GHz; 61.09; 1.12%); norm.: 3.775 GHz

Nicolaz CN, Zhadobov M, Desmots F, Sauleau R, Thouroude D, Michel D, Le Drean Y. Cell Biol Toxicol 2009; 25 (5): 471-478 Absence of direct effect of low-power millimeter-wave radiation at 60.4 GHz on endoplasmic reticulum stress. med./bio.
Exposure to 60.4 GHz did not modify endoplasmic reticulum protein folding and secretion, nor induced XBP1 or ATF6 transcription factors maturation. There were no significant changes in gene expression of BiP/GRP78 and HSP70. The data show that endoplasmic reticulum homeostasis does not undergo any modification at molecular level after exposure to low-power millimeter wave exposure at 60.4 GHz at 0.14 mW/cm².

145) **Radzievsky et al. (2004)**: (61.22 Ghz; 61.09; 0.22%); norm.: 3.8263 GHz

Radzievsky AA, Gordiienko OV, Szabo I, Alekseev SI, Ziskin MC. Millimeter wave-induced suppression of B16 F10 melanoma growth in mice: involvement of endogenous opioids. Bioelectromagnetics. 2004 Sep;25(6):466-73.

146) **Kalantaryan et al. (2010)**: (64.50 GHz; 65.23; 1.12%) %); norm.: 4.0313 GHz

Kalantaryan VP. Influence of low intensity coherent electromagnetic millimeter radiation (EMR) on aqua solution of DNA. Progress in Electromagnetics Research Letters 2011; 13: 1–9.

147) **Beneduci et al. (2005)**: (65.00 GHz; 65.23; 0.35%) %); norm.: 4.0313 GHz

Beneduci A, Chidichimo G, De Rose R, Filippelli L, Straface SV, Venuta S. Frequency and irradiation time-dependant antiproliferative effect of low-power millimeter waves on RPMI 7932 human melanoma cell line. Anticancer Res. 2005.

148) **Bantysh et al. (2018):** (130 GHz; 130.46; 0.35%); norm.: 4.0625 GHz

Bantysh BB, Krylov AY, Subbotina TI, Khadartsev AA, Ivanov DV, Yashin AA. Peculiar Effects of Electromagnetic Millimeter Waves on Tumor Development in BALB/c Mice. Bull Exp Biol Med. 2018 Sep;165(5):692-694. doi: 10.1007/s10517-018-4243-2.

In experimental mice exposed to electromagnetic radiation, the development of cancer process was slowed down throughout the observation period; moreover, no macroscopic signs of the tumors were revealed. However, in contrast to control mice, experimental animals demonstrated the formation of pathological reactions reflected by hepatic biochemical indices accompanied by the development of dystrophic and microcirculatory alterations in the liver tissue.

2.3 Electromagnetic frequencies that are proposed unhealthy, related to decoherent base signal at MHz and GHz, combined with estimated decoherent modulations, that fit in the algorithm

Name, (year):(applied frequency, calculated decoherent pointer frequency; difference between applied frequency and pointer state frequency)

1) **Guo et al. (2019)**: (220 MHz; 219.2; 0.37%)

Guo et al., (2019) 220 MHz (pulsed modulated) Sprague-Dawley rats 0.030 (whole body), 0.014W/kg (testis) 1 h/day, 7days/week, 30 days 20/group Decreased Leydig and Sertoli cells secreting factor levels, morphological alterations of the testis, increased levels of cleaved caspase 3, caspase 3, BAX/BCL2 ratio in the testis ($p < 0.05$).

Guo, L.; Lin, J.J.; Xue, Y.Z.; An, G.Z.; Zhang, J.P.; Zhang, K.Y.; He, W.; Wang, H.; Li, W.; Ding, G.R. Effects of 220 MHz pulsed modulated radiofrequency field on the sperm quality in rats. Int. J. Environ. Res. Public Health 2019, 16, 1286.

2) **d'Ambrosio et al. (2002):** (1748 MHz; 1753.5; 0.31%)

d'Ambrosio G, Massa R, Scarfi MR, Zeni O, Cytogenetic damage in human lymphocytes following GMSK phase modulated microwave exposure. Bioelectromagnetics 2002; 23 (1): 7-13.

A first set of experiments was performed by exposing the cultures to unmodulated (continuous wave) radiation and no significant difference was found (either in micronuclei or in cell proliferation kinetics). Other experiments were carried out by exposing the samples to phase modulated radiation, and a significant difference in micronuclei was found. This result would indicate a genotoxic effect of phase modulation.

3) **Vecsei (2018):** Pulsed 1750 MHZ; 1753.5; 0.20%)

4) **Vecsei (2018):** (pulsed 1947 MHz; 1973; 0.13%)

Vecsei Z., Balázs Knakker, Péter Juhász, György Thuróczy, Attila Trunk & István Hernádi. Short-term radiofrequency exposure from new generation mobile phones reduces EEG alpha power with no effects on cognitive performance. SCIENtIFIC REpoRTS | (2018) 8:18010 | DOI:10.1038/s41598-018-36353-9.

The study involved 60 healthy, young-adult university students (34 for UMTS and 26 for LTE) with double-blind administration of Real and Sham exposure in separate sessions. The system was set to WCDMA mode operating at the 1947 MHz carrier frequency (which corresponds to the operating frequency of UMTS MPs in Europe) with a wideband 5 MHz modulation of the RF carrier signal and of 1750 MHz (corresponding to one of the operating frequencies of LTE systems in Europe), and the LTE signal used 20 MHz of bandwidth (the allowed maximum). The averaged SAR was below 2 W/kg. EEG was recorded before, during and after RF exposure, and Stroop performance was assessed before and after EEG recording. Both RF exposure types caused a notable decrease in the alpha power over the whole scalp that persisted even after the cessation of the exposure, whereas no effects were found on any aspects of performance in the Stroop test. We can conclude that 20 min 3G (UMTS) or 4G (LTE) MP emitted RF exposure below the limit proposed by ICNIRP does not interfere with executive function measures, processing speed and selective attention as assessed by the Stroop test. In addition, both RF exposure types caused a notable decrease in EEG alpha power over the whole scalp that persisted even after cessation of the exposure. These results imply that the brain networks underlying global alpha oscillations might require minor reconfiguration to adapt to the acute local biophysical changes in the temporal cortex caused by focal RF exposure mimicking MP use. The results imply that the brain networks underlying global alpha oscillations might require minor reconfiguration to adapt to the local biophysical changes caused by focal RF exposure mimicking MP use.

5) **Zwamborn et al. (2003):** (pulsed 1.840 GHz; 1.860; 1.08%)

Zwamborn APM, Vossen SHJ, van Leersum BJA, Ouwens MA, Makel WN. Effects of Global Communication system radio-frequency fields on Well Being and Cognitive Functions of human subjects with and without subjective complaints. Published in: TNO Reports 2003; (FEL03C148): 1-89.

Electric field strength: 1 V/m peak value, electric field strength: 0.71 V/m effective value, SAR: 0.082 mW/kg maximum (10 g), SAR: 0.000383 µW/kg average over mass (partial body). A statistically significant relation between UMTS-like fields with a field strength of 1 V/m and an effect on the well-being was found (lower overall well-being). Further, a number of significant effects was revealed in the cognitive tasks.

6) **Broom et al. (2019):** (pulsed 1.846 GHz; 1.860; 0.74%)

Broom KA., Zenon Sienkiewicz et al. Early-Life Exposure to Pulsed LTE Radiofrequency Fields Causes Persistent Changes in Activity and Behavior in C57BL/6 J Mice September 2019, Bioelectromagnetics 40(7):498-511, DOI: 10.1002/bem.22217

Exposure to radiofrequency (RF) fields. This study investigated the effects of early-life exposure to pulsed long term evolution (LTE) 1,846 MHz downlink signals on innate mouse behavior. Animals were exposed for 30 min/day, 5 days/week at a whole-body average specific energy absorption rate (SAR) of 0.5 or 1 W/kg from late pregnancy (gestation day 13.5) to weaning (postnatal day 21). A behavioral tracking system measured locomotor, drinking, and feeding behavior in the home cage from 12 to 28 weeks of age. The exposure caused significant effects on both appetitive behaviors and activity of offspring that depended on the SAR. Compared with sham-exposed controls, exposure at 0.5 W/kg significantly decreased drinking frequency ($P \leq 0.000$) and significantly decreased distance moved ($P \leq 0.001$). In contrast, exposure at 1 W/kg significantly increased drinking frequency ($P \leq 0.001$) and significantly increased moving duration ($P \leq 0.005$). In the absence of other plausible explanations, it is concluded that repeated exposure to low-level RF fields in early life may have a persistent and long-term effect on adult behavior.

7) **Hae-June Lee et al. (2011)**: (modulated 1.95 GHz; 1.973; 1.15%)

Hae-June Lee, Young-Bae Jin, Jae-Seon Lee, Jeong-Ki Pack, Nam Kim, Yun-Sil Lee. One Year Simultaneous Combined Exposure of CDMA and WCDMA Radiofrequency Electromagnetic Fields to Rats. April 2011, International Journal of Radiation Biology 87(4):416-23. DOI: 10.3109/09553002.2010.537428

The results suggest that one---year chronic exposure to CDMA (849 MHz) RF at 2.0 W/kg for 45---min RF exposure periods
(total, 4 W/kg) did not increase chronic illness in rats, although there were some altered parameters in the complete blood count and serum chemistry.

8) **Tillmann et al. (2010)**: (modulated 1.97 GHz; 1.9726 GHz; 0.13%)

Tillmann et al., (2010), B6C3F1 mice (F) 24 months UMTS fields 48 W/m2 and 4.8 W/m2 + prenatal ENU treatment of 40mg/kg/b.w. 23.5 h/day, 7 days/week 60/group, Female lung carcinoma and lung tumor, rate in ENU-pretreated group (tumor promotion) ($p < 0.05$)

Tillmann T, Ernst H, Streckert J, Zhou Y, Taugner F, Hansen V, Dasenbrock C. Indication of cocarcinogenic potential of chronic UMTS-modulated radiofrequency exposure in an ethylnitrosourea mouse model. Int J Radiat Biol 2010; 86 (7): 529-541.

1,966 MHz, Exposure duration: continuous for 20 hr/day, 7 days/week for up to 24 months, power density: 4.8 W/m² average. The ENU-treated and UMTS-co-exposed (at 4.8 W/m²) animals displayed an enhanced lung tumour rate and an increased incidence of lung carcinomas as compared to the controls treated with ENU only. Furthermore, tumour multiplicity of the lung carcinomas was increased and the number of metastasising lung tumours was doubled in the ENU/UMTS co-exposure group as compared to the ENU control group. The authors conclude that this pilot study indicates a cocarcinogenic effect of lifelong UMTS exposure (4.8 W/m²) in female B6C3F1 offspring subjected to pretreatment with ethylnitrosourea.

9) **Lerchl et al. (2014)**: (modulated 1.97 GHz; 1.9726 GHz; 0.13%)

Lerchl et al., (2015) B6C3F1 mice (F) 24 months UMTS fields 0.04, 0.4, and 2 W/kg + prenatal ENU
treatment of 40mg/kg/b.w. 23.5 h/day, 7 days/week 96/group, Female lymphoma, lung adenoma and carcinoma, liver carcinoma (tumor promotion) ($p < 0.05$).

Lerchl A, Klose M, Grote K, Wilhelm AF, Spathmann O, Fiedler T, Streckert J, Hansen V, Clemens M. Tumor promotion by exposure to radiofrequency electromagnetic fields below exposure limits for humans. Biochem Biophys Res Commun 2015; 459 (4): 585-590.

The previous study indicated a cocarcinogenic effect of lifelong UMTS exposure (4.8 W/m²) in female B6C3F1 offspring subjected to pretreatment with ethylnitrosourea. Compared to the pilot study, higher numbers of animals per group were used and two additional exposure levels were included. The numbers of bronchiolo-alveolar adenoma in the lungs

were significantly increased in all exposure groups compared to the sham exposure and the numbers of bronchiolo-alveolar carcinoma were significantly elevated in the group with moderate exposure. Additionally, in all exposure groups, significantly higher rates of hepatocellular carcinoma were found when compared to the sham exposure. The numbers of animals bearing lymphomas were significantly elevated at moderate exposure compared to sham exposed mice. The numbers of multiple tumors (bronchiolo-alveolar adenomas) were found to be significantly elevated at low exposure in comparison to the sham exposure. The study confirms and extends the results of the pilot study of Tillmann et al., 2010 which indicated a tumor-promoting effect of lifelong exposure to radiofrequency electromagnetic fields in mice subjected to pretreatment with ethylnitrosourea. However, no clear dose-response relationship was found.

10) **Aydogan et al. (2015)**: (2100 MHz; 2092.2; 0.37%) (decoherent signal and modulated with estimated incoherent frequencies)

Aydogan F et al, (January 2015) The effect of 2100 MHz radiofrequency radiation of a 3G mobile phone on the parotid gland of rats, Am J Otolaryngol. 2015 Jan-Feb;36(1):39-46. doi: 10.1016/j.amjoto.2014.10.001. Epub 2014 Oct 5.

The effects of 2100-MHz radiofrequency radiation on nasal mucosa and mucociliary clearance in rats. med./bio.
Aydogan F, Aydin E, Koca G, Ozgur E, Atilla P, Tuzuner A, Demirci S, Tomruk A, Ozturk GG, Seyhan N, Korkmaz M, Muftuoglu S, Samim EE: Int Forum Allergy Rhinol 2015; 5 (7): 626-632, Journal PubMed doi:10.1002/alr.21509.

Radiofrequency radiation at 2100 MHz damaged the nasal septal mucosa, and disturbed the mucociliary clearance. Ciliary disorganization and ciliary loss in the epithelial cells resulted in deterioration of nasal mucociliary clearance.

11) **Guy et al. (1985)**: (modulated 2.45 GHz; 2.480 GHz; 1.2%)

Guy, A.W.; Chou, C.K.; Kunz, L.L.; Crowley, J.; Krupp, J. (1985, August) Effects of long-term low-level radiofrequency radiation exposure on rats. Volume 9. Summary. University of Washington, USAFSAM-TR-85-64.

12) **Chou et al., (1992)**: (2450 MHz pulse modulated); 2.480 GHz; 1.2%)

Chou, Sprague-Dawley rats (M) 25 months 0.144–0.4 W/kg 21.5 h/day, 7 days/week 200/group Total primary cancers malignant lymphoma thyroid cancer ($p < 0.05$).

Chou, C.K.; Guy, A.W.; Kunz, L.L.; Johnson, R.B.; Crowley, J.J.; Krupp, J.H. Long term, low-level microwave irradiation of rats. Bioelectromagnetics 1992, 13, 469–496.

13) **Gupta et al. (2018)**: (2450 MHz pulse modulated); 2.480 GHz; 1.2%)

Gupta SK, Mesharam MK, Krishnamurthy S. Electromagnetic radiation 2450 MHz exposure causes cognition deficit with mitochondrial dysfunction and activation of intrinsic pathway of apoptosis in rats. med./bio. J Biosci 2018; 43 (2): 263-276.

14) **Olakunle Bamikole et al. (2019)**: (2.5 GHz EMF emission indoor Wi-Fi device; 2.480 GHz, 0.81%)

Bamikole AO., Obajuluwa Adejoke Olukayode, Tiwa Obajuluwa, Okiki Pius, Oloyede Omotade Ibidun, Fadaka Oluwaseun Adewale, and Ojo Oluwafemi Adeleke.Exposure to a 2.5 GHz Non-ionizing Electromagnetic Field Alters Hematological Profiles, Biochemical Parameters, and Induces Oxidative Stress in Male Albino Rats. Biomed Environ Sci, 2019; 32(11): 860-863

15) **Bamdad et al. (2019):** (2.4-2.48 GHz Wi-Fi router devices: 2.44 GHz, 2.480 GHz, 0.16%)

Bamdad K, Adel Z, Esmaeili M. Complications of nonionizing radiofrequency on divided attention. J Cell Biochem. 2019 Feb 3. doi: 10.1002/jcb.28343.

16) **Ibitayo et al. (2017)** (2.5 GHz Wi-Fi device; 2.480 GHz, 0.81%)

Ibitayo AO, Afolabi OB, Akinyemi AJ, Ojiezeh TI, Adekoya KO, Ojewunmi OO. RAPD Profiling, DNA Fragmentation, and Histomorphometric Examination in Brains of Wistar Rats Exposed to Indoor 2.5 Ghz Wi-Fi Devices Radiation. RAPD

Profiling, DNA Fragmentation, and Histomorphometric Examination in Brains of Wistar Rats Exposed to Indoor 2.5 Ghz Wi-Fi Devices Radiation, Biomed Res Int. 2017;2017:8653286.

Alterations in harvested brain tissues were confirmed by histopathological analyses which showed vascular congestion and DNA damage in the brain was assayed using agarose gel electrophoresis. Histomorphometry analyses of their brain tissues showed perivascular congestion and tissue damage as well.

17) **Gang Yu, (2020):** 2575–2635 MHz (TDLTE): (2.605 GHz; 2.630; 0.95%)

Gang Yu, Zeping Tang, Hui Chen, Zhiyuan Chen, Lei Wang, Hui Cao, Gang Wang, Jiansheng Xing, Haotao Shen, Qing Cheng, Donghui Li, Guoren Wang, Yang Xiang, Yupeng Guan, Yabing Zhu, Zhenxiang Liu, Zhiming Bai. Long-term exposure to 4G smartphone radiofrequency electromagnetic radiation diminished male reproductive potential by directly disrupting Spock3–MMP2-BTB axis in the testes of adult rats, Science of The Total Environment, Volume 698, 1 January 2020, 133860

The present study was designed to investigate this issue by using 4G SRF-EMR in rats. The frequency band of the smartphones was 2575–2635 MHz (TDLTE). The electric field strength, power density of SRF-EMR, and SAR in the exposure area were respectively 37.93 V/m, 22.74 W/m2 and 1.05 W/kg. A unique exposure model using a 4G smartphone achieved localized exposure to the scrotum of the rats for 6 h each day (the smartphone was kept on active talk mode and received an external call for 1 min over 10 min intervals). Results showed that SRF-EMR exposure for 150 days decreased sperm quality and pup weight, accompanied by testicular injury. However, these adverse effects were not evident in rats exposed to SRF-EMR for 50 days or 100 days. Sequencing analysis and western blotting suggested Spock3 overexpression in the testes of rats exposed to SRF-EMR for 150 days. Inhibition of Spock3 overexpression improved sperm quality decline and alleviated testicular injury and BTB disorder in the exposed rats. Additionally, SRF-EMR exposure suppressed MMP2 activity, while increasing the activity of the MMP14–Spock3 complexes and decreasing MMP14–MMP2 complexes; these results were reversed by Spock3 inhibition. Thus, long-term exposure to 4G SRF-EMR diminished male fertility by directly disrupting the Spock3–MMP2–BTB axis in the testes of adult rats. To our knowledge, this is the first study to show direct toxicity of SRF-EMR on the testes emerging after long-term exposure.

18) **Wang et al. (2015):** (pulsed 2.856 GHz; 2.7896; 0.23%)

Wang C, Wang X, Zhou H, Dong G, Guan X, Wang L, Xu X, Wang S, Chen P, Peng R, Hu X. 2015 Effects of pulsed 2.856 GHz microwave exposure on BM-MSCs isolated from C57BL/6 mice. PLoS One. 2015 Feb 6;10(2): e0117550. doi:10.1371/journal.pone.0117550.

The increasing use of microwave devices over recent years has meant the bioeffects of microwave exposure have been widely investigated and reported. However, the exact biological fate of bone marrow MSCs (BM-MSCs) after microwave radiation remains unknown. In this study, the potential cytotoxicity on MSC proliferation, apoptosis, cell cycle, and in vitro differentiation were assayed following 2.856 GHz microwave exposure at a specific absorption rate (SAR) of 4 W/kg. Importantly, our findings indicated no significant changes in cell viability, cell division and apoptosis after microwave treatment. Furthermore, we detected no significant effects on the differentiation ability of these cells in vitro, with the exception of reduction in mRNA expression levels of osteopontin (OPN) and osteocalcin (OCN). These findings suggest that microwave treatment at a SAR of 4 W/kg has undefined adverse effects on BM-MSCs. However, the reduced-expression of proteins related to osteogenic differentiation suggests that microwave can influence at the mRNA expression genetic level.

19) **Pyrpasopoulou et al. (2004)**: (9.4 GHz, modulated; 9.352; 0.51%)

Pyrpasopoulou A. Vassiliki Kotoula, Angeliki Cheva, Georgios Karkavelas et al. Bone morphogenetic protein expression in newborn rat kidneys after prenatal exposure to radiofrequency radiation, April 2004, Bioelectromagnetics 25(3):216-27, DOI: 10.1002/bem.10185

GSM-like RFR interferes with gene expression during early gestation and results in aberrations of BMP expression in the new born.

2.4 Frequencies that are proposed healthy, related to the coherent frequency patterns at MHz and GHz, that fit in the proposed algorithm, but at a relatively high exposure rate.

Name, (year); (applied frequency, calculated coherent pointer frequency; difference between applied frequency and pointer frequency)

1) **García-Minguillán López et al. (2019):** (2.54 GHz; 2.545; 0.20%)

García-Minguillán Lópe O.z, Ana Jiménez Valbuena and Ceferino Maestú Unturbe. Significant Cellular Viability Dependence on Time Exposition at ELF-EMF and RF-EMF In Vitro Studies. Int. J. Environ. Res. Public Health 2019, 16, 2085; doi:10.3390/ijerph16122085.

The effect produced on NIH/3T3 cell viability after exposure to a 56.2 muW/cm2 EMF at 2.54 GHz for 15 min, 3 h, 6 h, 9 h, 15 h, 18 h and 21 h was measured.

2.5 Electromagnetic frequencies that are proposed unhealthy related to coherent base signal at MHz and GHz, combined with estimated decoherent modulations

Name, (year); (applied frequency, calculated coherent pointer frequency; difference between applied frequency and pointer frequency)

1) **Salama et al. (2010)**: 800 MHz (mobile phone in standby mode); (800 Mhz; 805.3; 0.66%)

Salama, 0.43 W/kg, Rabbits 8 h/day, 7 days/ week, 12 weeks 11/sex/group Decreased sperm concentration and motility, decrease in the diameter of seminiferous tubules ($p < 0.05$).

Salama, N.; Kishimoto, T.; Kanayama, H.O. Effects of exposure to a mobile phone on testicular function and structure in adult rabbit. Int. J. Androl. 2010, 33, 88–94.

2) **Repacholi et al. (1997)**: (modulated 900 MHz, 905.9; 0.65%)

Repacholi MH, Basten A, Gebski V, Noonan D, Finnie J, Harris AW. 1997. Lymphomas in E mu-Pim1 transgenic mice exposed to pulsed 900 MHz electromagnetic fields. Radiat Res 147: 631–640.

3) **Buttiglione et al. (2007)**: (modulated 900 MHz; 905.9; 0.66%)

Buttiglione M, Roca L, Montemurno E, Vitiello F, Capozzi V, Cibelli G. Radiofrequency radiation (900 MHz) induces Egr-1 gene expression and affects cell-cycle control in human neuroblastoma cells. J Cell Physiol (2007) 213(3):759–67

4) **Mausset-Bonnefont et al. (2004)**: 900 MHz (pulsed); (900; 905.9; 0.65%)

Mausset-Bonnefont AL, Hirbec H, Bonnefont X, Privat A, Vignon J, de Seze R. Acute exposure to GSM 900-MHz electromagnetic fields induces glial reactivity and biochemical modifications in the rat brain. Neurobiol Dis 2004; 17 (3): 445-454.

Acute exposure to high power GSM 900 MHz microwaves is able to induce 1) a strong glial immunoreactivity in different structures of the brain, 2) a significant reduction of the presence of NMDA receptors at the postsynaptic membrane level in the cortex and the striatum, and 3) biochemical modifications of neurotransmitter receptor properties. Although the authors showed that the rat general locomotor behavior was not significantly altered on the short term, the data provide the first evidence for rapid cellular and molecular alterations in the rat brain after an acute exposure to high power GSM 900 MHz microwaves.

5) **Schneider et al. (2014)**: 900 MHz (GSM); 905.9; 0.65%)

Schneider J., Manfred Stangassinger. Nonthermal Effects of Lifelong High-Frequency Electromagnetic Field Exposure on Social Memory Performance in Rats July 2014, Behavioral Neuroscience 128(5) DOI: 10.1037/a0037299

EMF-exposed females exhibited no differences in sniffing duration compared with controls. In contrast, the sniffing durations of EMF-exposed males at 3 months of age were significantly affected. At 6 months of age, GSM-exposed male adults showed a memory performance deficit. These findings provide new insight into the nonthermal effects of long-term high-frequency EMF exposure on memory.

6) **Pandey et al. (2018)**: 900 MHz (GSM); (900; 905.9; 0.65%)

Pandey et al. (2018) 900 MHz (GSM) Swiss albino mice, (Melatonin 5 mg/kg bw/day) 0.0054 – 0.0516 W/kg 6 h/day, 7 days/week, 35 days 15/group. Decreased sperm count, sperm head abnormalities, extensive DNA damage in germ cells, arrest in pre-meiotic stages of spermatogenesis, excess free radical generation resulting in histological and morphological changes in testis and germ cells morphology ($p < 0.05$).

Pandey, N.; Giri, S. Melatonin attenuates radiofrequency radiation (900 MHz)-induced oxidative stress, DNA damage and cell cycle arrest in germ cells of male Swiss albino mice. Toxicol. Ind. Health 2018, 34, 315–327.

7) **Narayanan et al. (2018)**: 900 MHz (GSM) (900 MHz; 905.9; 0.65%)

Narayanan et al., (2018): 900 MHz (GSM), 146.60 _W/cm2 1 h/day, 7 days/week, 4 weeks 6/group Wistar rats Increased MDA and caspase 3 levels, reduced sperm motility (NS), increased percentage of abnormal sperm ($p < 0.05$), loss of germ cells (spermatocytes and spermatids) in the testes.

Narayanan, S.N.; Lukose, S.T.; Arun, G.; Mohapatra, N.; Pamala, J.; Concessao, P.L.; Jetti, R.; Kedage, V.; Nalini, K.; Bhat, P.G. Modulatory effect of 900 MHz radiation on biochemical and reproductive parameters in rats. Bratisl. Lek. Listy 2018, 119, 581–587.

7b) **Falzone et al. (2011)**: 900 MHz (GSM) (900 MHz; 905.9; 0.65%)

Falzone N, Huyser C, Becker P, Leszczynski D, Franken DR. The effect of pulsed 900-MHz GSM mobile phone radiation on the acrosome reaction, head morphometry and zona binding of human spermatozoa. Int J Androl. 2011;34:20–26.

Falzone et al (2011) evaluated sperm-fertilizing competence following exposure to RF-EMR. To accomplish this, highly motile human spermatozoa collected from 12 healthy, were exposed for 1 hour to 900-MHz mobile phone radiation at an SAR of 2.0 W/kg, and the acrosome reaction was evaluated at various intervals after exposure by using the viability probe (7-aminoactinomycin, a fluorescent chemical compound) to assess the acrosome reaction in live spermatozoa only. Morphometric evaluation showed a significant decrease of the sperm head area and acrosome percentage of the head area among exposed compared with unexposed spermatozoa. The sperm competence to bind the zona pellucida following RF-EMR exposure decreased significantly compared with that of unexposed spermatozoa (Falzone et al, 2011). Therefore, the results of this study showed that although RF-EMR exposure does not seem to negatively affect the rate of the acrosome reaction, it significantly alters sperm morphometry and decreases the capability of spermatozoa to bind to the zona pellucida.

8) **Wyde et al., (2016)**: 900 MHz (GSM, CDMA) (900 MHz; 905.9; 0.65%)

Wyde et al., (2016) 900 MHz (GSM, CDMA) 1.5, 3,5 W/kg, Sprague-Dawley rats (M, F) Before birth trough 24 months, 9 h/day, 7 days/week 105/sex/group Male brain glioma and heart Schwannoma ($p < 0.05$).

Wyde M.E. et al. Report of Partial Findings from the National Toxicology Program Carcinogenesis Studies of Cell Phone Radiofrequency Radiation in Hsd: Sprague Dawley® SD rats (Whole Body Exposures) Draft 2-1-2018.

The U.S. National Toxicology Program (NTP) has carried out extensive rodent toxicology and carcinogenesis studies of radiofrequency radiation (RFR) at frequencies and modulations used in the U.S. telecommunications industry. This report presents partial findings from these studies. The occurrences of two tumor types in male Harlan Sprague Dawley rats exposed to RFR, 6 malignant gliomas in the brain and schwannomas of the heart, were considered of particulr interest and are the subject of this report.

Smith-Roe SL., Michael E. Wyde, Matthew D. Stout, John W. Winters. Evaluation of the genotoxicity of cell phone radiofrequency radiation in male and female rats and mice following subchronic exposure, Environment and Molecular Mutagenesis 61:276-290(2020).

The National Toxicology Program tested two common radiofrequency radiation (RFR) modulations emitted by cellular telephones in a 2-year rodent cancer bioassay that included interim assessments of additional animals for genotoxicity endpoints. The NTP bioassay was designed to evaluate nonthermal effects of cell phone RFR exposure, which meant that body temperature could not change more than 1 C under our exposure conditions. To meet that requirement, pilot studies conducted to establish acceptable SARs for the bioassay indicated that no body temperature increases over 1 C would be expected in rats (including pregnant rats) or mice at exposures up to 6.0 or 10.0 W/kg, respectively. Male and female Hsd:Sprague Dawley SD rats and B6C3F1/N mice were exposed from Gestation day 5 or Postnatal day 35, respectively, to code division multiple access (CDMA) or global system for mobile modulations over 18 hr/day, at 10-min intervals, in reverberation chambers at specific absorption rates of 1.5, 3, or 6 W/kg (rats, 900 MHz) or 2.5, 5, or 10 W/kg (mice, 1,900 MHz). After 19 (rats) or 14 (mice) weeks of exposure, animals were examined for evidence of RFR-associated genotoxicity using two different measures. Using the alkaline (pH > 13) comet assay, DNA damage was assessed in cells from three brain regions, liver cells, and peripheral blood leukocytes; using the micronucleus assay, chromosomal damage was assessed in immature and mature peripheral blood erythrocytes. Results of the comet assay showed significant increases in DNA damage in the frontal cortex of male mice (both modulations), leukocytes of female mice (CDMA only), and hippocampus of male rats (CDMA only). Increases in DNA damage judged to be equivocal were observed in several other tissues of rats and mice. No significant increases in micronucleated red blood cells were observed in rats or mice. In conclusion, these results suggest that exposure to RFR is associated with an increase in DNA damage. Environ. Mol. Mutagen. 61:276–290, 2020.

The NTP concluded that results demonstrated clear evidence of carcinogenic activity of cell phone RFR (both modulations) based on incidences of malignant schwannomas of the heart in male rats. Malignant gliomas in the brain were also observed in male rats exposed to cell phone RFR and were considered to be related to exposure. Female rats exhibited malignant schwannomas of the heart and malignant gliomas, but incidences of these tumors were considered equivocal. The observation that cell phone RFR affects heart and brain tissue in Sprague Dawley rats after long-term exposure was replicated in a similar study (that used only the GSM modulation) by the Ramazzini Institute (Falcioni et al. 2018). The U.S. Federal Communications Commission has set a guideline limit for RFR requiring that mobile devices emit an SAR of less than of 1.6 W/kg as measured in a volume containing 1 g of tissue absorbing the signal.

9) **Cammaerts et al. (2011):** 900 MHz (GSM) (902 MHz; 905.98; 0.66%)

Cammaerts, MC, Debeir O, Cammaerts R. 2011. Changes in Paramecium caudatum (protozoa) near a switched-on GSM telephone. Electromagn Biol Med. 2011, Mar;30(1):57-66. doi: 10.3109/15368378.2011.566778.

The protozoan Paramecium caudatum was examined under normal conditions versus aside a switched-on GSM telephone (900 MHz; 2 Watts). Exposed individuals moved more slowly and more sinuously than usual. Their physiology was affected: they became broader, their cytopharynx appeared broader, their pulse vesicles had difficult in expelling their content outside the cell, their cilia less efficiently moved, and trichocysts became more visible. All these effects might result from some bad functioning or damage of the cellular membrane. The first target of communication electromagnetic waves might thus be the cellular membrane

10) **Durdik et al. (2019)**: (modulated 915 MHz; 905.9; 1.01%)

Durdik M., Pavol Kosik, Eva Markova, Alexandra Somsedikova, Beata Gajdosechova,Ekaterina Nikitina, Eva Horvathova, Katarina Kozics, Devra Davis4 & Igor Belyaev. Microwaves from mobile phone induce reactive oxygen species but not DNA damage, preleukemic fusion genes and apoptosis in hematopoietic stem/progenitor cells. Scientific Reports | (2019) 9:16182 | https://doi.org/10.1038/s41598-019-52389-x 1

In this study (GSM MW with the frequency 915 MHz and 4 and 40 mW/kg) it has been investigated whether microwaves (MW) emitted by mobile phones could induce various biochemical markers of cellular damage including reactive oxygen species (ROS), DNA single and double strand breaks, PFG, and apoptosis in umbilical cord blood (UCB) cells including CD34+ hematopoietic stem/progenitor cells. UCB cells were exposed to MW pulsed signals from GSM900/UMTS test-mobile phone and ROS, apoptosis, DNA damage, and PFG were analyzed using flow cytometry, automated fluorescent

microscopy, imaging flow cytometry, comet assay, and RT-qPCR. In general, no persisting difference in DNA damage, PFG and apoptosis between exposed and sham-exposed samples was detected. However, we found increased ROS level after 1 h of UMTS exposure that was not evident 3 h post-exposure. We also found that the level of ROS rise with the higher degree of cellular differentiation. Our data show that UCB cells exposed to pulsed MW developed transient increase in ROS that did not result in sustained DNA damage and apoptosis.

11) **Çam et al. (2012)**: 900 MHz (GSM) (902 MHz; 905.98; 0.66%)

Çam ST, Seyhan N., 2012 Single-strand DNA breaks in human hair root cells exposed to mobile phone radiation. Int J Radiat Biol 88:420-424. doi: 10.3109/09553002.2012.666005.

To analyze the short-term effects of radiofrequency radiation (RFR) exposure on genomic deoxyribonucleic acid (DNA) of human hair root cells. SUBJECTS AND METHODS: Hair samples were collected from eight healthy human subjects immediately before and after using a 900-MHz GSM (Global System for Mobile Communications) mobile phone for 15 and 30 min. Single-strand DNA breaks of hair root cells from the samples were determined using the 'comet assay'. RESULTS: The data showed that talking on a mobile phone for 15 or 30 min significantly increased ($p < 0.05$) single-strand DNA breaks in cells of hair roots close to the phone. Comparing the 15-min and 30-min data using the paired t-test also showed that significantly more damages resulted after 30 min than after 15 min of phone use. CONCLUSIONS: A short-term exposure (15 and 30 min) to RFR (900-MHz) from a mobile phone caused a significant increase in DNA single-strand breaks in human hair root cells located around the ear which is used for the phone calls

12) **Belyaev al. (2006)**: (GSM modulated 915 MHz; 905.9; 1.01%)

Belyaev IY, Koch CB, Terenius O, Röxstrom-Lindquist K, Malmgren LO, Sommer WH, Salford LG, Persson BR. Exposure of rat brain to 915 MHz GSM microwaves induces changes in gene expression but not double stranded DNA breaks or effects on chromatin conformation. med./bio. Bioelectromagnetics 2006; 27 (4): 295-306

Effects of microwave exposure were found on neither conformation of chromatin nor DNA double-strand breaks. In cerebellum from all exposed animals, 11 genes were upregulated in a range of 1.34-2.74 fold and one gene was downregulated 0.48-fold. The induced genes encode proteins with diverse functions including neurotransmitter regulation, blood-brain barrier, and melatonin production. The results show that GSM microwaves at 915 MHz did not induce DNA double-strand breaks or changes in chromatin conformation, but affected gene expression in rat brain cells.

13) **Yamaguchi et al. (2003)**: pulsed 1439 MHz; 1431.7; 0.51%)

Yamaguchi H, Tsurita G, Ueno S, Watanabe S, Wake K, Taki M, Nagawa H. 1439 MHz pulsed TDMA fields affect performance of rats in a T-maze task only when body temperature is elevated. Bioelectromagnetics 2003; 24 (4): 223-230.

To assess the effects on learning and memory in rats of short term (4 days) or long term (4 weeks) exposure to a pulsed 1439 MHz, time division multiple access (TDMA) field based on the personal digital cellular (PDC) system used in cellular phones.
The animals exposed to electromagnetic waves with the brain average SAR of 25 W/kg for 4 days showed statistically significant decreases in the transition in number of correct choices in the reversal task. However, rats exposed to the brain average SAR of 7.5 W/kg for either 4 days or for 4 weeks showed no T-maze performance impairments. In conclusion, exposure to a 1439 MHz TDMA field, as used in cellular phones, at SARs much stronger than those emitted by cellular phones did not affect the learning and memory processes of rats when exposure did not cause thermal effects.

14) **Czyz et al., (2004):** (1710 MHz, modulated) (1710 MHZ; 1696.8; 0.78%)

Czyz J., Kaomei Guan Qinghua Zeng Teodora Nikolova Armin Meister Frank Schönborn Jürgen Schuderer Niels Kuster Anna M. Wobus. High frequency electromagnetic fields (GSM signals) affect gene expression levels in tumor suppressor p53-deficient embryonic stem cells. Bio Electromagnetics, Volume25, Issue4, May 2004.

The data indicate that the genetic background determines cellular responses to GSM modulated EMF.

15) **Diem et al. (2005)**: (modulated 1800 MHz) (1800 MHz, 1812.0; 0.66%)

Diem E, Schwarz C, Adlkofer F, Jahn O, Rudiger H. Non-thermal DNA breakage by mobile-phone radiation (1800 MHz) in human fibroblasts and in transformed GFSH-R17 rat granulosa cells in vitro. Mutat Res. 2005;583(2):178–183. doi:10.1016/j.mrgentox. 2005.03.006

16) **Falcioni et al., (2018)**: (1800 MHz (GSM); (1800 MHz, 1812.0; 0.66%)

Falcioni et al., Sprague-Dawley rats (M, F) Before birth trough spontaneous death 1800 MHz (GSM) 0.1 W/Kg, 0.03 W/Kg, 0.001W/Kg 19 h/day, 7 days/week Groups I,II: 400/sex/group Groups III, IV: 200/sex/group Male heart Schwannoma ($p < 0.05$) and female brain glioma (NS).

Falcioni L, Bua L, Tibaldi E, Lauriola M, De Angelis L, Gnudi F, Mandrioli D, Manservigi M, Manservisi F, Manzoli I, Menghetti I,
Montella R, Panzacchi S, Sgargi D, Strollo V, Vornoli A, Belpoggi F. 2018. Report of final results regarding brain and heart tumors in Sprague-Dawley rats exposed from prenatal life until natural death to mobile phone radiofrequency field representative of a 1.8 GHz GSM base station environmental emission. Environ Res 165: 496–503.

Four groups of817, 811, 411, 409 male and female Sprague-Dawley rats of our colony were exposed from prenatal life (12th day of mother gestation) until natural death to a 1.8 GHz GSM far field respectively of 0 (control, sham exposure), 5, 25, 50V/m with a whole-body exposure for 19h/day. A statistically significant increase in the incidence of heart Schwannomas was observed in treated male rats at the highest dose (50 V/m). Furthermore, an increase in the incidence of heart Schwann cells hyperplasia was observed in treated male and female rats at the highest dose (50V/m), although this was not statistically significant. An increase in the incidence of malignant glial tumors was observed in treated female rats at the highest dose (50V/m), although not statistically significant. Conclusions: The RI findings on far field exposure to RFR are consistent with and reinforce the results of the NTP study on near field exposure, as both reported an increase in the incidence of tumors of the brain and heart in RFR-exposed Sprague-Dawley rats. These tumors are of the same histotype of those observed in some epidemiological studies on cell phone users. These experimental studies provide sufficient evidence to call for the reevaluation of IARC conclusions regarding the carcinogenic potential of RFR in humans.

17) **Liu et al. (2013)**: (1800 MHz, pulsed GSM); (1800 MHz, 1812.0; 0.66%)

Liu C, Gao P, Xu SC, Wang Y, Chen CH, He MD, Yu ZP, Zhang L, Zhou Z. Mobile phone radiation induces mode dependent DNA damage in a mouse spermatocyte-derived cell line: a protective role of melatonin. Int J Radiat Biol. 2013. 89: 993-1001. doi: 10.3109/09553002.2013.811309.

A mouse spermatocyte-derived GC-2 cell line was exposed to a commercial mobile phone handset once every 20 min in standby, listen, dialed or dialing modes for 24 h., 1800 NHZ pulsed and 0.13 W/kg. DNA damage was determined using an alkaline comet assay. RESULTS: The levels of DNA damage were significantly increased following exposure to MPR in the listen, dialed and dialing modes. Moreover, there were significantly higher increases in the dialled and dialing modes than in the listen mode. These results regarding mode-dependent DNA damage have important implications for the safety of inappropriate mobile phone use by males of reproductive age.

18) **Bua et al. (2018)**: (1800 MHz, GSM); (1800 MHz, 1812.0; 0.66%)

Bua, L.; Tibaldi, E.; Lauriola, M.; De Angelis, L.; Gnudi, F.; Mandrioli, D.; Manservigi, M.; Manservisi, F.; Manzoli, I.; et al. Report of final results regarding brain and heart tumors in Sprague-Dawley rats exposed from prenatal life until natural death to mobile phone radiofrequency field representative of a 1.8 GHz GSM base station environmental emission. Environ. Res. 2018, 165, 496–503.

19) **Pawlak et al. (2018)**: (1800 MHz, GSM); (1800 MHz, 1812.0; 0.66%)

Pawlak K., Bartosz Bojarski, Zenon Nieckarz, Marcin Lis, Tomasz Wojnar. Effect of an 1800 MHz electromagnetic field emitted during embryogenesis on the https://doi.org/10.2754/avb201887010065 blood picture of one-day-old domestic hen chicks (Gallus gallus domesticus), Acta Vet. Brno 2018, 87: 65-71,

The aim of the study was to determine the effect of an 1800 MHz GSM electromagnetic field emission on the blood picture of one-day-old domestic hen chicks. Embryos developing in eggs were situated in the area where electric and magnetic fields ranged from 4.23 V/m to 6.25 V/m (± 0.01 V/m). Power density fluctuated between 0.090 W/m2 and 0.110 W/m2 (± 0.001 W/m2), while frequency reached the value of 1800 MHz. The SAR value calculated for the experimental group amounted to 4.2 × 10-4 W/kg. During the experiment, chick embryos were exposed to artificial electromagnetic fields throughout incubation for 13 ´ 2 min/day, 4 ´ 10 min/day and 1 ´ 40 min/day. The study shows an increase in the red blood cell count, haemoglobin concentration, haematocrit, white blood cell count, segmented heterophils and the heterophil/lymphocyte ratio, and a decrease in lymphocyte percentage of embryos exposed to an 1800 MHz electromagnetic field. The observed changes may be indicative of the stress-inducing effect of EMF on living organisms.

20) **Franzellitti et al. (2010)**: (1800 MHz, GSM); (1800 MHz, 1812.0; 0.66%)

Franzellitti S, Valbonesi P, Ciancaglini N, Biondi C, Contin A, Bersani F, Fabbri E. Transient DNA damage induced by high-frequency electromagnetic fields (GSM 1.8 GHz) in the human trophoblast HTR-8/SVneo cell line evaluated with the alkaline comet assay. Mutation Research, 01 Jan 2010, 683(1-2):35-42, DOI: 10.1016/j.mrfmmm.2009.10.004 PMID: 19822160.

The amplitude-modulated signals GSM-217 Hz and GSM-Talk induced a significant increase in comet parameters in trophoblast cells after 16 and 24h of exposure, while the un-modulated CW was ineffective. However, alterations were rapidly recovered and the DNA integrity of HF-EMF exposed cells was similar to that of sham-exposed cells within 2h of recovery in the absence irradiation. Our data suggest that HF-EMF with a carrier frequency and modulation scheme typical of the GSM signal may affect the DNA integrity.

21) **Poque et al. (2020):** (1800 MHz, GSM); (1800 MHz, 1812.0; 0.66%)

Poque E, Arnaud-Cormos D, Patrignoni L, Ruigrok HJ, Poulletier de Gannes F, Hurtier A, Renom R, Garenne A, Lagroye I, Leveque P, Percherancier Y. Effects of radiofrequency fields on RAS and ERK kinases activity in live cells using the Bioluminescence Resonance Energy Transfer technique. med./bio. [Wirkungen von hochfrequenten Feldern auf die RAS- und ERK-Kinase-Aktivität in lebenden Zellen mit Hilfe der Biolumineszenz-Resonanz-Energietransfer-Technik].Int J Radiat Biol 2020: 1-24 [im Druck], Journal PubMed doi:10.1080/09553002.2020.1730016.

The study was conducted to re-evaluate the effect of low-level 1800 MHz RF signals (up to public exposure level for local exposure) on RAS/MAPK activation in live cells. Material and methods: Using molecular probes based on the Bioluminescence Resonance Energy Transfer technique (BRET), we assessed the effect of Continuous wave (CW) and Global System for Mobile (GSM)-modulated 1800 MHz signals (up to 2 W/kg) on ERK and RAS kinases' activity in live HuH7 cells. Results: We found that radiofrequency field (RF) exposure for 24h altered neither basal level of RAS and ERK activation nor the potency of phorbol-12-myristate-13-acetate (PMA) to activate RAS and ERK kinases, whatever the Specific Absorption Rate (SAR) or signal used. However, we found that exposure to GSM-modulated 1800 MHz signals at 2 W/kg decreased the PMA maximal efficacy to activate both RAS and ERK kinases' activity. Exposure with CW 1800 MHz signal at 2 W/kg only decreased maximal efficacy of PMA to activate ERK but not RAS. No effects of RF exposure at 0.5 W/kg was observed on maximal efficacy of PMA to activate either RAS or ERK whatever the signal used. Conclusion: Our results indicate that RF exposure decreases the efficiency of the cascade of events, which, from the binding of PMA to its receptor(s), leads to the activation of RAS and ERK kinases.

22) **Nylund et al. (2009)**: (1800 MHz, GSM); (1800 MHz, 1812.0; 0.66%)

Nylund R, Tammio H, Kuster N, Leszczynski D, Proteomic Analysis of the Response of Human Endothelial Cell Line EA.hy926 to 1800 GSM Mobile Phone Radiation. med./bio.J Proteomics Bioinform 2009; 2: 455-462.

In conclusion, the data suggest that the 900 MHz and 1800 MHz GSM exposures, SAR: 2 W/kg average, might affect the expression of some proteins in the EA.hy926 cell line. The discrepancy observed here between the expression changes of GRP78 detected with different methods confirms the importance of validation of the results obtained with two-dimensional electrophoresis using other methods, e.g. Western blot.

23) **Koca et al. (2013)**: (1800 MHz, GSM); (1800 MHz, 1812.0; 0.66%)

Koca O, Gökçe AM, Öztürk MI, Ercan F, Yurdakul N, Karaman MI. 2013. Effects of intensive cell phone (Philips Genic 900) use on the rat kidney tissue. Urol J.2013 Spring;10:886-891.

To investigate effects of electromagnetic radiation (EMR) emitted by cell phones on the rat kidney tissue: 1,800 MHz, Exposure duration: 8 h/day speech mode, 16 h/day standby mode for 20 days, SAR: 1.52 W/kg. Twenty-one male Albino rats were divided into 3 groups, each comprising 7 rats. Group 1 was exposed to a cell phone in speech mode for 8 hours/day for 20 days and their kidneys were removed. Group 2 was exposed to EMR for 20 days and then their kidneys were removed after an interval of 20 days. Cell phone used in the present study was Philips Genie 900, which has the highest specific absorption rate on the market. Light microscopic examination of the kidney tissues obtained from the first group of rats revealed glomerular damage, dilatation of Bowman's capsule, formation of large spaces between the tubules, tubular damage, perivascular edema, and inflammatory cell infiltration. The mean severity score was 4.64 ± 1.7 in group 1, 4.50 ± 0.8 in group 2, and 0 in group 3. While there was no significant difference between group 1 and group 2 ($P > .05$), the mean severity scores of groups 1 and 2 were significantly higher than that of the control group ($P = .001$ for each). CONCLUSION: Considering the damage in rat kidney tissue caused by EMR-emitting cell phones, high-risk individuals should take protective measures.

24) **Meo et al. (2013)**: pulsed 1800 MHz (1800 MHz, 1812.0; 0.66%)

Meo SA, Al Rubeaan K. 2013. Effects of exposure to electromagnetic field radiation (EMFR) generated by activated mobile phones on fasting blood glucose. Int J Occup Med Environ Health 26:235-241.

The aim was to determine the effects of exposure to electromagnetic field radiation generated by mobile phones on fasting blood glucose in Wistar Albino rats. 40 Male Albino rats (Wistar Strain) were divided into 5 equally numerous groups. Group A served as the control one, group B received mobile phone radiation for less than 15 min/day, group C: 15-30 min/day, group D: 31-45 min/day, and group E: 46-60 min/day for a total period of 3 months. RESULTS: Wister Albino rats exposed to mobile phone radiation for longer than 15 min a day for a total period of 3 months had significantly higher fasting blood glucose ($p < 0.015$) and serum insulin ($p < 0.01$) compared to the control group. HOMA-IR for insulin resistance was significantly increased ($p < 0.003$) in the groups that were exposed for 15-30 and 46-60 min/day compared to the control rats. CONCLUSION: The results of the present study show an association between long-term exposure to activated mobile phones and increase in fasting blood glucose and serum insulin in Albino rats.

25a) **Zhi-qiang Li et al. (2020)**: pulsed GSM, 1800 MHz (1800 MHz, 1812.0; 0.66%)

25b) **Zhi-qiang Li et al. (2020)**: pulsed Wifi, (2400 MHz; 2415.9; 0.66%)

Zhi-qiang Li, Yuan Zhang, Yue-MengWan, Qiong Zhou, Chang Liu, Hui-XinWu, Yun-ZhengMu, Yue-FengHe, Ritika Rauniyar and Xi-NanWu. Testing of behavioral and cognitive development in rats after prenatal exposure to 1800 and 2400MHz radiofrequency fields. Journal of Radiation Research, Vol. 61, No. 2, 2020, pp. 197–206, doi: 10.1093/jrr/rrz097, Advance Access Publication: 11 January 2020

Pregnant female rats were exposed to radiofrequency fields beginning on the 21st day of pregnancy. The indicators of physiological and behavioral development were observed and measured in the offspring rats: Y maze measured at 3-weeks postnatal, open field at 7-weeks postnatal, and the expression of N-methyl-D-aspartate receptors (NMDARs) measured by reverse transcription-PCR in the hippocampus at 9-weeks postnatal. The body weight of the 1800 MHz group and the 1800 MHz + WiFi group showed a downward trend. The eye-opening time of newborn rats was much earlier in the WiFi group than in the control group. Compared to the control group, the overall path length of the 1800MHz+WiFi group was shortened and the stationary time was delayed. The path length of theWiFi group was shortened and the average velocity was increased in the error arm. The 1800MHz+WiFi group displayed an increased trend in path length, duration, entry times and stationary time in the central area. In both the 1800 MHz + WiFi and WiFi groups, NR2A and NR2B expression was down-regulated, while NR2D, NR3A andNR3B were up-regulated. Moreover, NR1 and NR2C in the WiFi groupwere also up-regulated. Prenatal exposure to 1800MHz and WiFi radiofrequencymay affect the behavioural and cognitive development of offspring rats, which may be associated with altered mRNA expression of NMDARs in the hippocampus.

26) **Wyde ME et al. (2016)**: (modulated 1900 MHz) (1900; 1908; 0.42%)

Wyde et al., (2016) 1900 MHz (GSM, CDMA) 2.5, 5, and 10 W/Kg B6C3F1/N mice (M, F) Before birth trough 24 Months 9 h/day, 7 days/week 105/sex/group Not any increased tumor incidence (NS).
20) **Gautam et al., (2019)**: **1915 MHz (UMTS):** (1915 MHz; 1908.9**;** 0.32%)

Gautam et al., (2019) 1915 MHz (UMTS) Wistar rats 0.26 W/kg 2 h/day, 7 days/week, 45 days 8/group Decreased weight of the sperm count (NS), viability and HOS tail-coiled spermatozoa ($p < 0.05$), increased MDA and ROS levels ($p < 0.05$, $p < 0.01$), reduced mitochondrial activity ($p < 0.01$), morphological alterations in sperm tail and membrane.

27) **Dasdag et al., (2015)**: 2400 MHz (from Wi-Fi system); (2400 MHz; 2415.9; 0.66%)

Dasdag et al. Wistar rats 2420 muW/kg 24 h/day, 7 days/week, 12 months 8/group Increased sperm head defects ($p<0.05$), decreased weight of the epididymis and seminal vesicles, seminiferous tubules diameter and tunica albuginea thickness ($p<0.01$, $p<0.001$, $p<0.0001$).

Dasdag, S., Akdag, M. Z., Erdal, M. E., Erdal, N., Ay, O. I., Ay, M. E., Yegin, K. (2015a). Effects of 2.4 GHz radiofrequency radiation emitted from Wi-Fi equipment on microRNA expression in brain tissue. International Journal of Radiation Biology, 91(7), 555–561. Dasdag, S., Taş, M., Akdag, M. Z., & Yegin, K. (2015).

Effect of longterm exposure of 2.4 GHz radiofrequency radiation emitted from Wi-Fi equipment on testes functions. Electromagnetic Biology and Medicine, 34(1), 37–42.

28) **Akdag et al., (2016):** 2400 MHz (from Wi-Fi system); (2400 MHz; 2415.9; 0.66%)

Akdag, Wistar rats 2420 W/kg 24 h/day, 7 days/week, 12 months 8/group Increased DNA damage (as percentage tail DNA value by Comet assay) in the testes. Akdag MZ, Dasdag S, Canturk F, Karabulut D, Caner Y, Adalier N. Does prolonged radiofrequency radiation emitted from Wi-Fi devices induce DNA damage in various tissues of rats? J Chem Neuroanat. 2016 Sep;75(Pt B):116-22.

29) **Bektas et al. (2020)**: (modulated 2400 MHz; 2415.9; 0.66%)

Bektas H., Suleyman Dasdag and Mehmet Selcuk Bektas, Comparison of effects of 2.4 GHz Wi-Fi and mobile phone exposure on human placenta and cord blood. BIOTECHNOLOGY & BIOTECHNOLOGICAL EQUIPMENT 2020, VOL. 34, NO. 1, 154–162, https://doi.org/10.1080/13102818.2020.1725639

The results of this study indicated that mobile phone exposure during pregnancy could have an important potential to cause oxidative stress and DNA damage in cord blood and placenta. The results of the study showed an increase in 8-OHdG, MDA, PCO and TOS in cord blood and placenta in the group exposed to mobile phones during gestation. The results of this study also indicated that combined effects of Wi-Fi plus mobile phone exposure have a higher potential to cause synergistic harmful effects.

30) **Margaritis et al., (2014):** 2440 MHz (from Wi-Fi system); (2440 MHz; 2415.9; 0.10%)

Margaritis LH., A.K.Manta, K.D. Kokkaliaris, C.D. Kokkaliaris, D.Schiza, K. Alimisis, G.Barkas, E.Georgiou, O.Giannakopoulou, I. Kollia, G.Kontogianni, A.Kourouzidou, A.Myari, F. Roumelioti, A. Skouroliakou, V. Sykioti, G. Varda, K. Xenos, K.Ziomas, Drosophila oogenesis as a bio- marker responding to EMF sources, Electromagn Biol Med. Electromagn Biol Med. 33(3): 165-89. 2014.

All EMF sources used created statistically significant effects regarding fecundity and cell death-apoptosis induction, even at very low intensity levels (0.3 V/m blue tooth radiation), well below ICNIRP's guidelines, suggesting that Drosophila oogenesis system is suitable to be used as a biomarker for exploring potential EMF bioactivity.

31) **Ramundo-Orlando et al., (2007):** (130 GHz; 130.46; 0.35%)

Ramundo-Orlando A, Gallerano GP, Stano P, Doria A, Giovenale E, Messina G, Cappelli M, D'Arienzo M, Spassovsky I. Permeability changes induced by 130 GHz pulsed radiation on cationic liposomes loaded with carbonic anhydrase. Bioelectromagnetics 2007; 28 (8): 587-598.

The effect of 130 GHz radiation pulse-modulated at low frequencies of 5, 7, or 10 Hz, and at time-averaged incident intensity (IAV) up to 17 mW/cm2 was studied at room temperature (22°C). The data indicate that interactions can take place between lipid bilayer and 130 GHz pulsed irradiation affecting its permeability, and that this is not simply caused by heating. 130 GHz exposure pulse modulated at low frequencies (5, 7, or 10 Hz) can enhance the permeability of cationic enzyme-containing liposomes.

2.6 Frequencies that are proposed healthy, related to coherent base signal at MHz and GHz, combined with coherent modulations that fit in the proposed algorithm.

Name, (year); (applied frequency and modulations, calculated coherent pointer frequency; difference between applied frequency and pointer frequency)

1) **Chen X. et al. (2009)**: (300-ns: 3.33 MHz; 3.314, 0.48%); (2 Hz; 2; 0%)

Chen, X., Swanson, J. R., Kolb, J.F., Nuccitelli, R., Schoenbach K.H. (2009) Histopathology of Normal Skin and Melanomas after Nanosecond Pulsed Electric Field Treatment. Melanoma Research, 19, 361-371.

2) **Yao et al. (2008)**: pulsed (10 MHz; 9.94, 0.71%; 1 Hz; 1.0; 0.0%)

Yao, C., Mi, Y., Hu, X., Li, C., Sun, C., Tang, J., Wu, X. (2008). Experiment and mechanism research of SKOV3 cancer cell apoptosis induced by nanosecond pulsed electric field, Proceedings of 30th Annual International IEEE EMBS Conference, Vancouver, British Columbia, Canada, 2008.

3) **Ren Z. et al. (2015)**: (10 MHz; 9.94, 0.71%; 0.5 Hz; 0.5; 0.00%)

Ren Z., Xinhua Chen, Guangying Cui, Shengyong Yin, Luyan Chen, Jianwen Jiang, Zhenhua Hu, Haiyang Xie, Shusen Zheng, Lin Zhou. Nanosecond Pulsed Electric Field Inhibits Cancer Growth Followed by Alteration in Expressions of NF-κB and Wnt/ β-Catenin Signaling Molecules, PLOS ONE | DOI:10.1371/journal.pone.0117550 February 6, 2015.

4) **Wang J. et al. (2012)**: (10 MHz; 9.94 MHz; 0.71%) (0.5 Hz, 0.5 Hz; 0.0%)

Wang J., Jinsong Guo, Shan Wu, Hongqing Feng, Shujun Sun, Jie Pan, Jue Zhang, Stephen J. Beebe. Synergistic Effects of Nanosecond Pulsed Electric Fields Combined with Low Concentration of emcitabine on Human Oral Squamous Cell Carcinoma In Vitro, PLOS ONE | www.plosone.org 1 August 2012 | Volume 7 | Issue 8 | e43213.

5) **Grospietsch et al. (1995)**: (150 MHz; 150.99; 0.51%) (72 Hz; 72 Hz; 0%).

Grospietsch T, Schulz O, Hoelzel R, Lamprecht I, Kramer KD. Stimulating effects of modulated 150 MHz electromagnetic fields on the growth of Escherichia coli in a cavity resonator. med./bio. Bioelectrochem Bioenerg 1995; 37 (1): 17-23.

A stimulation effect of electromagnetic field exposure on the growth of E. coli was observed. The growth behaviour was identical within the various modulation frequencies and unmodulated field conditions. Microthermal effects at cellular level could not be excluded. Modulation type: pulsed, Exposure duration: continuously for 6 h modulation-frequency: 72 Hz
electric field strength: 1.6 kV/m maximum

6) **Hinrikus et al. (2016)**: (mod. 450 MHz; 453.0; 0.66%); (40 Hz; 40.5 Hz; 1.2%)

Hinrikus H, Bachmann M, Karai D, Lass J. Mechanism of low-level microwave radiation effect on nervous system. Electromagn Biol Med. 2016 Nov 22:1-11.

7) **Oberto et al. (2007)**: (900 Mhz; 905.9; 0.66%); (217 Hz; 216.0; 0.46%)

Oberto G, Rolfo K, Yu P, Carbonatto M, Peano S, Kuster N, Ebert S, Tofani S. Carcinogenicity Study of 217 Hz Pulsed 900 MHz Electromagnetic Fields in Pim1 Transgenic Mice. med./bio. Radiat Res 2007; 168 (3): 316-326.

A total of 500 mice, 50 per sex per group, were exposed, sham-exposed or used as cage controls. This study was one of two independent studies performed to investigate carcinogenic potential of radiofrequency exposure. No significant effect of the radiofrequency irradiation under the exposure conditions used was found on the incidence of any neoplastic or non-neoplastic lesion, and thus these data did not provide evidence that radiofrequency irradiation possesses carcinogenic potential.

2.7 Electromagnetic frequencies that are proposed healthy related to coherent base signal at MHz and GHz, combined with estimated decoherent modulations

Name, (year); (applied frequency and modulations, calculated coherent pointer frequency; difference between applied frequency and pointer frequency)

1) **Utteridge et al. (2002);** (GSM pulsed 898.4 MHz; 905.9; 0.84%)

Utteridge TD, Gebski V, Finnie JW, Vernon-Roberts B, Kuchel TR. Long-term exposure of E-mu-Pim1 transgenic mice to 898.4 MHz microwaves does not increase lymphoma incidence. med./bio. Radiat Res 2002; 158 (3): 357-364

The results showed no significant difference in the incidence of lymphomas between exposed and sham-exposed groups at any of the exposure levels. No dose-response effect was found. SAR: 0.25 W/kg, 1 W/kg, 2 W/kg, W/kg.

2) **Hae-June Lee et al. (2011);** (GSM pulsed 848.5 MHz; 848.4; 0.01%)

Hae-June Lee,Yeung Bae Jin, Jae-Seon Lee, SooYong Choi,Tae-Hong Kim, Jeong-Ki Pack, HyungDoChoi, NamKim, and Yun-Sil Lee. Lymphoma Development of Simultaneously Combined Exposuret oTwo Radiofrequency Signals in AKR/JMice, Bioelectromagnetics 32:485^492 (2011).

Carcinogenic effects of combined signal RF-EMFs on AKR/J mice, which were used for the lymphoma animal model, were investigated. The carrier frequency of the CDMA signal is 848.5 MHz and the channel bandwidth is 1.23 MHz. The cellular CDMA system corresponds to a socalled second-generation (2G) wireless communication
system. The carrier frequency of the WCDMA signal is 1950 MHz and the channel bandwidth is 5 MHz. Six-week-old AKR/J mice were simultaneously exposed to two types of RF signals: single code division multiple access (CDMA) and wideband code division multiple access (WCDMA). AKR/J mice were exposed to combined RFEMFs for 45 min/day, 5 days/week, for a total of 42 weeks. The whole-body average specific absorption rate (SAR) of CDMA and WCDMA fields was 2.0 W/kg each, 4.0 W/kg in total. When we examined final survival, lymphoma incidence, and splenomegaly incidence, no differences were found between sham- and RF-exposed mice. However, occurrence of metastasis infiltration to the brain in lymphoma-bearing mice was significantly different in RF-exposed mice when compared to sham-exposed mice, even though no consistent correlation (increase or decrease) was observed between male and female mice. However, infiltration occurrence to liver, lung, and spleen was not different between the groups. From the results, we suggested that simultaneous exposure to CDMA and WCDMA RF-EMFs did not affect lymphoma development in AKR/J mice. Bioelectromagnetics 32:485–492, 2011.

3) **Ziemann et al. (2009)**: 902 MHz (GSM) (902 MHz; 905.98; 0.44%)

Ziemann C, Brockmeyer H, Reddy SB, Vijayalaxmi, Prihoda TJ, Kuster N, Tillmann T, Dasenbrock C. Absence of genotoxic potential of 902 MHz (GSM) and 1747 MHz (DCS) wireless communication signals: In vivo two-year bioassay in B6C3F1 mice. med./bio., Int J Radiat Biol 2009; 85 (5): 454-464.

The average number of survivors analyzed per treatment group was 39. There were no significant differences in the frequency of micronuclei between radiofrequency-exposed, sham-exposed, and cage control mice, irrespective of the staining/counting method used. Micronuclei were significantly increased in polychromatic and normochromatic erythrocytes of the positive control mice. The data did not indicate radiofrequency-induced genotoxicity in mice after two years of exposure. SAR: 0.4 W/kg maximum (whole body) (low exposure group), SAR: 1.3 W/kg maximum (whole

body) (medium exposure group), SAR: 4 W/kg maximum (whole body) (high exposure group), SAR: 0.18 W/kg peak value (partial body) (low exposure group), SAR: 1.9 W/kg peak value (partial body) (high exposure group)

4) **Tsurita et al. (2000)**: pulsed 1439 MHz; 1431.7; 0.51%)

Tsurita G, Nagawa H, Ueno S, Watanabe S, Taki M, Bioelectromagnetics 2000; 21 (5): 364-371. Biological and morphological effects on the brain after exposure of rats to a 1439 MHz TDMA field. med./bio.

A 1439 MHz TDMA field did not induce observable changes in the permeability of the blood-brain barrier, morphological changes in the cerebellum, or body mass changes.

5) **Yamashita et al. (2010)**: pulsed 1439 MHz; 1431.7; 0.51%)

Yamashita H, Hata K, Yamaguchi H, Tsurita G, Wake K, Watanabe S, Taki M, Ueno S, Nagawa H. Short-term exposure to a 1439-MHz TDMA signal exerts no estrogenic effect in rats. Bioelectromagnetics 2010; 31 (7): 573-575.

The short-term exposure to a 1439 MHz electromagnetic field, as used in Japanese mobile phones, altered neither the serum estrogen concentration nor estrogenic activity in female ovariectomized rats.

2.8 Frequencies that are proposed healthy, related to decoherent frequency signals at MHz and GHz (not modulated), that <u>do not fit</u> in the proposed algorithm

Name, (year): (applied frequency, calculated decoherent pointer frequency; difference between applied frequency and pointer frequency)

1) **Adey et al. (1999)**: (836.6 Mhz; 826.8; 1.19%)

Adey et al 1999; NS tumors in F-344 rats exposed to a single dose of n-ethyl-N-nitrosourea (ENU) transplacentally, 836.55 MHz DAMPS.

Focus formation of C3H/10T1/2 cells and exposure to 836.55 MHz modulated radiofrequency field. med./bio.
Cain CD, Thomas DL, Adey WR. Focus formation of C3H/10T1/2 cells and exposure to 836.55 MHz modulated radiofrequency field. med./bio. Bioelectromagnetics 1997; 18 (3): 237-243.

Spontaneous and Nitrosourea-induced Primary Tumors of the Central Nervous System in Fischer 344 Rats Exposed to Frequency-modulated Microwave Fields, April 2000Cancer Research 60(7):1857-63. Energy absorption rates (SARs) in the rats' brains were similar to localized peak brain exposures of a phone user (female, 236 g, <u>1.0 W/kg; male, 450 g, 1.2 W/kg</u>).

Although consistent but not attaining significance in the experiment overall (spontaneous CNS tumors, $P < 0.08$ one-tailed; $P < 0.16$ two-tailed; ENU-induced CNS tumors, $P < 0.08$ one-tailed, $P < 0.16$ two-tailed), the trend was significant ($P < 0.015$ one-tailed, $P < 0.03$, two-tailed) in rats that received ENU and died prior to experiment termination, with a primary brain tumor as the cause of death. We discuss differences in the signalling structure of digital and FM fields. Certain bioeffects induced by either amplitude-modulated or pulsed radiofrequency fields at a thermal levels have not been seen with fields of similar average power but unvarying in intensity (continuous wave or frequency-modulated fields).

2) **Son et al. (2015):** (1950 MHz; 1972.6; 1.15%)

Son Y, Jeong YJ, Kwon JH, Choi HD, Pack JK, Kim N, Lee YS, Lee HJ. The Effect of Sub-Chronic Whole-Body Exposure to a 1,950 MHz Electromagnetic Field on the Hippocampus in the Mouse Brain. med./bio.JEES 2015; 15 (3): 151-157.

No significant differences were found between exposed and sham exposed mice in any parameter.

The authors conclude that exposure of mice to a 1950 MHz electromagnetic field has no effect on cognitive functions and hippocampal histology. 1,950 MHz, Exposure duration: continuous for 2 hours/day for 60 days, SAR: 5 W/kg.

3) **Koyama et al. (2019)**; (40 GHz; 39.67; 0.83%)

Koyama S., Eijiro Narita, Yukihisa Suzuki, Takeo Shiina, Masao Taki, Naoki Shinohara and Junji Miyakoshi. Long-term exposure to a 40-GHz electromagnetic field does not affect genotoxicity or heat shock protein expression in HCE-T or SRA01/04 cells. Journal of Radiation Research, Vol. 60, No. 4, 2019, pp. 417–423 doi: 10.1093/jrr/rrz017

We exposed the cells to 40-GHz millimeter waves at 1mW/cm2 for 24h. We observed no statistically significant increase in the micronucleus (MN) frequency or the level of DNA strand breaks in cells exposed to 40-GHz millimeter waves relative to sham-exposed and incubator controls. Heat shock protein (Hsp) expression also exhibited no statistically significant response to the 40-GHz exposure. These results indicate that exposure to 40 GHz millimeter waves under these conditions has little or no effect on MN formation, DNA strand breaks, or Hsp expression in HCE-T or SRA01/04 cells. The results of the study suggest that exposure of eye epithelial cells to 40-GHz millimeter-wave radiation has little or no effect on genotoxicity or protein expression.

4) **Gurbuz et al., (2014):** (2100 MHz; 2092.2; 0.37%)

Gurbuz N, Sirav B, Colbay M, Yetkin I, Seyhan N. No genotoxic effect in exfoliated bladder cells of rat under the exposure of 1800 and 2100 MHz radio frequency radiation. med./bio. Electromagn Biol Med 2014; 33 (4): 296-301

No significant differences were found in the Micronucleus formation between the exposure groups or between the individual exposure groups and their respective control groups. The authors conclude that there is no evidence for genotoxic effects of exposure of rats to 1800 or 2100 MHz electromagnetic in exfoliated bladder cells. (Remark Geesink: 2100 MHz positioned at decoherent zone).

5) **Cohen et al. (2010):** (99 GHz; 100.1; 1.13%)

Cohen I, Cahan R, Shani G, Cohen E, Abramovich A. Effect of 99 GHz continuous millimeter wave electro-magnetic radiation on E. coli viability and metabolic activity. Int J Radiat Biol 2010; 86 (5): 390-399.

The data showed that 1 hour of exposure to 99 GHz continuous wave electromagnetic field irradiation had no effect on Escherichia coli viability and colony characterisation. The authors conclude that exposure of Escherichia coli to millimeter wave 99 GHz irradiation (continuous wave) for a short period did not affect the viability of Escherichia coli bacterial cells. However, 0.2 mW/cm² exposure, for 19 h caused a slight proliferation but did not influence the metabolic activities (of about 90 biochemical reactions that were examined). Hence, the authors assume that the slight proliferation (half order of magnitude) after 19 h of exposure does not have a biological meaning. (Remark Geesink: 99 GHz is positioned at the border of a coherent frequency band).

2.9 Frequencies that are proposed unhealthy, related to coherent frequency signals at MHz and GHz (not modulated), that do not fit in the proposed algorithm

Name, (year); (applied frequency and modulations, calculated coherent pointer frequency; difference between applied frequency and pointer frequency)

1)**Diem et al. (2005)**: (not modulated 1800 MHz) (1800 MHz, 1812.0; 0.66%)

Diem E, Schwarz C, Adlkofer F, Jahn O, Rudiger H. Non-thermal DNA breakage by mobile-phone radiation (1800 MHz) in human fibroblasts and in transformed GFSH-R17 rat granulosa cells in vitro. Mutat Res. 2005;583(2):178–183. doi:10.1016/j.mrgentox. 2005.03.006.

(2.0 W/kg, during 4, 16 and 24 h; effects occurred (after 16 h irradiation) in both cell types and after different modulations. The intermittent exposure showed a stronger effect than continuous exposure. The authors conclude that the induced DNA damage cannot be based on thermal effects).

2) **Aldad et al. (2012**): 800 MH; 805.3; 0.66%)

3) **Aldad et al. (2012):** 1,900 MHz; 1908.9; 0.47%)

Aldad TS, Gan G, Gao X-B, Taylor HS. 2012 Fetal Radiofrequency radiation from 800-1900 MH-rated cellular telephone affects neurodevelopment and behavior in mice. Scientific Rep 2, article 312.

Neurobehavioral disorders are increasingly prevalent in children, however their etiology is not well understood. An association between prenatal cellular telephone use and hyperactivity in children has been postulated, yet the direct effects of radiofrequency radiation exposure on neurodevelopment remain unknown. Here we used a mouse model to demonstrate that inutero radiofrequency exposure from cellular telephones does affect adult behavior. 800–1,900 MHz exposure duration: continuous for 0, 9, 15 or 24 hours/day on day 1-17 of gestation SAR: 1.6 W/kg. Mice exposed in-utero were hyperactive and had impaired memory as determined using the object recognition, light/dark box and step-down assays. Whole cell patch clamp recordings of miniature excitatory postsynaptic currents (mEPSCs) revealed that these behavioral changes were due to altered neuronal developmental programming. Exposed mice had dose-responsive impaired glutamatergic synaptic transmission onto layer V pyramidal neurons of the prefrontal cortex. We present the first experimental evidence of neuropathology due to in-utero cellular telephone radiation.

2.10 Electromagnetic frequencies that are proposed healthy, related to decoherent base signal at MHz and GHz, combined with estimated decoherent modulations, that do not fit in the proposed algorithm

Name, (year): (applied frequency, calculated decoherent pointer frequency; difference between applied frequency and pointer frequency)

1)**Ziemann et al. (2009)**: 1747 MHz (GSM) (1747 MHz; 1753.5; 0.37%)

Ziemann C, Brockmeyer H, Reddy SB, Vijayalaxmi, Prihoda TJ, Kuster N, Tillmann T, Dasenbrock C. Absence of genotoxic potential of 902 MHz (GSM) and 1747 MHz (DCS) wireless communication signals: In vivo two-year bioassay in B6C3F1 mice. med./bio., Int J Radiat Biol 2009; 85 (5): 454-464.

Exposure duration: continuous for 2 h/day, 5 days/weeks for 2 years (see also add. information for exp. setup). SAR: 0.4 W/kg maximum (whole body) (low exposure group), SAR: 1.3 W/kg maximum (whole body) (medium exposure group), SAR: 4 W/kg maximum (whole body) (high exposure group), SAR: 0.14 W/kg peak value (partial body) (low exposure group), SAR: 3.3 W/kg peak value (partial body) (high exposure group)

There were no significant differences in the frequency of micronuclei between radiofrequency-exposed, sham-exposed, and cage control mice, irrespective of the staining/counting method used. Micronuclei were significantly increased in polychromatic and normochromatic erythrocytes of the positive control mice. The data did not indicate radiofrequency-induced genotoxicity in mice after two years of exposure.

2) **Brescia et al. (2009)**: (modulated 1950 MHz; 1972.6; 1.15%)

Brescia F, Sarti M, Massa R, Calabrese ML, Sannino A, Scarfi MR. Reactive oxygen species formation is not enhanced by exposure to UMTS 1950 MHz radiation and co-exposure to ferrous ions in Jurkat cells. med./bio. Bioelectromagnetics 2009; 30 (7): 525-535.

Exposure duration: 5 min - 60 min or 24 h, SAR: 0.5 W/kg and SAR: 2 W/kg. The data indicate that non-thermal radiofrequency exposures do not increase spontaneous reactive oxygen species formation in any of the experimental conditions investigated. Consistent with the lack of reactive oxygen species formation, no change in cell viability was found in radiofrequency exposed cells. Similar results were obtained when co-exposures were considered: combined

exposures to radiofrequency and iron sulfate (as stress-inducer) did not increase reactive oxygen species production induced by the chemical treatment alone.

3) **Hae-June Lee. (2011)**; (GSM pulsed 1950 MHz; 1972.6; 1.15%)

Hae-June Lee,Yeung Bae Jin, Jae-Seon Lee, SooYong Choi,Tae-Hong Kim, Jeong-Ki Pack, HyungDoChoi, NamKim, and Yun-Sil Lee. Lymphoma Development of Simultaneously Combined Exposuret oTwo Radiofrequency Signals in AKR/JMice, Bioelectromagnetics 32:485^492 (2011).

Carcinogenic effects of combined signal RF-EMFs on AKR/J mice, which were used for the lymphoma animal model, were investigated. The carrier frequency of the CDMA signal is 848.5 MHz and the channel bandwidth is 1.23 MHz. The cellular CDMA system corresponds to a socalled second-generation (2G) wireless communication
system. The carrier frequency of the WCDMA signal is 1950 MHz and the channel bandwidth is 5 MHz. Six-week-old AKR/J mice were simultaneously exposed to two types of RF signals: single code division multiple access (CDMA) and wideband code division multiple access (WCDMA). AKR/J mice were exposed to combined RFEMFs for 45 min/day, 5 days/week, for a total of 42 weeks. The whole-body average specific absorption rate (SAR) of CDMA and WCDMA fields was 2.0 W/kg each, 4.0 W/kg in total. When we examined final survival, lymphoma incidence, and splenomegaly incidence, no differences were found between sham- and RF-exposed mice. However, occurrence of metastasis infiltration to the brain in lymphoma-bearing mice was significantly different in RF-exposed mice when compared to sham-exposed mice, even though no consistent correlation (increase or decrease) was observed between male and female mice. However, infiltration occurrence to liver, lung, and spleen was not different between the groups. From the results, we suggested that simultaneous exposure to CDMA and WCDMA RF-EMFs did not affect lymphoma development in AKR/J mice.

4) **Durdik et al. (2019)**: (modulated 1947.4 MHz; 1972.6; 1.28%)

Matus Durdik, Pavol Kosik, Eva Markova, Alexandra Somsedikova, Beata Gajdosechova,Ekaterina Nikitina, Eva Horvathova, Katarina Kozics, Devra Davis4 & Igor Belyaev. Microwaves from mobile phone induce reactive oxygen species but not DNA damage, preleukemic fusion genes and apoptosis in hematopoietic stem/progenitor cells. Scientific Reports | (2019) 9:16182 | https://doi.org/10.1038/s41598-019-52389-x 1

In this study (*UMTS MW frequency 1947.4 MHz and the SAR of 40 mW/kg for 1 or 3 h) i*t has been investigated whether microwaves (MW) emitted by mobile phones could induce various biochemical markers of cellular damage including reactive oxygen species (ROS), DNA single and double strand breaks, PFG, and apoptosis in umbilical cord blood (UCB) cells including CD34+ hematopoietic stem/progenitor cells. UCB cells were exposed to MW pulsed signals from GSM900/UMTS test-mobile phone and ROS, apoptosis, DNA damage, and PFG were analyzed using flow cytometry, automated fluorescent microscopy, imaging flow cytometry, comet assay, and RT-qPCR. In general, no persisting difference in DNA damage, PFG and apoptosis between exposed and sham-exposed samples was detected. However, we found increased ROS level after 1 h of UMTS exposure that was not evident 3 h post-exposure. We also found that the level of ROS rise with the higher degree of cellular differentiation. Our data show that UCB cells exposed to pulsed MW developed transient increase in ROS that did not result in sustained DNA damage and apoptosis.

2.11 Electromagnetic frequencies that are proposed healthy, related to coherent base signal at MHz and GHz, combined with estimated decoherent modulations, that do not fit in the proposed algorithm

1) **Kuznar et al. (2016):** (5.8 GHz; 5.73; 1.28%)

Kuzniar A, Laffeber C, Eppink B, Bezstarosti K, Dekkers D, Woelders H, Zwamborn AP, Demmers J, Lebbink JH, Kanaar R. Semi-quantitative proteomics of mammalian cells upon short-term exposure to non-ionizing electromagnetic fields. med./bio.Published in: PLoS One 2017; 12 (2): e0170762

WiFi (5.8 GHz, E = 9.5 V/m RMS) signals for 24 hrs: the results indicate that less than 1% of the quantitated human or mouse proteome responds to the EMFs by small changes in protein abundance. Further network-based analysis of the differentially regulated proteins did not detect significantly perturbed cellular processes or pathways in human and

mouse cells in response to ELF, UMTS or WiFi exposure. In conclusion, our extensive bioinformatics analyses of semi-quantitative mass spectrometry data do not support the notion that the short-time exposures to non-ionizing EMFs have a consistent biologically significant bearing on mammalian cells in culture.

Appendix 3.

Analyses of frequency patterns of unhealthy and healthy electromagnetic signals, related to MHz and GHz

3.1 Table of frequencies that are unhealthy, related to decoherent frequency patterns at MHz and GHz, that fit in the proposed algorithm

1) Brown-Woodman et al. (1988): norm.: 3.4714 GHz
2) Tofani et al. (1986): norm.: 3.4714 GHz
3) Lary et al. (1982, 1983): norm.: 3.4714 GHz
4) Bawin et al. (1973): norm.: 2.352 GHz
5) Guo et al. (2019): norm.: 3.520 GHz
6) Klos-Witkowska et al. (2019): norm.: 3.680 GHz
7) Jauchem and Frei (1997): norm.: 2.800 GHz
8) Holt JA (1977): norm.: 3.472 GHz
9) Sanders et al. (1980): norm.: 2.364 GHz
10) Frei et al. (1989): norm.: 2.800 GHz
11) Daniells et al. (1998): norm.: 3.000 GHz
12) Mashevich et al. (2003): norm.: 3.340 GHz
13) Mashevich et al.: (2003): norm.: 3.320 GHz
14) Maskey et al. (2014): norm.: 3.340 GHz
15) Donnellan et al. (1997): norm.: 3.340 GHz
16) Maskey et al. (2010): norm.: 3.340 GHz
17) Kim et al. (2018): norm.: 3.340 GHz
18) Pavicic I and Trosic I (2006): norm.: 3.456 GHz
19) Zmyslony et al. (2004): norm.: 3.720 GHz
20) Pavicic I and Trosic I (2008): norm.: 3.740 GHz
21) Maes et al. (1997): norm.: 3.7408 GHz
22) Herrala et al. (2018): norm.: 3.488 GHz
23) Luukkonen et al. (2009): norm.: 3.488 GHz
24) Hao et al. (2012): norm.: 3.664 GHz
25) Yang, L. et al. (2012): norm.: 3.664 GHz
26) Johnson and Guy (1972): norm.: 3.672 GHz
27) Zmyslony et al. (2004): norm.: 3.720 GHz
28) Maes et al. (1997): norm.: 3.741 GHz
29) Jauchem and Frei (2000): norm.: 4.000 GHz
30) De Pomerai et al. (2003): norm.: 4.000 GHz
31) Todorova et al. (2020): norm.: 4.000 GHz
32) Todorova et al. (2020): norm.: 2.500 GHz
33) Todorova et al. (2020): norm.: 2.500 GHz
34) Lu et al. (1992): norm.: norm.: 2.500 GHz
35) Oscar and Hawkins (1977): norm.: 2.600 GHz
36) Schirmacher et al. (1999): norm.: 2.500 GHz
37) Mancinelli et al. (2004): norm.: 3.900 GHz
38) Miyakoshi et al. (2005): norm.: 3.900 GHz
39) Iyama et al. (2004): norm.: norm.: 4.000 GHz
40) Senavirathna et al. (2014): norm.: 4.000 GHz
41) Esmekaya et al. (2013): norm.: 2.100 GHz
42) Esmekaya et al. (2017): norm.: 2.100 GHz
43) Bedir et al. (2015): norm.: 2.100 GHz
44) Sahin et al. (2016): norm.: 2.100 GHz

45) Gokcek-Sarac et al. (2017): norm.: 2.100 GHz
46) Jong Jin Oh et al. (2018): norm.: 2.100 GHz
47) Kesari et al. (2014): norm.: 2.115 GHz
48) Chandel et al. (2019): norm.: 2.350 GHz
49) Shandalal et al. (1979): norm.: 2.375 GHz
50) Lai et al. (1987, 1988): norm.: 2.450 GHz
51) Deshmukh et al. (2015): norm.: 2.450 GHz
52) D'Andrea et al. (1986): norm.: 2.450 GHz
53) Switzer and Mitchell (1977): norm.: 2.450 GHz
54) Meena et al., (2014): norm.: norm.: 2.450 GHz
55) Szmigielski et al. (1982): norm.: 2.450 GHz
56) Kesari et al. (2010): norm.: 2.450 GHz
57) Shokri S. et al. (2015): norm.: 2.450 GHz
58) Marcickiewicz et al. (1986): norm.: 2.450 GHz
59) Roszkowski et al. (1980b): norm.: 2.450 GHz
60) Szudzinski et al. (1982): norm.: 2.450 GHz
61) Usikalu et al. (2013): norm.: 2.450 GHz
62) Megha et al. (2015): norm.: 2.450 GHz)
63) Karimi et al. (2018): norm.: 2.450 GHz
64) Varghese et al. (2018): norm.: 2.450 GHz
65) Topsakal et al. (2017): norm.: 2.450 GHz
66) Figueiredo et al. (2004): norm.: 2.500 GHz
67) Liburdy R. (1979): norm. 2.600 GHz
68) Thomas et al. (1982): norm.: 2.800 GHz
69) Albert et al. (1977): norm.: 2.800 GHz
70) Frei and Jauchem (1989): norm.: 2.800 GHz
71) Gandhi et al. (1989): norm.: 2.800 GHz
72) Hai-juan Li et al. (2015): norm.: 2.856 GHz
73) Zuo H. et al. (2014): norm.: 2.856 GHz
74) Siekierzynski et al. (1972): norm.: 2.950 GHz
75) Pu et al. (1997): norm.: 3.000 GHz
76) D'Ándrea et al., (1994): norm.: 2.800 GHz
77) Jensh et al. (1984): norm.: 3.000 GHz
78) Goldstein and Sisko et al. (1974): norm.: 2.325 GHz
79) Zhang Y et al. (2014): norm.: 2.354 GHz
80) Sharma et al. (2014): norm.: 2.500 GHz
81) Millenbaugh et al. (2008): norm.: 2.1875 GHz
82) Sypniewska et al. (2008): norm. 2.1875 GHz
83) Foster et al. (2008): norm.: 2.1875 GHz
84) Makar et al. (2005): norm.: 2.638 GHz
85) Lushnikov et al. (2003): norm.: 2.625 GHz
86) Gapeev et al. (2003): norm.: 2.625 GHz
87) Frei et al. (1995): 2.1875 GHz
88) Kesari et al. (2009) norm.: 3.125 GHz
89) Albini et al. (2014): norm.: 3.125 GHz
90) D'Agostino et al. (2018): norm.: 3.336 GHz
91) Habauzit et al. (2018): norm.: 3.750 GHz
92) Le Quément et al. (2014): norm.: 3.775 GHz
93) Mahamoud et al. (2019): norm.: 3.775 GHz
94) Le Pogam et al. (2019): norm.: 3.775 GHz
95) Foster et al. (2003); norm.: 2.9375 GHz
96) Homenko et al. (2009): norm.: 3.125 GHz
97) Tafforeau et al. (2004): norm.: 3.281 GHz
98) Sheng Zhi Tan et al. (2019): norm.: 2.500 GHz
99) Sheng Zhi Tan et al. (2019): norm.: 2.656 GHz
100) Ahlberg Gagnér et al. (2019): norm.: 2.656 GHz
101) Wilmink et al. (2010): norm.: 2.4609 GHz
102) Ol'shevskaia et al. (2009): norm.: 2.597 GHz

73.1) Hui Wang et al. (2017): norm.: 2.856 GHz
84.2) Gapeyev et al. (2011): norm.: 2.638 GHz
91.2) Bellossi et al. (2018): norm. 3.750 GHz

3.2 Table of frequencies that are healthy, related to coherent frequency patterns at MHz and GHz, that fit in the proposed algorithm

103) Kyung Shin Kang et al. (2013): norm.: 4.0960 GHz
104) Kyung Shin Kang et al. (2013): norm.: 4.0960 GHz
105) Takebe et al. (2013): norm.: 4.0960 GHz
106) Bandyopadhyay et al. (2014): norm.: 4.0960 GHz
107) Usselman et al. (2016): norm.: 2.8672 GHz
108) Kyung Shin Kang et al. (2013): norm.: 3.0720 GHz
109) Takebe et al. (2013): norm.: 3.0720 GHz
110) Agulan et al. (2015): norm.: 3.389 GHz
111) Bandyopadhyay et al. (2014): norm.: 3.8605 GHz;
112) Zou et al. (2007): norm.: 2.560 GHz
113) Pokorny et al. (2009): norm.: 4.096 GHz
114) Chen X. et al. (2012, 2014): norm.: 2.560 GHz
115) Bandyopadhyay et al. (2014): norm.: 2.560 GHz
116) Stolfa et al. (2007): norm.: 2.7136 GHz
117) Garon et al. (2007): norm.: 3.200 GHz
118) Lary et al., (1983): norm.: 3.200 GHz
119) Alessio et al. (2019): norm.: 2.7040 GHz
120) Roti et al. (2001): norm.: 3.3425 GHz
121) LaRegina et al. (2003): norm.: 3.3425 GHz
122) Roti et al. (2001): norm.: 3.3910 GHz
123) LaRegina, (2003): norm.: 3.3910 GHz
124) Lee et al., (2010): norm.: 3.394 GHz
125) Kim et al., (2010): norm.: 3.394 GHz
126) Keleş et al. (2018, 2019): norm.: 3.600 GHz
127) Surducan et al. (2020): norm.: 3.660 GHz
128) D'Andrea et al. (2000): 3.660 GHz
129) Masuda al. (2009): norm.: 3.660 GHz
130) Trošic et al., (2013): norm.: 3.660 GHz
131) Furtado-Filho et al., (2015): norm.: 3.8 GHz
132) Seyednour et al. (2011): norm.: 3.8 GHz
133) Gibot et al. (2019): norm.: 3.0 GHz
134) Gibot et al. (2019): norm.: 2.4 GHz
135) Vijayalaxmi et al. (2003): norm.: 3.2 GHz
136) Anderson et al., (2004): norm.: 3.2 GHz
137) Gurbuz et al., (2014): norm.: 3.6 GHz
138) Guler et al., (2016): norm.: 3.6 GHz
139) McNamee et al. (2003): norm.: 3.8 GHz
140) Miyakoshi et al. (2019): norm.: 2.9 GHz
141) Hansteen et al. (2009): norm.: 4.125 GHz
142) Hansteen et al. (2009): norm.: 2.250 GHz
143) Beneduci et al. (2005): norm.: 2.875 GHz
144) Nicolaz et al. (2009): norm.: 3.775 GHz
145) Radzievsky et al. (2004): norm.: 3.8263 GHz
146) Kalantaryan et al. (2010): norm.: 4.0313 GHz
147) Beneduci et al. (2005): norm.: 4.0313 GHz
148) Bantysh et al. (2018): norm.: 4.0625 GHz

143.2) Samoilov et al. (2015): norm.: 3.375 GHz

3.3 Frequencies that are unhealthy, related to decoherent frequency signals at MHz and GHz (not modulated), that fit in the proposed algorithm

Algorithmic decoherent reference scale:

2.0922 2.2042 2.3379 2.4797 2.6301 2.7896 2.9489 3.1278 3.3063 3.5069 3.7196 3.9452 GHz

Applied frequencies and calculated decoherent pointer frequency:

2.0922

41) 2.100 GHz 42) 2.100 GHz 43) 2.100 GHz 44) 2.100 GHz 45) 2.100 GHz 46) 2.100 GHz 47) 2.115 GHz

2.2042

81) 2.1875 GHz 82) 2.1875 GHz 83) 2.1875 GHz 87) 2.1875 GHz

2.3379

78) 2.325 GHz 48) 2.350 GHz 4) 2.352 GHz 79) 2.354 GHz 9) 2.364 GHz 49) 2.375 GHz

2.4797

101) 2.4609 GHz 50) 2.450 GHz 51) 2.450 GHz 52) 2.450 GHz 53) 2.450 GHz 54) 2.450 GHz 55) 2.450 GHz 56) 2.450 GHz 57) 2.450 GHz 58) 2.450 GHz 59) 2.450 GHz 60) 2.450 GHz 61) 2.450 GHz 62) 2.450 GHz 63) 2.450 GHz 64) 2.450 GHz 65) 2.450 GHz 32) 2.500 GHz 33) 2.500 GHz 34) 2.500 GHz 36) 2.500 GHz 66) 2.500 GHz 80) 2.500 GHz 98) 2.500 GHz

2.6301

102) 2.597 35) 2.600 GHz 67) 2.600 GHz 85) 2.625 GHz 86) 2.625 GHz 84) 2.638 GHz 84.2) 2.638 99) 2.656 GHz 100) 2.656 GHz

2.7896

7) 2.800 GHz 10) 2.800 GHz 68) 2.800 GHz 69) 2.800 GHz 70) 2.800 GHz 71) 2.800 GHz 76) 2.800 GHz 72) 2.856 GHz 73) 2.856 GHz 73.1) 2.856 GHz

2.9489

95) 2.9375 GHz 74) 2.950 GHz 11) 3.000 GHz 75) 3.000 GHz 77) 3.000 GHz

3.1278

88) 3.125 GHz 89) 3.125 GHz 96) 3.125 GHz

3.3063

97) 3.281 GHz 90) 3.336 GHz 12) 3.340 GHz 14) 3.340 GHz 15) 3.340 GHz 16) 3.340 GHz 17) 3.340 GHz

3.5069

18) 3.456 GHz 1) 3.4714 GHz 2) 3.4714 GHz 3) 3.4714 GHz 8) 3.472 GHz 22) 3.488 GHz 23) 3.488 GHz 5) 3.520 GHz

3.7196

24) 3.664 GHz 25) 3.664 GHz 26) 3.672 GHz 6) 3.680 GHz 19) 3.720 GHz 27) 3.720 GHz 20) 3.740 GHz 21) 3.741 GHz 28) 3.741 GHz 91) 3.750 GHz 91.2) 3.750 92) 3.775 GHz 93) 3.775 GHz 94) 3.775 GHz

3.9452

37) 3.900 GHz 38) 3.900 GHz 29) 4.000 GHz 30) 4.000 GHz 31) 4.000 GHz 39) 4.000 GHz 40) 4.000 GHz

Algorithmic coherent reference scale:

2.1475 2.2624 2.4159 2.5452 2.71785 2.8633 3.03695 3.22125 3.39365 3.6239 3.8178 4.0768 GHz

Applied frequencies and calculated coherent pointer frequencies:

2.1475

2.2624

142) 2.250 GHz

2.4159

134) 2.400 GHz

2.5452

112) 2.560 GHz 114) 2.560 GHz 115) 2.560 GHz

2.71785

119) 2.7040 GHz 116) 2.7136 GHz

2.8633

107) 2.8672 GHz 143) 2.875 GHz 140) 2.9 GHz

3.03695

133) 3.0 GHz 108) 3.0720 GHz 109) 3.0720 GHz

3.22125

117) 3.200 GHz 118) 3.200 GHz 135) 3.200 GHz 136) 3.200 GHz

3.39365

120) 3.3425 GHz 121) 3.3425 GHz 143.2) 3.375 110) 3.389 GHz 122) 3.3910 GHz 123) 3.3910 GHz 124) 3.394 GHz 125) 3.394 GHz

3.6239

126) 3.600 GHz 137) 3.600 GHz 127)3.660 GHz 128) 3.660 GHz 129) 3.660 GHz 130) 3.660 GHz 138) 3.600 GHz

3.8178

144) 3.775 GHz 131) 3.800 GHz 132) 3.800 GHz 139) 3.800 GHz 145) 3.8263 GHz 111) 3.8605 GHz

144) Nicolaz et al. 2009: (60.4 GHz; 61.09; 1.12%); norm.: 3.775 GHz

4.0768

146) 4.0313 GHz 147) 4.0313 GHz 148) 4.0625 GHz 103) 4.096 GHz 104) 4.096 GHz 105) 4.096 GHz 106) 4.096 GHz 113) 4.096 GHz
141) 4.125 GHz

3.4 Graph 13: Normalized frequencies, that are healthy (green) or unhealthy (red), related to frequency patterns at MHz and GHz, that fit in the proposed algorithm

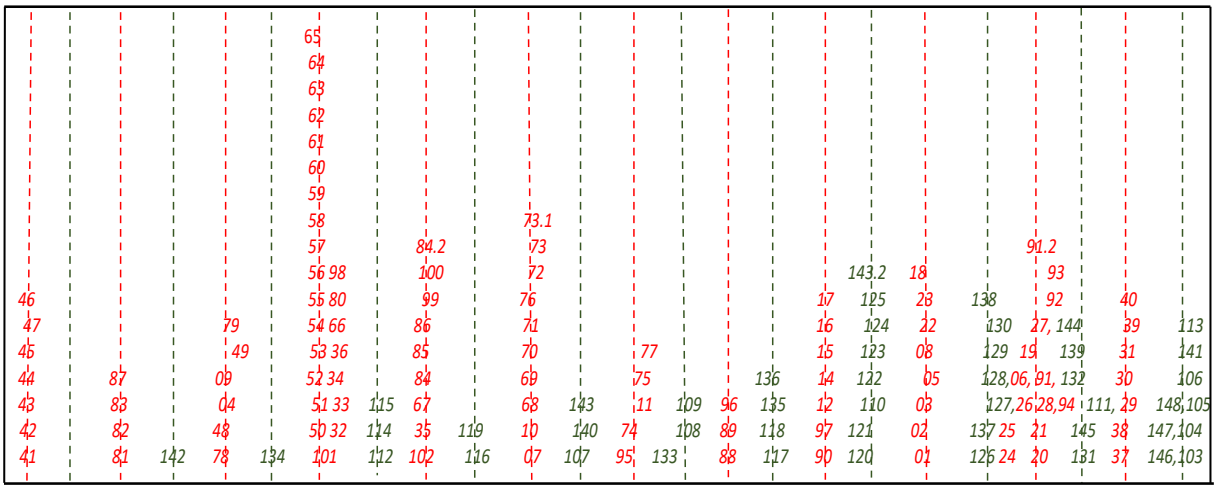

Figure 6. *Measured frequency data of living cells systems that are health-sustaining (coherent data: green), or detrimental for health (decoherent data: red) versus calculated normalized frequencies, 1970 till 2020. Biological effects measured following exposures or endogenous effects of living cells in vitro and in vivo at frequencies in the bands of MHz, GHz and THz. Green numbers plotted on a logarithmic x-axis represent calculated normalized GHz-health-sustaining frequencies; red numbers represent calculated GHz-health-destabilizing frequencies. Each point: green numbers (see references) or red numbers (see references) indicated in the graph is taken from published biological data and are a typical frequency for a biological experiment(s). For clarity, points are randomly distributed along the Y-axis; Yellow lines are proposed transition frequencies (Geesink, 2020).*